PRELIMINARY UPDATED GROUNDWATER FLOW AND TRANSPORT MODELING REPORT FOR CLIFFSIDE STEAM STATION, MOORESBORO, NORTH CAROLINA

November 2018

Prepared for
Duke Energy Carolinas, LLC

Investigators
Regina Graziano, M.S. – SynTerra Corporation
Ronald W. Falta, Ph.D. – Falta Environmental, LLC
Jonathan Ebenhack, M.S. – SynTerra Corporation
Rong Yu, Ph.D. – SynTerra Corporation
Lawrence C. Murdoch, Ph.D. – FRx, Inc.

TABLE OF CONTENTS

LIST OF TABLES

LIST OF FIGURES

EXECUTIVE SUMMARY

Duke Energy Carolinas, LLC (Duke Energy) owns and operates the Cliffside Steam Station (CSS), or the Site, which is located in Mooresboro, Rutherford and Cleveland Counties, North Carolina. The CSS began operation in 1940 as a coal-fired generating station. Units 1 through 4 were retired in October 2011, and currently only Units 5 and 6 are in operation at the CSS. The coal combustion residuals (CCR) and other liquid discharges from coal combustion processes at the CSS have historically been managed in the CSS ash basins, which consist of the active ash basin, the Former Units 1-4 ash basin, and the Unit 5 inactive ash basin. Discharge from the active ash basin is currently permitted by the North Carolina Department of Environmental Quality (NCDEQ) Division of Water Resources (DWR) under National Pollutant Discharge Elimination System (NPDES) Permit NC0005088. Duke also operates a Coal Combustion Products (CCP) Industrial Landfill (CCP Landfill) in accordance with the North Carolina Department of Environmental Quality (NCDEQ) Solid Waste Section (SWS) on the property.

Preliminary numerical simulations of groundwater flow and transport have been calibrated to current conditions and used to evaluate different scenarios being considered as options for closure of the ash basin. The predictive simulations presented herein are not intended to represent a final detailed closure design. These simulations use conceptual designs that are subject to change as the closure plans are finalized. The simulations are intended to show the key characteristics of groundwater flow and mobile constituent transport that are expected to result from the closure actions. It should be noted that for groundwater modeling purposes, a reasonable assumption was made for initiation dates for each of the closure options. The assumed dates were based on information provided by Duke Energy that is currently evolving and may vary from dates provided in contemporary documents. The potential variance in closure dates presented in the preliminary groundwater model is inconsequential to the results of the model as it does not produce substantial changes in the modeled scenarios. This preliminary model report is intended to provide basic model development information and simulations of conceptual basin closure designs. A more detailed model report is planned for inclusion in the groundwater corrective action plan (CAP) scheduled for completion in December 2019.

The model simulations were developed using flow and transport models MODFLOW and MT3DMS. Boron was the constituent of interest (COI) selected to estimate the time to achieve compliance because it is highly mobile in groundwater and tends to have the largest extent of migration. The less mobile, more reactive constituents (i.e. arsenic, selenium, chromium, etc.) will follow the same flow path as boron; however, they generally are not present at concentrations greater than the 15A NCAC 02L .0202 Groundwater Quality Standard for boron (2L standard) beyond the compliance boundary.

The results of the model simulations indicate the boron plume configuration over time is somewhat different for the three closure scenarios: excavation, final cover and hybrid (Figure ES-1 and ES-2)[1]. The differences are caused by changes to the groundwater flow field that would occur following excavation. In the excavation scenario, the original Suck Creek footprint, which was a deeply cut hydraulic channel, was simulated as a drain within the active ash basin making boron migrate into the Suck Creek channel. The former Suck Creek footprint changes the hydraulics of the groundwater system ultimately causing boron to migrate to the original Suck Creek footprint and reduces migration to the north of the compliance boundary. Without any additional corrective action, it is expected that excavation could meet the 2L standard (potential compliance boundary) within 100 years, final cover scenario could meet the 2L standard in 500 years, and the hybrid scenario could meet the 2L standard in 400 years. These times would likely be greatly reduced if an engineered control system were used to control the boron plume, though the three closure scenarios predict there are no potential human health or environmental risks. Three closure-specific compliance boundaries[2] were used to evaluate the results:

- Excavation scenario is evaluated using a compliance boundary that is 250 ft. from the current waste boundary.
- Final Cover scenario is evaluated using a compliance boundary that is 500 feet (ft.) from the current waste boundary.
- Hybrid scenario is evaluated using a compliance boundary 250 ft. from the final waste boundary.

A reference location near the compliance boundary was also used to evaluate changes in boron concentrations over time for the three closure designs, in the absence of any additional corrective action. The boron concentrations exceed the 2L standard at the reference locations during historical operation of the ash basin. The boron concentrations decrease over the next 100-500 years with compliance achieved at this location by 2150 for excavation, 2525 for the final cover, and 2400 for hybrid design.

Domestic wells near the CSS are outside the groundwater flow system containing the ash basins. Domestic wells are not affected by constituents released from the ash basins, or by the different ash basin closure options based upon the simulations.

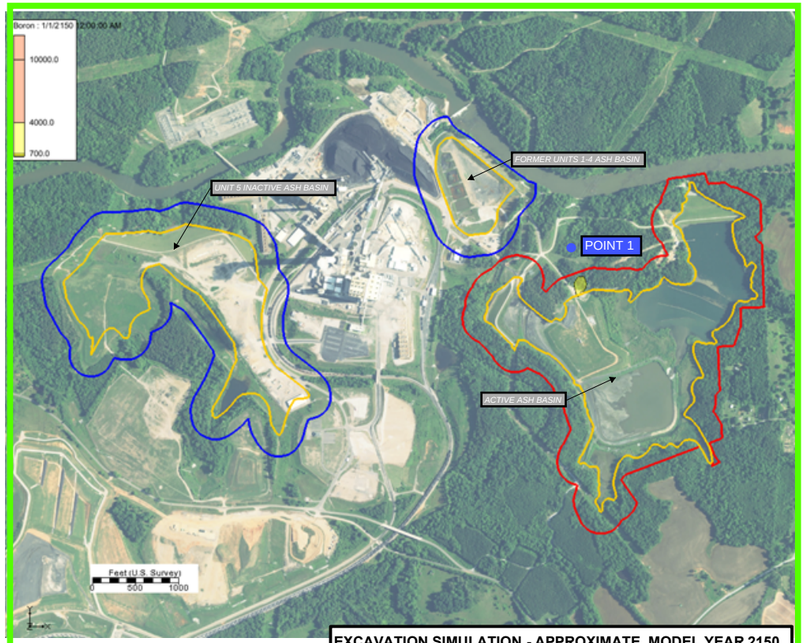

EXCAVATION SIMULATION - APPROXIMATE MODEL YEAR 2150

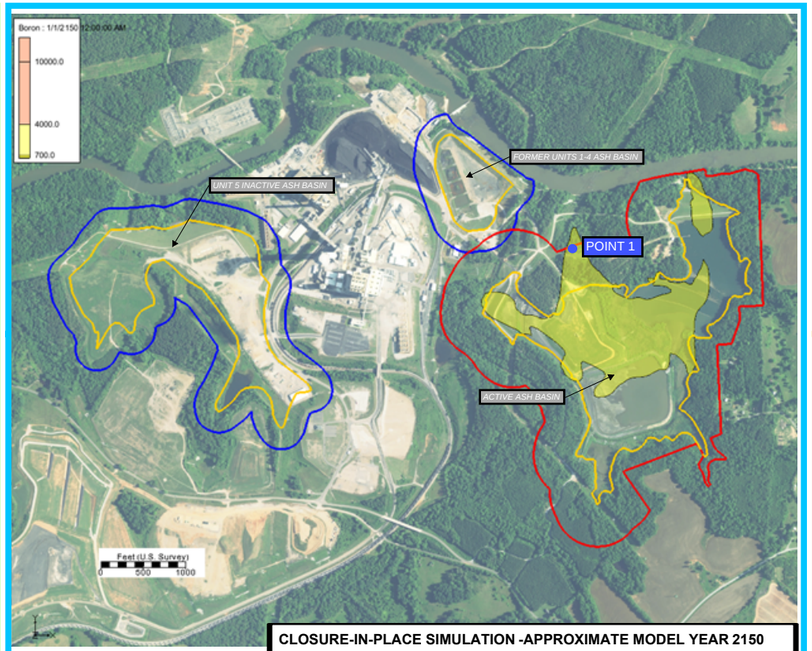

CLOSURE-IN-PLACE SIMULATION -APPROXIMATE MODEL YEAR 2150

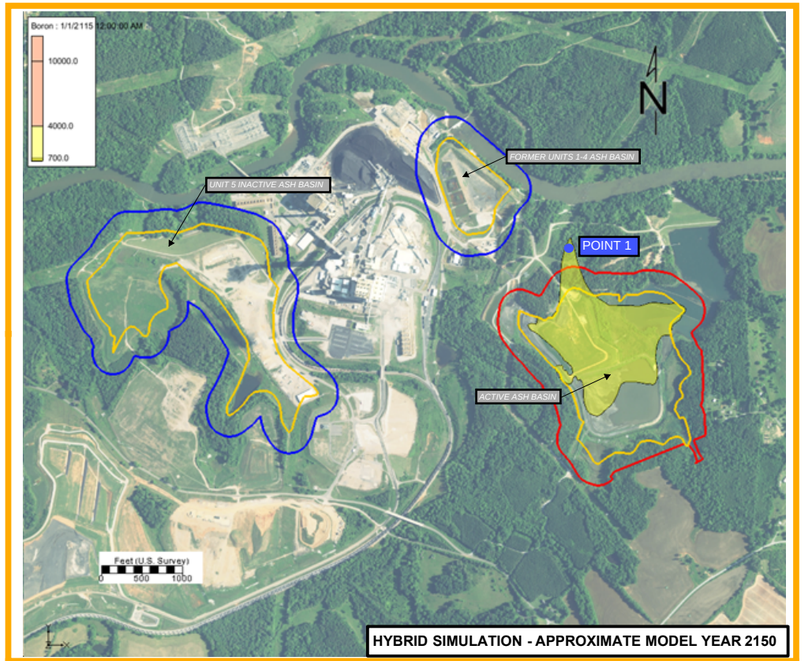

HYBRID SIMULATION - APPROXIMATE MODEL YEAR 2150

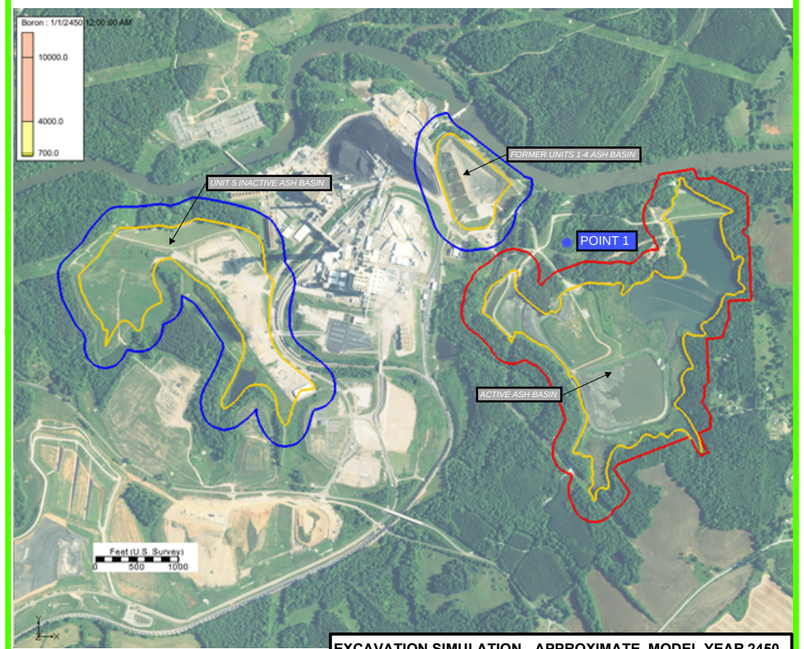

EXCAVATION SIMULATION - APPROXIMATE MODEL YEAR 2450

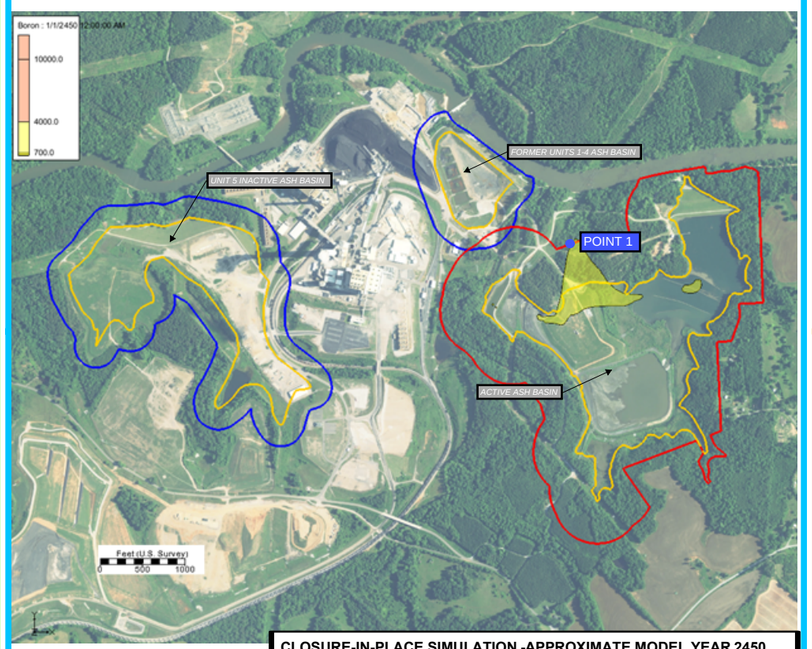

CLOSURE-IN-PLACE SIMULATION -APPROXIMATE MODEL YEAR 2450

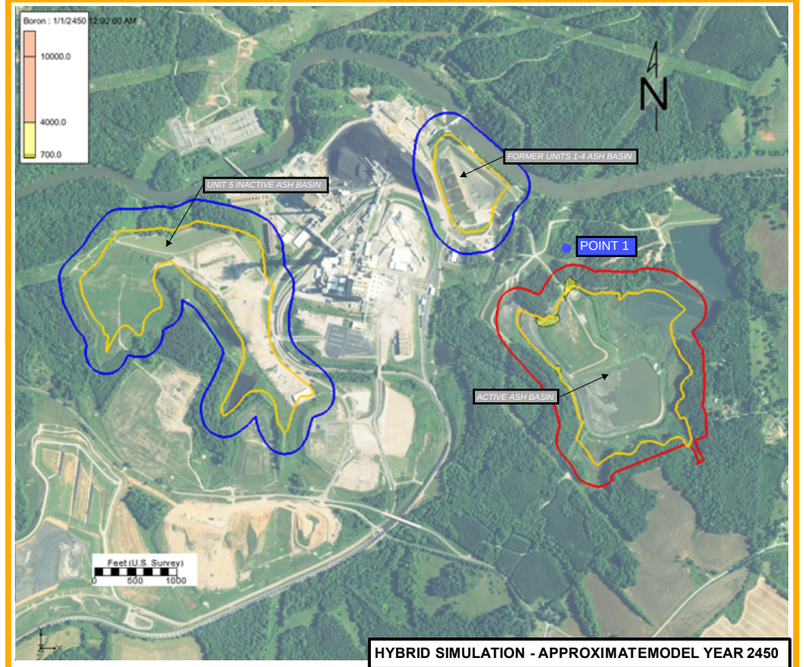

HYBRID SIMULATION - APPROXIMATEMODEL YEAR 2450

LEGEND

- BORON CONCENTRATION RANGE (4,000 - 10,000 µg/L)
- BORON CONCENTRATION RANGE (700 - 4,000 µg/L)
- ACTIVE & INACTVE ASH BASIN WASTE BOUNDARY
- POTENTIAL ACTIVE ASH BASIN COMPLIANCE BOUNDARY
- POTENTIAL INACTIVE ASH BASIN COMPLIANCE BOUNDARY

NOTES:

1) THE MODELED TIME TO RETURN TO COMPLIANCE WITH 2L GROUNDWATER STANDARDS IS APPROXIMATELY 50 TO 100 YEARS FOR THE EXCAVATION SIMULATION AND APPROXIMATELY 400 TO 500 YEARS FOR THE CLOSURE-IN-PLACE SIMULATION USING BORON IN THE TRANSITION ZONE AS THE BASIS FOR THE ESTIMATE. FORMER UNITS 1-4 ASH BASIN IS EXCAVATED IN ALL SIMULATIONS.
2) TRANSITION ZONE RESULTS SHOWN SINCE THIS REPRESENTS THE MOST TRANSMISSIVE ZONE.
3) THREE CLOSURE-SPECIFIC COMPLIANCE BOUNDARIES WERE USED TO EVALUATE THE RESULTS:
   a) EXCAVATION SIMULATION IS EVALUATED USING A COMPLIANCE BOUNDARY THAT IS 250 FT FROM THE CURRENT WASTE BOUNDARY.
   b) CLOSURE-IN-PLACE IS EVALUATED USING A COMPLIANCE BOUNDARY THAT IS 250 FT FROM THE CURRENT WASTE BOUNDARY FOR BASINS WITHOUT NPDES PERMITS.
   c) CLOSURE-IN-PLACE SIMULATION IS EVALUATED USING A COMPLIANCE BOUNDARY THAT IS 500 FT FROM THE CURRENT WASTE BOUNDARY FOR THE ACTIVE ASH BASIN.
   d) HYBRID SIMULATION IS EVALUATED USING A COMPLIANCE BOUNDARY 250 FT FROM THE FINAL WASTE BOUNDARY.
4) THE THREE MODEL SIMULATIONS ARE BASED ON THE COMPLETION DATES FOR THOSE ACTIVITIES. THESE DATES ARE:
   EXCAVATION - YEAR 2030
   CLOSURE-IN-PLACE - YEAR 2022
   HYBRID - YEAR 2022
5) SEE FIGURE 2 FOR TIME VS. CONCENTRATION PLOTS OF BORON AT POINT 1.
6) CLOSURE-IN-PLACE EXTENT AND HYBRID WASTE BOUNDARY PROVIDED BY WOOD PLC.
7) AERIAL PHOTOGRAPHY OBTAINED FROM DIGITALGLOBE VIA ESRI ARCGIS ONLINE. IMAGE COLLECTED ON APRIL 1, 2017.
8) DRAWING HAS BEEN SET WITH A PROJECTION OF NORTH CAROLINA STATE PLANE COORDINATE SYSTEM FIPS 3200 (NAD83).

RESPONSE TO ITEM 5 - FIGURE ES-1
SIMULATED BORON CONCENTRATIONS
TRANSITION ZONE
EXCAVATION, CLOSURE-IN-PLACE, AND HYBRID SIMULATIONS
CLIFFSIDE STEAM STATION
DUKE ENERGY CAROLINAS, LLC
MOORESBORO, NORTH CAROLINA

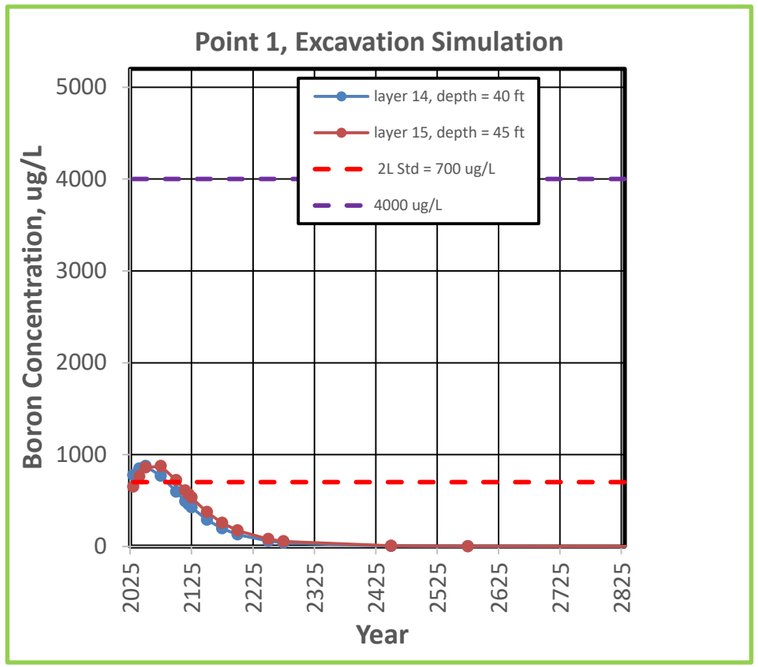

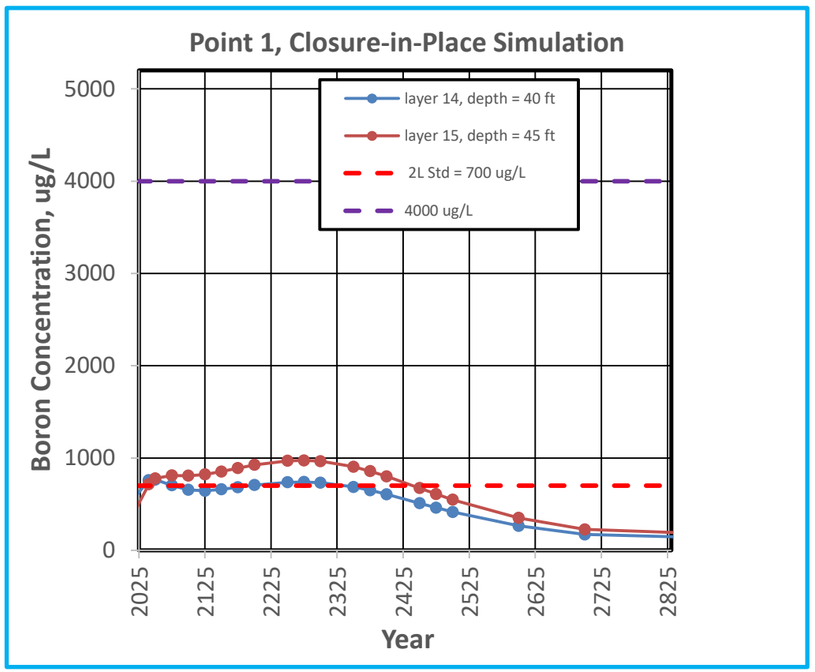

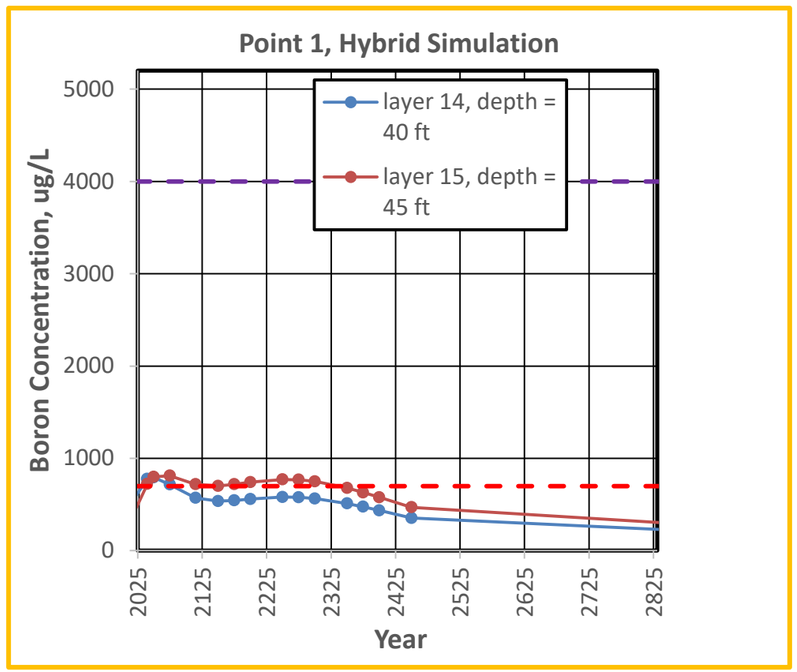

NOTES:
THE START DATES FOR THE THREE MODEL SIMULATIONS ARE BASED ON THE COMPLETION DATES FOR THOSE ACTIVITIES.
THESE DATES ARE:

- EXCAVATION – YEAR 2030
- CLOSURE – IN-PLACE – YEAR 2022
- HYBRID – YEAR 2023

TRANSITION ZONE RESULTS SHOWN

FIGURE ES-2
BORON TIME VS. CONCENTRATION PLOTS
TRANSITION ZONE
EXCAVATION, CLOSURE-IN-PLACE, AND HYBRID SIMULATIONS
CLIFFSIDE STEAM STATION
DUKE ENERGY CAROLINAS, LLC
MOORESBORO, NORTH CAROLINA

P:\Duke Energy Progress.1026\500.Client Attorney Privilege\DEQ August 1 Letter - Responses\Item 5\Cliffside\Figure 2 - Response to Item 5_Cliffside.pptx

1.0 INTRODUCTION

Duke Energy Carolinas, LLC (Duke Energy) owns and operates the Rogers Energy Complex; henceforth referred to as the Cliffside Steam Station (CSS), or the Site, which is located in Mooresboro, Rutherford and Cleveland Counties, North Carolina. The CSS began operation in 1940 as a coal-fired generating station with a capacity of 198 MW from Units 1-4. The CSS was expanded to 754 MW in 1972 when Unit 5 was commissioned. Unit 6 went on-line in 2012. Units 1 through 4 were retired in October 2011, and currently only Units 5 and 6 are in operation at the CSS with a current generating capacity of 1,381 MW. The coal ash residue and other liquid discharges from coal combustion processes at the CSS have historically been managed in the CSS ash basins, which consist of the active ash basin, the Former Units 1-4 ash basin, and the Unit 5 inactive ash basin. Discharge from the active ash basin is currently permitted by the North Carolina Department of Environmental Quality (NCDEQ) Division of Water Resources (DWR) under National Pollutant Discharge Elimination System (NPDES) Permit NC0005088. Duke also operates a Coal Combustion Products (CCP) Industrial Landfill (CCP Landfill) in accordance with the North Carolina Department of Environmental Quality (NCDEQ) Solid Waste Sections (SWS) on the property. Preliminary numerical simulations of groundwater flow and transport have been calibrated to current conditions and used to evaluate different scenarios being considered as options for closure of the ash basin. The methods and results of those simulations are described in this report.

1.1 General Setting and Background

The CSS is located in the Piedmont region of North Carolina. The area surrounding the CSS generally consists of residential properties, undeveloped land, and the Broad River (Figure 1-1). The CSS site occupies approximately 1,000 acres. The CSS is situated between the Broad River to the north and McCraw Road (Duke Power Road) to the south, with additional land south of Duke Power Road where the CCP Landfill is located. The CCP Landfill is located south of Duke Power Road and northeast of the intersection of Old U.S. Highway 221A and Ballenger Road. The Former Units 1-4 ash basin is located immediately east of the Former Units 1-4 and northeast of Unit 6 along the Broad River (Figure 1-1). The Unit 5 inactive ash basin is located west and southwest of Unit 5 and Unit 6 (Figure 1-1). The active ash basin is located east of Unit 6 and the ash storage area is located just north of the active ash basin (Figure 1-1).

The topography in the area is hilly with approximate high elevations of 856 feet southwest of the Unit 5 inactive ash basin, 848 feet west of Unit 5 inactive ash basin, and 832 feet southwest of the active ash basin. The low elevation is approximately 664 feet at the interface with the Broad River on the northern extent of the site. The elevation of the Broad River is approximately 656 feet in the vicinity of the Site and the river flows from west to east. Overall topography generally slopes from south-to-north towards the Broad River. Surface water drainage generally follows site topography and flows from the south to the north across the Site except where natural drainage patterns have been modified by the ash basin or other construction. Suck Creek, located between the active ash basin and the Former Units 1-4 ash basin and CSS Plant, transects the Site generally from south to north and discharges to the Broad River. Unnamed drainage features are located near the western and eastern edges of the Site and generally flow north to the Broad River. The approximate pond elevation for the active ash basin is 762 feet.

The CSS began commercial operations in July 1940 with Units 1 through 4. Unit 5 began operations in 1972. Construction of Unit 6 began in 2008 and began commercial operations in 2012. Units 1 through 4 were retired from service in October 2011, and Units 5 and 6 continue to operate and use the active ash basin. Unit 5 currently operates with dry bottom ash and dry fly ash handling. Unit 6 operates with dry bottom ash and dry fly ash handling. The CSS ash basin system consists of an active ash basin, the Former Units 1-4 ash basin, and the Unit 5 inactive ash basin. The ash storage area is located north of the active ash basin.

The Former Units 1-4 ash basin was constructed in 1957 and began operations the same year. The Former Units 1-4 ash basin was retired in 1977 once it reached capacity. Stormwater ponds were constructed on top of the Former Units 1-4 ash basin and were operated until the basin was excavated in 2017.

The Unit 5 inactive ash basin was constructed in 1970 (in advance of Unit 5 operations) and received sluiced ash from Unit 5 starting in 1972. The ash basin was retired in 1980 when it reached full capacity. The Unit 5 inactive ash basin is currently covered with a layer of topsoil with stable vegetation and is used as a laydown yard for the CSS site. The Unit 5 inactive ash basin currently receives stormwater from a localized drainage area. The stormwater is discharged out of NPDES stormwater outfall SW009.

The active ash basin was constructed in 1975 and began receiving sluiced ash from Unit 5 that same year. The ash basin expanded in 1980 to its current footprint. An unlined dry ash storage area is located north of the active ash basin. The ash storage area was likely created when ash was removed from the active ash basin in the 1980s to provide additional capacity for sluiced ash. An area east of the ash storage area may be a spoils area remnant of soil from embankment dam construction. The active ash basin receives waste water inflows from Units 5 and 6, however, the active ash basin has not received ash since April 2018 which is dry handled and disposed of in the onsite CCP landfill. The active ash basin is an integral part of the CSS site's wastewater treatment system and historically received inflows from the ash removal system, station yard drain sump, stormwater flows, station wastewater, and other permitted discharges. Inflows to the active ash basin are variable based on Unit 5 and Unit 6 operations.

Duke Energy operates the CCP Landfill in accordance with the NCDEQ Industrial Solid Waste Permit No. 81-06. The CCP landfill is constructed with an engineered liner and leachate collection system. The CCP landfill is permitted to receive fly ash, bottom ash, boiler slag, coal mill rejects/pyrites, flue gas desulfurization sludge, gypsum, leachate basin sludge, non-hazardous sandblast material, limestone, lime, ball mill rejects, coal carbon, sulfur pellets, cation and anion resins, sediment from sumps, cooling tower sludge, filter bags, conditioning agents (e.g. lime kiln dust), soil material that contains any of the above material and soil used for operations, incidental amounts of geotextile used in the management of the CCP's, and vacuum truck waste.

The subsurface at the Site is composed of residual soil/saprolite, a transition zone, and bedrock. Typically, the residual soil/saprolite is partially saturated and the water table fluctuates within it. Water movement is generally preferential through the weathered/fractured and fractured bedrock of the transition zone (i.e., enhanced permeability zone). Groundwater within the Site area exists under unconfined, or water table, conditions within the saprolite, transition zone and in fractures and joints of the underlying bedrock. The shallow water table and bedrock water-bearing zones are interconnected. The saprolite, where saturated thickness is sufficient, acts as a reservoir for supplying groundwater to the fractures and joints in the bedrock. Shallow groundwater generally flows from local recharge zones in topographically high areas, such as

ridges, toward groundwater discharge zones, such as river/stream valleys. Groundwater flow in the vicinity of the CSS site is generally in a northern direction towards the Broad River.

The groundwater flow and transport model for the CSS site has been under development since late 2017. The original CSS groundwater flow and transport model was completed in December 2015 (HDR, 2015) and revised in March 2016 (HDR, 2016). The present model domain has been greatly expanded in the horizontal direction compared to the 2015 model, and the number of model layers in the vertical direction has been increased from 9 to 28. The earlier model was calibrated to hydraulic heads and COI concentrations measured in 2015. Since that time, significant site activities have taken place including the installation of many additional monitoring wells. The current model has been accordingly revised with respect to the 2015 model. These additional data have further improved the predictive capability and reduce uncertainty in the model results. To take advantage of this potential, the model was recalibrated using data from both the new and existing groundwater wells.

The following data sources were used during calibration of the revised groundwater flow and fate and transport model:

- Average site-wide water levels measured in CAMA/CCR/Compliance groundwater monitoring wells through April 2018.
- Groundwater quality data obtained from CAMA/CCR/Compliance sampling events conducted in April 2018.
- Surface water elevations, as described in the CSA Update report (SynTerra, 2018).
- Surface water elevations from October 2018 survey
- Estimated recharge, as described in the CSA Update report (SynTerra, 2018).

The study consists of three main activities: developing a calibrated steady-state flow model of current conditions, developing historical transient model of boron transport that is calibrated to current conditions, and performing predictive simulations of the possible closure actions at the CSS site. The predictive simulations include consideration of a complete excavation closure scenario, a final cover closure scenario, and a hybrid closure scenario.

Excavation of the Former Units 1-4 ash basin was completed in early 2017 and the CCR materials were transferred to the CCP Landfill. The complete excavation scenario includes

excavating the active ash basin, ash storage area, and Unit 5 inactive ash basin and transporting the CCR material to the onsite CCP landfill for disposal.

The final cover scenario includes modifications to the Unit 5 inactive ash basin and the active ash basin. A low permeability cap will be built on the entire Unit 5 inactive ash basin. In the active ash basin, portions of the basin will be excavated and other portions will be covered with a low permeability cap. In the active ash basin CCR material will be excavated from the northeastern portion of the basin (south of the downstream dam), from behind the up-gradient dam in the western portion of the basin near Suck Creek, from the southern finger regions of the basin, and from the ash storage area. The CCR material will be stacked in the interior of the active ash basin and the excavated regions will be regraded with fill material. The downstream dam will be lowered by approximately 10 to 30 feet and graded to slope to the east. A low permeability cap will be built on the ash stack in the active ash basin and a drainage system will be built surrounding the ash stack. The drainage system is designed to flow from the northwest of the active ash basin at the upstream dam and from the southwest of the active ash basin towards the regraded downstream dam to the Broad River.

The hybrid closure scenario reduces the footprint of the active ash basin similar to the final cover scenario, however the downstream dam will be fully removed and the upstream dam will be lowered by 20 feet.

1.2 Study Objectives

The overall objective of the groundwater flow and transport modeling effort is to predict the performance of three closure scenarios. The goal is for these predictions to guide decisions during the selection of closure actions. The flow and transport models have been undergoing a process of continuous improvement and refinement by including new field data. The continuous improvement process is designed to increase the accuracy and reliability of the performance predictions.

The objective of this model is to describe a subset of the overall results of simulations of boron transport in saprolite, the transition zone, and the underlying fractured rock. The predictive simulations shown here are not intended to represent a final detailed closure design. These simulations use conceptual designs that are subject to change as the closure plans are

finalized. The simulations are intended to show the key characteristics of groundwater flow and mobile constituent transport that are expected to result from the closure actions. Model simulations and the results presented do not include any active form of groundwater remediation. The relative benefits of various groundwater remediation alternatives will be addressed in the CAP.

2.0 CONCEPTUAL MODEL

The Site conceptual model for the CSS Site is primarily based on the 2015 Comprehensive Site Assessment (CSA) report (HDR, 2015a), and the 2018 CSA Update (2018, CSA) for the CSS (SynTerra, 2018). The 2018 CSA Update report contains extensive detail and data related to most aspects of the Site conceptual model that are used here.

2.1 Aquifer System Framework

The groundwater system at the Site consists of an unconfined aquifer. Depending on the local topography and hydrogeology, the water table surface may exist in the saprolite, the transition zone, or in the fractured bedrock. At some isolated locations along streambeds, the upper units (saprolite and transition zone) are absent. At other locations, the upper units may be unsaturated, with the water table located in deeper units (fractured bedrock).

The hydraulic conductivity at the CSS site has been measured in a series of slug tests in the different hydrologic units. Eighteen (18) slug tests were performed in the coal ash, with conductivities ranging from 0.14 feet/day (ft/d) to 108 ft/d. Fifty-one (51) slug tests performed in saprolite wells yielded hydraulic conductivities ranging from 0.28 ft/d to 42.5 ft/d. Ninety-nine (99) slug tests performed in the transition zone wells gave results ranging from 0.0007 ft/d to 45.4 ft/d. Thirty-eight (38) slug tests conducted in bedrock wells gave hydraulic conductivity values ranging from 0.001 ft/d to 126 ft/d. It should be noted that the bedrock wells are screened near the top of the bedrock surface, and the conductivity of the deeper bedrock would be expected to be lower. The range of observed conductivity in the transition zone and bedrock wells (from nearly zero to 126 ft/d) highlights the very large degree of heterogeneity in the multi-unit system.

2.2 Groundwater Flow System

The unconfined groundwater system at the CSS is dominated by flow towards the Broad River north of the ash basins, and towards Suck Creek, which flows in a north easterly direction between the Unit 5 inactive ash basin and the active ash basin. A groundwater ridge exists south of Suck Creek, and approximately follows the topography along Prospect Church Road and Fox Place Road (Figure 1-1).

The groundwater system is recharged from infiltrating rainwater, and from water that infiltrates from the active ash basin pond. The average value of recharge in the vicinity of the CSS was estimated at 7.5 inches per year. The North Carolina map of recharge by Haven (2003) does not show values for Cleveland County, but the average value in adjacent counties is consistent with this estimate. A reduced rate of recharge (0.004 inches per year) was assumed for the power plant and large buildings, and an infiltration rate of zero was assumed for the Broad River and Suck Creek. An infiltration rate of zero was also used in the pond areas of the active ash basin. The capped areas of the CCP Landfill was assigned very low infiltration rate of 0.00054 in/yr based on results from landfill cover simulations.

There are 77 private water wells that have been identified within one-half mile of the three ash basins' compliance boundaries (SynTerra, 2018). Most of these wells are located east and south of the active ash basin, and west of the CCP landfill. Pumping rates for the private wells were not available, and completion depths were only available for a few wells. Sixteen private water wells were not included in the model boundary because they are located north of the Broad River which is a hydrological boundary.

2.3 Hydrologic Boundaries

The major discharge features for the shallow water system serve as hydrologic boundaries to the shallow groundwater system. The Broad River, Suck Creek and smaller drainages in the region of the CSS serve as the major hydrologic boundaries in the area.

2.4 Hydraulic Boundaries

The shallow groundwater system does not appear to contain impermeable barriers or boundaries in the study area, but it does include hydraulic boundaries between zones of different hydraulic conductivity. The degree of fracturing, and thus the hydraulic conductivity, is expected to decrease with depth in metamorphic rock. This will result in blocks of unfractured rock where the hydraulic conductivity is quite low to negligible. However, isolated fractures may occur that result in large local hydraulic conductivities, and the locations of these fractures is difficult to predict or to comprehensively map. It was assumed that the rock was impermeable below the depth of the bottom modeled layer, and a no-flow boundary was used to represent this condition.

2.5 Sources and Sinks

Ash pore water seepage out of the active ash basin and areal recharge (rainfall infiltration) are sources of water to the groundwater system. Groundwater discharges to the Broad River, Suck Creek, and other small drainages. Private water wells within the model area remove only a small amount of water from the overall hydrologic system.

2.6 Water Budget

Over the long term, the rate of water inflow to the study area is equal to the rate of water outflow from the study area. Water enters the groundwater system from the active ash basin pond and recharge. Water leaves the system through discharge to the Broad River, Suck Creek, and other small drainages and through private wells.

2.7 Modeled Constituents of Interest

Arsenic, boron, chromium, hexavalent chromium, cobalt, iron, manganese, pH, strontium, sulfate, thallium, TDS, vanadium, total uranium, and radium have been identified as constituents of interest (COIs) for groundwater at the CSS (SynTerra, 2018).

The COIs that were initially selected for modeling at the CSS were boron, sulfate, and TDS. Boron is the best (most conservative, or proxy) constituent for tracking historical and future plume migration because it is almost always present in plumes from CCR releases at concentrations higher than background. Boron is also not subject to appreciable chemical attenuation under normal aquifer conditions (low reactivity, low K_d).

Boron is present in the active ash basin, Unit 5 inactive ash basin, ash storage area and beneath the Former Units 1-4 ash basin. Dissolved boron is found below all ash basins and the ash storage area. Boron is found in monitoring wells screened in the saprolite, the transition zone, and the bedrock. Boron concentrations in background monitoring wells are below 2L standards, and less than the laboratory detection limit. Other conservative constituents have similar K_d values but are not present in large concentrations in the source area or are present naturally in regional groundwater. Attenuation for these conservative COIs primarily occurs through physical means (i.e., dispersion, dilution, and diffusion). This preliminary model report will focus exclusively on boron because boron is the dominant mobile constituent.

The remaining COIs were not considered for the modeling exercise for one or more of the following reasons: 1) concentrations in the ash pore water do not greatly exceed background levels; and 2) there is no discernable plume of the constituent extending downgradient from the ash basin. The reactive, non-conservative parameters subject to chemical attenuation have relatively high K_d (i.e., greater than 10 L/kg) under all probable pH and E_H conditions at the CSS. The relatively high K_d values are due to sorption, ion exchange, and (co)precipitation. Therefore, their migration potential is significantly limited, meaning that the plume is small and sometimes discontinuous.

2.8 Constituent Transport

The COIs that are present in the coal ash dissolve into the ash pore water. As water infiltrates through the ash, water containing COIs can enter the groundwater system. Once in the groundwater system, the COIs are transported by advection and dispersion and are subject to retardation due to sorption to solids. If the COIs reach a hydrologic boundary or water sink, they are removed from the groundwater system, and they enter the surface water system, where in general, they are greatly diluted.

3.0 COMPUTER MODEL

3.1 Model Selection

The numerical groundwater flow model was developed using MODFLOW (McDonald and Harbaugh, 1988), a three-dimensional (3D) finite difference groundwater model created by the United States Geological Survey (USGS). The chemical transport model is a new version the Modular 3-D Transport Multi-Species (MT3DMS) model (Zheng and Wang, 1999). MODFLOW and MT3DMS are widely used in industry and government, and are considered to be industry standards. The models were assembled using the Aquaveo GMS 10.3 graphical user interface (http://www.aquaveo.com/).

3.2 Model Description

MODFLOW uses Darcy's law and the conservation of mass to derive water balance equations for each finite difference cell. MODFLOW considers 3D transient groundwater flow in confined and unconfined heterogeneous systems, and it can include dynamic interaction with pumping wells, recharge, evapotranspiration, rivers, streams, springs, lakes, and swamps.

This study uses the MODFLOW-NWT version (Niswonger, et al., 2011). The NWT version of MODFLOW provides improved numerical stability and accuracy for modeling problems with variable water tables. That improved capability is helpful in the present work where the position of the water table in the ash basin can fluctuate depending on the conditions under which the basin is operated and the various closure scenario simulations.

Some of the flow models were challenging to run due to the topography and layers that become unsaturated in the model. It was found that using the NWT solver options "MODERATE" with the xMD matrix solver could overcome these difficulties.

MT3DMS uses the groundwater flow field from MODFLOW to simulate 3D advection and dispersion of the dissolved COIs including the effects of retardation due to COI adsorption on the soil and rock matrix.

4.0 GROUNDWATER FLOW AND TRANSPORT MODEL CONSTRUCTION

The flow and transport model for this site was built through a series of steps.

- Step 1: Build a 3D model of the Site hydrostratigraphy based on field data.
- Step 2: Determine the model domain and construction of the numerical grid.
- Step 3: Populate the numerical grid with flow parameters
- Step 4: Calibrate the steady-state flow model to current hydraulic heads with adjustments of the flow parameters
- Step 5: Develop a transient model of historical flow and transport to provide time-dependent constituent transport development.
- Step 6: Calibration to recent boron concentration field data to ensure the model reproduces the observed boron plumes.

The process of revising the model involved using the initial updated model as a starting point and following an iterative process of adjusting parameters until the model adequately predicted the observed heads and concentrations.

4.1 Model Domain and Grid

The initial steps in the model grid generation process were the determination of the model domain, and the construction of a 3D hydrostratigraphic model. The model has dimensions of about 13,900 ft. by 9,400 ft. and it is oriented in a North-South orientation. (Figure 4-1). The model is generally bounded to the north by the Broad River, and to the east by Ashworth Creek. The distance to the boundary from the ash basin is large enough to prevent boundary conditions from artificially affecting the results near the basin.

The ground surface of the model was developed by HDR and was interpolated from the North Carolina Floodplain Mapping Program's 2010 Light Detection and Ranging (LiDAR) elevation data. These data were supplemented by on-site surveys conducted by Duke Energy in 2014. The elevations used for the top of the ash surface in the active ash basin and Unit 5 inactive ash basin were modified from the bathymetric data to provide a model surface that can accommodate planned regrading of ash for the final cover or hybrid closure options. For current

conditions simulations, the part of the ash in the model that is above the current ash surface elevation is given a large hydraulic conductivity.

The hydrostratigraphic model (called a solids model in GMS) consists of five units: ash, saprolite, transition zone, upper fractured bedrock, and deeper bedrock. The contact elevations between these units were determined from boring logs from previous studies by HDR (2015a, 2016). The contact elevations were estimated by HDR for locations where well logs were not available by extrapolation of the borehole data using the Leapfrog Hydro geologic modeling tool. This program was used by HDR to develop surfaces defining the top of the saprolite, transition zone, and bedrock. While the contact between the upper units (ash, saprolite, transition zone, bedrock) are well defined, the division of the bedrock into an upper fractured zone and deeper bedrock was subjective. For the purposes of model construction, the upper fractured zone is approximately 100 feet thick. The deeper bedrock extends another 450 feet below the upper zone for a total bedrock thickness of 550 feet in the model. The upper bedrock zone in the model was given a heterogeneous hydraulic conductivity distribution to represent more and less fractured zones.

Figure 4-2 shows a fence diagram of the 3D hydrostratigraphic unit viewed from the northwest, with a vertical exaggeration of 5x. The light grey material corresponds to the ash in the basins, the light orange material is the saprolite, the red material is the transition zone, the light purple material is the upper fractured part of the bedrock, and the black material is the deep bedrock.

The numerical model grid is shown in Figure 4-3. The grid is discretized in the vertical direction using the solids model (Figure 4-2) to define the numerical model layers. The top 8 model layers represent the active ash basin, including the dams that form the active ash basin, and the CCP Landfill. Model layers 9-13 represent the saprolite. Model layer 14-16 represents the transition zone. Model layers 16-22 represent the upper fractured part of the bedrock, while model layers 23 to 28 represent deeper parts of the bedrock (which also may be fractured). Model layer 16 represents some areas that have both transition zone and fractured bedrock characteristics. The model varies in thickness from about 600 ft. to 650 ft.

The discretization in the horizontal direction is variable with smaller grid cells in and around the ash basin area. The minimum horizontal grid spacing in the finely divided areas is

about 30 ft., while the maximum grid spacing near the outer edges of the model is about 160 ft. The grid contains a total of 766,371 active cells in 28 layers.

4.2 Hydraulic Parameters

The horizontal hydraulic conductivity and the horizontal to vertical hydraulic conductivity anisotropy ratio are the main hydraulic parameters in the model. The distribution of these parameters is based primarily on the model hydrostratigraphy, with additional horizontal and vertical variation. Most of the hydraulic parameter distributions in the model were heterogeneous across a model layer. The geometries and parameter values of the heterogeneous distributions were determined during the flow model calibration process. Initial estimates of parameters were based on literature values, results of slug and core tests, and simulations performed using a preliminary flow model. The hydraulic parameter values were adjusted during the flow model calibration process described in Section 5.0 to provide a best fit to observed water levels in observation wells. Slug test data from wells at the Duke Energy coal ash basin sites in North Carolina are shown in Figures 4-4 through 4-7.

The hydraulic conductivity of coal ash measured at 14 sites in North Carolina ranges over about 4 orders of magnitude, with a median value of about 1.6 ft/d (Figure 4-4). Ash hydraulic conductivity values measured in slug tests at the CSS ranged from 0.14 ft/d to 108 ft/d. The current conditions flow model is insensitive to the ash conductivity, but the predicted heads in the final cover simulations are sensitive to the ash hydraulic conductivity. In late 2018, three pumping tests were conducted within the active ash basin including the underlying saprolite and in the ash material within the basin to help refine the value of these unit specific parameters. Results of these tests are expected to yield an estimate of the ash properties that is more representative of site conditions. The simulations will be revised when the data from the pumping tests have been evaluated. Results from the revised simulations will be presented in future versions of the flow and transport model.

The hydraulic conductivities from hundreds of slug tests performed in saprolite wells at 10 Piedmont sites are shown in Figure 4-5. These also range over 4 or more orders of magnitude, and have a median value of 1.0 ft/d. Saprolite slug tests performed at the CSS ranged from 0.28 ft/d to 42.5 ft/d. Transition zone hydraulic conductivities from hundreds of slug tests

at 10 Piedmont sites are shown in Figure 4-6. These range over 6 orders of magnitude, with a median value of 0.97 ft/d. The measured values at the CSS range from 0.0007 ft/d to 45.4 ft/d.

Slug test results from bedrock from hundreds of wells at 10 Piedmont sites in North Carolina (Figure 4-7) range over more than 6 orders of magnitude, with a median value of 0.5 ft/d. It is possible that this median value is larger than the true average value for bedrock for three reasons. First, the bedrock wells are almost all screened in the uppermost few tens of feet of the bedrock, which is expected to be more highly fractured than deeper bedrock zones. Second, the wells are normally screened in zones with visible flowing fractures, rather than in zones with intact unfractured rock. Finally, wells that do not produce water are not slug tested. These factors likely bias the slug test data to higher values than may be representative of the bedrock as a whole. At the CSS, the measured values from slug tests in shallow bedrock ranged from 0.001 ft/d to 126 ft/d.

4.3 Flow Model Boundary Conditions

The Broad River forms a hydraulic boundary north of the ash basins. The river is treated as a highly conductive general head boundary in the uppermost active model layer with an elevation ranging from approximately 665 ft. to 655 ft. Suck Creek is located between the power plant and active ash basin and is treated as a general head boundary. The specified water elevations here range from a maximum of 767 ft. in the southern part of Suck Creek, to 658 ft where it enters the Broad River.

The eastern part of the model is bounded by Ashworth Creek which is simulated as a drain. Ashworth Creek flows from the south and discharges into the Broad River.

The southern model boundary does not align with any clearly defined hydraulic features. This boundary is located almost a mile from the ash basin, and there is a major groundwater divide between the model boundary and the active ash basin. Part of the southern model boundary is treated as a general head boundary with the head set to an elevation of 30 feet below the ground surface, except in stream valleys, where a no flow boundary is used perpendicular to the streams. The flow in these valleys is dominated by flow towards the streams, which are modeled as drains. The western boundary is treated as a general head boundary with the head set 30 feet below the ground surface, and as a no flow boundary as it crosses several creeks

approximately perpendicular to the streams, which are treated as drains in the model. This boundary is approximately a ½ mile away from the Unit 5 inactive ash basin.

4.4 Flow Model Sources and Sinks

The flow model sources and sinks consist of the Broad River and Suck Creek, the active ash basin pond, Ashworth Creek, recharge, streams, water supply wells, and wet areas that are assumed to directly drain into the active ash basin pond.

Recharge is a significant hydrologic parameter in the model, and the distribution of recharge zones in the model is shown in Figure 4-8. As described in Section 2.2, the recharge rate for the CSS Site was estimated to be 7.5 inches/year. The recharge rate for the CSS Plant was set to 0.004 inch per year due to the large areas of roof and pavement. The active ash basin pond and sluicing channel are treated as general head boundaries and have zero rainfall recharge, but part of the southern active ash basin has an increased rate of 14 inches per year to simulate sluicing which was terminated in April 2018. The recharge rate in the dams were set to 2 inches per year. The recharge rate through the CCP Landfill was set to 0.00054 inches per year based on landfill cover simulations.

The Broad River, Suck Creek, and the active ash basin ponds were treated as general head zones in the model (Figures 4-9 and 4-10). The northern active ash basin pond is maintained at an elevation of 759.4 ft. and the southern active ash basin has a head elevation of 765 ft. Suck Creek ranges from an elevation of 767 ft. in the upstream part of Suck Creek to an elevation of 658 ft. at the confluence of Suck Creek and the Broad River. The Broad River ranges from an elevation of 664.8 ft. at the western border of the model to 653.7 ft. at the eastern border of the model.

The many creeks exert a significant local control on the hydrology in the model. These features are shown as green lines in Figure 4-9. The position of these creeks was determined mainly from the topographic map (Figure 1-1), supplemented by a site visit where a survey of drainage features near the ash basins and various creeks onsite was conducted. The elevation of locations along the creeks were determined from either the surface LiDAR elevations or survey data, and were assumed to be 2 feet below the ground surface. The creeks were simulated using the DRAIN feature in MODFLOW with a high conductance value (100 $ft^2/d/ft$).

The southern part of the active ash basin contains several areas of standing water and was modeled as wetland area using the DRAIN feature. (Figure 4-10). The ash basin upstream dam contains a one main waste water channel (former sluicing channel) at an approximate elevation of 766 feet, and this is included in the model as a general head (Figure 4-9).

Figure 4-11 shows the location of private water supply wells in the model area. There are no public supply wells that were identified within a 0.5 mile radius of the ash basin compliance boundary (SynTerra, 2018).

There are 77 private wells inside the model boundary. This number is larger than the 71 wells that were identified within a 0.5 mile radius of the ash basin compliance boundary (SynTerra, 2018) due to the fact that the model extends about a mile beyond the ash basin waste boundary. Where depth data were available, the private wells were represented as screened over the known depth. In most cases, the well depths were unknown, and the wells were assumed to be screened in the upper part of the transition zone and/or fractured bedrock in model layers 14-16. The pumping rates from the wells were unknown, but the model simulated a pumping rate of +280 gals/day, which is an average water use for a family of four (Treece et al. 1990; North Carolina Water Use, 1987, and 1995). Septic return was assumed to be 94% of the pumping rate, based on Treece et al. (1990), Daniels et al. (1997) and Radcliffe et al. (2006). The septic return was injected into layer 14 in the model.

4.5 Flow Model Calibration Targets

The steady state flow model calibration targets were the 249 water level measurements made in observations wells in the 2nd quarter of 2018. These wells include wells screened in each of the hydrostratigraphic units, including many sets of nested wells. Wells not included in the calibration were classified as a ‘dry’ or a ‘did not produce’ well.

4.6 Transport Model Parameters

The transport model uses a MODFLOW simulation to provide the groundwater velocity field. The MODFLOW simulation reflects post-1975 flow conditions at the active ash basin, where Suck Creek has been rerouted, and the original channel has been dammed to form the ash basin. The flow model has transient changes that reflect the start and end of operation of the Unit 5 inactive ash basin and capping of the CCP Landfill. The transport model begins in 1957,

with the Former Units 1-4 ash basin serving as the only source of boron in the model. The additional boron sources (active ash basin, Unit 5 inactive ash basin, and ash storage area) are activated in 1975 in the transport model, and all of the boron sources in the ash layers are held at a specified concentration until the end of the simulation in 2018.

The key transport model parameters (besides the flow field) are the boron source concentrations in the ash and the boron soil-water distribution coefficient (K_d). The other model parameters are the longitudinal, transverse, and vertical dispersivity, and the effective porosity. The boron source concentrations in the ash basins and ash storage area were initially estimated from the ash pore water concentrations and from concentrations in nearby wells. During the transport model calibration process, the basins and other areas were subdivided, and different concentrations were assigned to different zones at different times. Source concentrations of the boron are held constant at the specified levels in the ash layers during the historical transport simulation, but they are allowed to vary in time during the predictive simulations that follow.

The numerical treatment of adsorption in the model requires special consideration because part of the system is a porous media (ash, saprolite, and transition zone) with a relatively high porosity, while the bedrock is a fractured media with very low matrix porosity and permeability. As a result, transport in the fractured bedrock occurs almost entirely through the fractures. The MODFLOW and MT3DMS flow and transport models used here simulated the fractured bedrock as an equivalent porous media. With this approach, an effective hydraulic conductivity is assigned to the fractured rock zones so that it produces the correct Darcy flux (volume of water per area of media per time) for a given hydraulic gradient. However, because the water flows almost entirely through the fractures, this approach requires that a small effective porosity value (~0.01 or less) be used for the transport calculations to compute a realistic flow velocity.

The COI retardation factor is computed internally in the MT3DMS code using a conventional approach:

$$R = 1 + \frac{\rho_b K_d}{\phi}$$

Where ρ_b is the bulk density and ϕ is the porosity. If typical porous media values are used for the bulk density and K_d, the resulting retardation factor in the fractured media becomes unrealistically large due to the low porosity value. In the current model, the calibrated boron K_d value was 0.53 mL/g for the saprolite and transition zone. Considering the fractured bedrock, with a bulk density of 1.6 g/mL and a porosity of 0.01, a K_d value of 0.53 mL/g results in a retardation factor of 90, which is unrealistically high for boron transport. To avoid this problem, the boron was assigned a much lower K_d value in the bedrock layers of the model so that it would have a reasonable retardation factor during transport through the fractured media.

Ash leaching tests were performed on 6 samples from the active ash basin using US EPA (LEAF) Method 1316. The leaching data were analyzed to develop a K_d (partition coefficient) value for boron in the coal ash. The average of those test values was 0.53 mL/g. The modeling approach for the predictive simulations of future boron transport allow the boron concentration in the ash to vary with time in response to flushing by groundwater. Using the K_d value that is derived from ash leaching tests ensures that the model response of the boron in the ash to groundwater flushing is realistic.

Linear adsorption K_d values for CSS COIs were measured in the laboratory using samples from the coal ash and native aquifer materials obtained from the Site (Langley and Oza, 2015). In general, the measured K_d values for the constituents were highly variable, and the variability within a given material type was larger than the variability between different materials. A summary of the measured K_d values is given by Langley and Oza (2015). The K_d value for the boron in the aquifer material outside of the ash basin was treated as a calibration parameter. Boron is expected to be mobile, and to have a low K_d value. The calibrated K_d values for the saprolite and transition zone layers were 0.5 mL/g. In the fractured bedrock, a much lower value was used as described above of 0.02 mL/g.

The longitudinal dispersivity was assigned a value of 20 ft., the transverse dispersivity was set to 2 ft., and the vertical dispersivity was set to 0.2 ft. The effective porosity was set to a value of 0.3 in the unconsolidated layers, and to 0.01 in all of the bedrock layers. The soil dry bulk density was set to 1.6 g/mL.

4.7 Transport Model Boundary Conditions

The transport model boundary conditions are no flow on the exterior edges of the model except where constant or general head boundaries exist, where they are specified as a concentration of zero. All of the constant head water bodies (river, streams, and pond), have a fixed concentration of zero. As water containing dissolved constituents enters these zones, the dissolved mass is removed from the model. The infiltrating rainwater is assumed to be clean, and enters from the top of the model. The ponded ash basin water receives special treatment, where the water level is maintained using a constant head hydraulic boundary, but the boron concentration is specified in model cells below the water surface.

The initial condition for the current conditions transport model (back in 1957) is one of zero concentration of boron everywhere in the model. No background concentrations are considered.

4.8 Transport Model Sources and Sinks

The ash basins and ash storage area are the source of boron in the model. During the historical transport simulation, these sources are simulated by holding the boron concentration constant in cells located inside the ash in these zones. The boron concentrations from the historical transport simulation form the initial condition for the predictive simulations of future transport at the Site. The predictive simulations do not hold the boron concentrations constant in the ash source zones, and this mobile constituent can wash out of the ash over time. The boron K_d value used for the ash was measured in ash leaching tests (described in Section 4.5) using ash from the Site to ensure that the simulated boron leaching rate is realistic.

Impacted soil and rock at the Site can continue to serve as a source for groundwater contamination by the boron at the Site. This potential is fully accounted for in the model by continuously tracking the boron concentrations in time in the saprolite, transition zone, and rock materials throughout the model. The historical transport model simulates the migration of boron through the soil and rock from the active ash basin, and these results are used as the starting concentrations for the predictive simulations. Therefore, even if all of the coal ash is excavated, the transport model predicts ongoing impacts to groundwater from the impacted soil beneath the ash.

The transport model sinks are the constant head river, ponds, creeks, and drains. As groundwater enters these features, it is removed along with any dissolved constituent mass. Similarly, if water containing a constituent were to encounter a pumping well, the constituent is removed with the water.

4.9 Transport Model Calibration Targets

The transport model calibration targets are boron concentrations measured in 170 monitoring wells in the 2nd quarter of 2018. All sampled wells are included in the calibration.

5.0 MODEL CALIBRATION TO CURRENT CONDITIONS

5.1 Flow Model

The flow model was calibrated in stages starting with a relatively simple layered model. All calibration was done by trial and error, simultaneously matching the recent water levels measured in observation wells (Table 5-1). Additional flow model calibration was required to also match the current conditions boron distribution. The primary calibration parameters are the three-dimensional distribution of hydraulic conductivity. Each model layer has been subdivided into hydraulic conductivity zones. These model conductivity zones are shown in Figures 5-1through 5-8, and the base calibrated hydraulic conductivity values for each layer are listed in Table 5-2.

Starting at the top, in layers 1-8, the layers represent both the coal ash and the ash basin dam. The dam fill material has a calibrated conductivity of 0.07-0.5 ft/d. This relatively variable conductivity of the dam fill was required in order to simultaneously match hydraulic heads of wells in and below the dam.

In the current steady-state flow model, the grid cells in the Unit 5 inactive ash basin and active ash basin were set at a higher elevation than the current ash elevations to simulate future closure scenarios where ash would be stacked. A high hydraulic conductivity (200 ft/d) was applied to stacked areas above the current ash basin elevations. The hydraulic conductivity of the ash was assumed to be 2.0 ft/d. The current conditions flow model is insensitive to the ash conductivity because the water levels around the active ash basin are controlled by the active ash basin pond elevation. The value of 2.0 ft/d that was used is close to the median of more than 200 slug tests performed at 14 coal ash basin sites in North Carolina shown in Figure 4-4, and it falls within the range of values measured at the Site. Although the current conditions model is insensitive to this parameter, the predictive final cover and hybrid simulations are more sensitive to the ash conductivity. Three pumping tests in the CSS ash basins were recently performed in late 2018 to improve the understanding of the coal ash hydraulic conductivity at the CSS. The data will be incorporated into an updated version of this model at a later date.

The calibrated background hydraulic conductivity for the saprolite (layers 9-13) was 2 ft/d, which slightly higher than the average value for slug tests performed in saprolite at 10 coal

ash basin sites in the Piedmont of North Carolina, however is the estimated average for slug tests performed at the CSS (Figure 4-5). This material is heterogeneous and zones of both higher and lower conductivity were required to match the hydraulic heads and boron transport (Figures 5-2a through 5-2d, and Table 5-2). The range of saprolite conductivity in the model goes from 0.05 ft/d to 4.0 ft/d, which falls within the range of values measured in slug tests in the 10 Piedmont Sites shown in Figure 4-5.

The conductivity of the saprolite was made slightly higher to the west of Suck Creek to better match the observed monitoring wells. A high hydraulic conductivity of 5 ft/d represents the alluvial channel along the Broad River. These units are thin below the center of the active ash basin dam. To the east of the dam, a zone of high permeability was required to match the high boron concentrations seen in wells in this area. Within the active ash basin, a zone of lower conductivity (0.5 ft/day) was needed in some sections under the active ash basin to reproduce the higher hydraulic heads observed.

The calibrated background conductivity for the transition zone (layers 14-15) was 3.0 ft/d. This value falls near the average value for slug tests performed in the transition zone at 10 Piedmont Sites in North Carolina (Figure 4-6). The transition zone is heterogeneous, with values ranging from 0.08 ft/d to 5.0 ft/d (Figure 5-3a through 3b and Table 5-2).

The upper bedrock zone in the model includes layers 16-20, and is approximately 70 feet thick. The background conductivity value used in the model of 0.04 ft/d falls within the range of values measured from slug tests at 10 Piedmont sites in North Carolina, and in slug tests performed at the CSS (Figure 4-7). The background conductivity value used in the model is somewhat lower than the median value measured in slug tests, to better match observed heads.

Model layer 16 represents some areas of transition zone and fractured bedrock, but it has a lower background conductivity than the shallower layers (Figure 5.4). Just west of the active ash basin, a zone of “high” conductivity (1 ft/day) was required in order to recreate the observed boron transport in this area. Higher hydraulic conductivities were used around U5-2BR; U5-5BR; GWA-31BRA (Figure 5-10) to better calibrate the hydraulic heads within these areas. The slug test analysis for U5-2BR was approximately 3 ft/d, which is close to the hydraulic conductivity used in the model calibration in this area.

The upper bedrock conductivity in layers 17-20 ranges from 0.006 ft/d to 2 ft/d in the model (Figure 5-5a through 5-5d and Table 5-2). The very low value was used to better match the hydraulic head elevations observed in two wells (GWA-12BRU and GWA-54BRO) west of the active ash basin dam. West of the southern active ash basin pond a low value was used to improve calibration to measured boron concentrations in GWA-27BR.

The deep bedrock layer extends 500 feet (layers 21-28) below the upper bedrock, and was assigned a uniform value of 0.006 ft/d (Figure 5-6a, Figure 5-6b, Figure 5-7 and Table 5-2). Figures 5-6a and 5-6b show some zones with hydraulic conductivities higher than the uniform value to calibrate observed wells within layers 21-22. The flow model calibration is insensitive to this value, but the model conductivity is high enough to allow some water flow in the deep bedrock. Combined with the low rock porosity (0.01), and the high mobility of boron, this combination results in deep predicted migration of low concentrations of boron beneath the active ash basin dam. There are four bedrock wells located in layers 20-22, (GWA-14BR, GWA-31BRA, GWA-32BR, GWA-33BR), where the hydraulic conductivity was made high to better match the low heads within the wells. Slug tests performed in these wells indicated high hydraulic conductivity, ranging up to 9 ft/d. Additional deeper bedrock wells are planned in the vicinity of the active ash basin dams and hydraulic and COI concentration data from those wells will be used to refine the calibration of shallow and deeper bedrock parameters in a future version of the flow and transport model.

The final calibrated flow model has a mean head residual of -0.12 ft., a root mean squared error (RMSE) of 4.22 ft., and a normalized root mean square error (NRMSE) of 2.29%. The range of heads at the Site is about 184 ft. with a maximum of 838.62 ft. and a minimum of 654.43 ft. A comparison of the observed and simulated water levels is listed in Table 5-1 and the observed and simulated levels are cross-plotted in Figure 5-8. Table 5-2 lists the best-fit hydraulic parameters from the calibration effort.

The computed heads in the transition zone (model layer 15) are shown in Figure 5-9. Figure 5-10 shows the simulated heads in the second fractured bedrock model layer (model layer 17). These are similar to the shallower heads. The calibration wells are also shown in this figure (many of the nested wells plot on top of each other). The green, yellow and red bars indicate the magnitude of model error at each well. The green color indicates that the difference is less than

9 ft. and the yellow color indicates a difference of 9 to 18 ft., the red color indicates the difference of 18 ft. or higher. The head gradients become extremely steep downgradient of the downstream dam, and are dominated by various creeks at the site.

Under current conditions, groundwater flow in the vicinity of the CSS is dominated by the Broad River, smaller creeks, and the pond in the active ash basin. Flow near the CSS occurs between two groundwater divide ridges, shown in yellow on Figure 5-11. These groundwater divides separate the Suck Creek drainage basin and CSS from the surrounding regions. In the southern region between these two groundwater divides, flow is towards and down the Suck Creek drainage (Figure 5-11). The eastern portion of the area is controlled by the active ash basin pond. Flow into the active ash basin pond occurs along the south and east edge of the pond. Ash pore water flows out on the north and west edge towards Suck Creek and the Broad River (Figure 5-11). Flow in the western portion between the groundwater divides is north-northeast towards the Broad River and east towards Suck Creek. Outside of the groundwater divides surrounding the CSS, flow occurs to the southeast towards Ashworth Creek and to the northwest and north towards the Broad River (Figure 5-11). All flow within the groundwater divides around the CSS discharges to the Suck Creek and Broad River (Figure 5-11).

5.2 Flow Model Sensitivity Analysis

A parameter sensitivity analysis was performed by varying the main hydraulic parameters (recharge, ash conductivity, saprolite conductivity, transition zone conductivity, and upper and lower bedrock conductivity) in the current conditions flow model. Starting with the calibrated model, each parameter was halved and doubled to evaluate the model sensitivity. Only the main background conductivity values were varied in this study. Table 5-3 shows the results of the flow parameter sensitivity study. The model is sensitive to the recharge rate, and is moderately sensitive to the saprolite, transition zone, and shallower bedrock conductivities. The model is insensitive to the ash conductivity and to the conductivity of the deeper bedrock. As discussed earlier, additional testing of the ash and deeper bedrock units from pumping tests and geophysical testing will take place in the near future, and these results will be incorporated into a later version of this model.

5.3 Historical Transport Model Calibration

The groundwater flow simulation used in the historical transport model reflects post-1975 flow conditions at the active ash basin, where Suck Creek has been rerouted, and the original channel has been dammed to form the ash basin. For the period of 1957 to the early 1970s, the Former Units 1-4 ash basin was the only significant source of boron to the groundwater. The Former Units 1-4 ash basin is not affected by flow conditions at the active ash basin, so this approximation of the early time groundwater flow field is reasonable. The flow model has transient changes that reflect the start and end of operation of the Unit 5 inactive ash basin and capping of the CCP Landfill.

The boron transport model begins in 1957, with the Former Units 1-4 ash basin serving as the only source of boron in the model. The additional boron sources (active ash basin, Unit 5 inactive ash basin, and ash storage area) are activated in 1975 in the transport model, and all of the boron sources in the ash layers are held at a specified concentration until the end of the simulation in 2018.

The transport simulations used 19 spatial zones of specified boron source concentration (Figure 5-12 and Table 5-4). The active ash basin was split into several different zones: one zone that represents the active ash basin pond, one that represents the southern part of the active ash basin, one that represents the sluicing channel, and several patched areas to reflect concentrations in the observation wells. These zones were assigned very similar boron concentrations. The ash storage area was treated as a separate boron source zone and was split into three sections. The Former Units 1-4 ash basin had a very low boron source since it was excavated and to reflect the historical and recent observed concentrations. The Unit 5 inactive ash basin also has a relatively low boron concentration applied to match current boron concentrations. The concentration of boron was held constant at specified values in the ash material in these zones during the historical transport simulations.

The calibrated K_d values for the boron was 0.50 in the saprolite and transition zone materials, and 0.02 in the bedrock. The effective porosity was set to 0.3 in the unconsolidated layers, and 0.01 in the bedrock layers.

Table 5-5 compares measured (2nd quarter, 2018) and simulated current conditions boron concentrations. The simulated boron concentrations in the saprolite zone (model layer 13) and the transition zone/upper part of the bedrock (model layer 16), are shown in Figure 5-13. The model predicts boron transport above the 2L standard from the ash basin to the north of the compliance boundary of the active ash basin in the ash storage area. This boron migration appears to mainly occur in the saprolite, with less migration in the transition zone and in the bedrock. Several deep wells are planned to be installed in the ash basin dam to help improve the understanding of possible boron transport in the bedrock near the ash basin dam. Overall, the simulated boron concentrations appear to reasonably match the observed concentrations in most areas, and the model simulated boundary where the 2L standard is exceeded is similar to the observed locations.

5.4 Transport Model Sensitivity

The most important transport model parameter for the boron is the K_d. The effective porosity affects transport velocity, but it also appears in the denominator of the retardation factor equation. Considering a Darcy velocity of V, the actual COI velocity, V_c is affected by both the porosity and the retardation factor:

$$V_c = \frac{V}{\phi R} = \frac{V}{\phi + \rho_b K_d}$$

The denominator of this relationship tends to be dominated by the K_d term unless it is very small. This is the reason why a small K_d value is assigned to the bedrock, where the effective porosity is due to the fractures, and is low. The transport model sensitivity to the K_d values was evaluated by running the boron transport simulation with K_d values that were 5 times smaller, and 5 times larger than the calibrated values (0.5 mL/g in the saprolite and transition zone, and 0.02 mL/g in the bedrock). The results of this study are shown in Table 5-6. The simulation results are seen to be sensitive to the K_d value range tested here. The calibrated value produces a normalized root mean square error of 3.5%. This slightly decreases to 3.4% for the high K_d case and increases to 5.3% for the low K_d case. In terms of the boron plume behavior, the low K_d simulation over-predicts the boron concentrations in wells, while the high K_d simulation under-predicts the boron concentrations in wells.

6.0 PREDICTIVE SIMULATIONS OF CLOSURE SCENARIOS

The simulated April 2018 boron distribution was used as the initial condition in closure simulations of future flow and transport at the CSS. There are three main simulated scenarios including an excavation scenario, final cover scenario, and hybrid scenario. In the excavation scenario all of the ash in the ash basins is excavated and be placed on the onsite CCP landfill. In the final cover scenario, a final cover system is installed over the active ash basin and Unit 5 inactive ash basin and the Former Units 1-4 ash basin is excavated. In the hybrid scenario, part of the ash is excavated from the active ash basin and moved to the southern part of the active ash basin where it is capped with a final cover system, Unit 5 inactive ash basin is capped, and the Former Units 1-4 ash basin is excavated. In all three scenarios, the ash layers in the Former Units 1-4 ash basin was simulated using a high hydraulic conductivity (200 ft/d) and boron concentrations that were set to zero.

The current plans call for the CSS active ash basin pond to be decanted (drained of free-standing water) beginning in 2019. The decanting of the ash basin pond is expected to take approximately one year. Ash basin pond decanting will have a major effect on the groundwater flow field near the active ash basin downstream dam, because the pond level will be lowered approximately 65 feet, removing free-standing water.

After the active ash basin pond decanting, the final site closure activities will start and will continue for several years. It is assumed that final cover construction can be completed in 2 years, and will be completed in the year 2022. Hybrid construction is assumed to be completed in approximately 2-3 years, in years 2022-2023. The excavation construction is assumed to be completed in 10 years, in year 2030.

The predictive simulations are run in two steps. The first step is a simulation that starts in 2020, and uses the groundwater flow field after the active ash basin pond is decanted. The starting boron distribution for this simulation is the simulated April 2018 concentration distribution. This simulation step continues for a period of 2 years (for the final cover system and the hybrid design) or for 10 years (for excavation) ending in either 2022, or 2030. The second step assumes that construction activities have been completed and uses the final excavation, hybrid, or final cover system flow field for transport simulations. These simulations

start in 2022 or 2030, and continue for 1000 years or until the boron concentrations beyond the current compliance boundary decrease below 2L standards. New potential compliance boundaries have recently been developed for the excavation and hybrid closure actions, and these potential boundaries are shown on the related figures in this report. These potential compliance boundaries for the excavation and hybrid scenarios are located at 250 feet from the waste, or at 50 feet inside the property line, whichever is closer to the waste. For the final cover scenario, the compliance boundary is 500 feet from the waste boundary in the active ash basin and 250 feet from the Former Units 1-4 ash basin and Unit 5 inactive ash basin waste boundaries, or at the property line.

6.1 Interim Period with Active Ash Basin Pond Decanted

This simulation represents an interim period after the active ash basin pond is decanted, but before closure action construction is completed. Decanting of the active ash basin pond is simulated by removing the generalized head zone that represents the pond in the current conditions flow simulation, and replacing it with a small drain area at an elevation of 693 ft., which is approximately 65 feet below the current active ash basin free water surface. The drain area is located in the deepest part of the current active ash basin pond. Recharge at a rate of 7.5 inches per year is added to the active ash basin, and boron initial conditions come from the historical transport simulation. Boron concentrations in the ash are no longer held constant, and the boron can leach from the ash according to its K_d value (which was derived from ash leaching tests). Boron present in the underlying soil and rock is mobile, and moves in response to the groundwater flow with adsorption occurring according to the soil or rock K_d value. The surface drains in the southern part of the active ash basin are removed in this simulation. Figure 6-1 shows the simulated steady-state hydraulic heads after the pond is decanted. The primary changes to groundwater flow after decanting the ash basin pond is increased gradients in the pond region (Figure 6-1). Figure 6-2 shows the simulated boron distribution in the transition zone in 2030 with the ash basin decanted.

6.2 Excavation Scenario

These simulations begin in 2030 using the boron distribution from the decanted pond simulation described above. Excavation is simulated by setting the boron concentration in the ash layers to zero in the active ash basin, ash storage area, Former Units 1-4 ash basin, and Unit

5 inactive ash basin. The concentrations of boron in the remaining impacted soil underneath the ash basin are set to the values from the decanted pond simulation. The ash layers, former Unit 5 inactive ash basin dam, and dowmstream dam in the active ash basin are given a very high hydraulic conductivity to simulate excavation, and the upstream dam is lowered about 20 feet to keep Suck Creek in place. Recharge occurs in the ash basin footprint at the background level of 7.5 inches per year. The previous active ash basin surface water features are removed and a small stream network is added to the active ash basin and Unit 5 inactive ash basin. The new drainages follow the original Suck Creek pathway within the active ash basin and southern drainages in the Unit 5 inactive ash basin and were simulated along the top of the saprolite surface. This drain network simulates the springs and streams that will form in the active ash basin and Unit 5 inactive ash basin (Figure 6-3) that may need to be collected and discharged per a NPDES permit for a period of time.

The steady-state hydraulic heads in the transition zone are shown in Figure 6-4 for the excavation case. The groundwater levels are now at or below the original ground surface. Flow in the active ash basin footprint is now mainly towards the former channel of Suck Creek.

The simulated boron concentrations in the transition zone (model layer 15) are shown for the years 2050, 2115, and 2450 for the excavation scenario Figure 6-5. The predicted boron concentrations in the shallow bedrock (model layer 17) are shown for the years 2050, 2115, and 2450 in Figure 6-6. The red line is the potential compliance boundary following ash basin excavation within the active ash basin, the blue line is the potential compliance boundary for Former Units 1-4 ash basin and Unit 5 inactive ash basin, and the gold line is the waste boundaries. These simulations suggest that boron may continue to migrate beyond the current compliance boundary north of the active ash basin at concentrations slightly greater than the 2L standard concentration for over 100 years.

A location was chosen to produce boron concentration versus time (time-series) plots (Figure 6-7). This point is located at the current compliance boundary north of the active ash basin. No other locations were chosen because the model simulation did not predict boron concentration greater than the 2L standard beyond the potential compliance boundary. The predicted concentrations in the transition zone and shallow bedrock at location 1 are shown in Figure 6-8.

6.3 Final Cover Scenario

The final cover simulation begins in 2022 using the boron distribution from the decanted active ash basin simulations described above. The active ash basin and Unit 5 inactive ash basin cover design used in the model is based on a draft closure plan design developed by AECOM (AECOM. Following active ash basin pond decanting, this draft design calls for the upstream dam to be lowered approximately 15 ft., and for the downstream dam to be regraded to form a gentle slope from west to east. The ash is to be regraded inside the southern portion of the active ash basin and will be stacked towards the center with the highest elevation of about 780 ft. The cover system consists of an impermeable geomembrane, covered with about 2 feet of soil and a grass surface. The surface drainage ditches follow along the perimeter of the active ash basin and converge to a single channel south of the downstream dam (Figure 6-9). This perimeter ditch is included in the model as a drain at an elevation that is 5 feet below the final ground surface.

The Unit 5 inactive ash basin main dam will be lowered and the ash will be piled into two separate stacks. A drainage system is proposed to run along most of the perimeter of the Unit 5 inactive ash basin and will drain out to the north where the main dam is located. These ditches are included in the model but they do not remove much if any groundwater from the Unit 5 area. Figure 6-9 shows the drain network that was used in the final cover simulation to simulate this drainage system. The numbered nodes along the drain arcs are locations where the drain elevation was specified using the Closure Plan (AECOM. Drain elevations between these nodes were interpolated along the arcs. The drains are simulated using the MODFLOW DRAIN feature, using a relatively high conductance of 10.0 $ft^2/d/ft$. Groundwater flow into these drains is removed from the model. If this closure option is selected, the discharge from the drainage system may need to be collected, treated and discharged per the NPDES permit for a period of time.

The final cover system is simulated by removing all of the original ash basin surface water features and replacing them with the designed drainage network. The ash properties are adjusted to reflect regrading of the ash in the area near the dam, and the recharge rate through the cover is set to 0.00054 inches per year. This value is based on landfill cover simulations performed using the Hydrologic Evaluation of Landfill Performance program (HELP) by

AECOM. The boron initial conditions come from the dewatered active ash basin pond simulation in the year 2022. The boron concentrations in the ash are variable in time, and the K_d value in the ash was set to value measured in ash leaching tests performed with ash from the basin (0.53 mL/g).

The steady-state hydraulic heads in the transition zone are shown in Figure 6-10. Hydraulic heads for the final cover design are controlled by the Broad River, Suck Creek, and changes to the dowmstream dam in the active ash basin. The drainage system around the active ash basin ash stack is predicted to remove approximately 140 gpm of groundwater, while the drainage system around the Unit 5 inactive ash basin removes only a few gpm of groundwater.

The simulated boron concentrations in the transition zone (model layer 15) are shown for the years 2050, 2150, and 2450 for the final cover simulation in Figure 6-11. The predicted boron concentrations in the shallow bedrock (model layer 17) are shown for the years 2050, 2150, and 2450 in Figure 6-12. The red outline is the current active ash basins compliance boundary, the blue line is the potential Former Units 1-4 ash basin and the Unit 5 inactive ash basin compliance boundary, and the gold outline is the waste boundaries. The final cover simulations suggest that boron may continue to migrate beyond the current compliance boundary north of the active ash basin at low concentrations but possibly greater than the 2L standard for over 500 years.

As before, one location was chosen to produce boron concentration versus time (time-series) plots (Figure 6-7). Location 1 is located at the compliance boundary north of the active ash basin. No other locations were chosen because the model simulation did not predict boron concentrations greater than the 2L standard beyond the compliance boundary. The predicted concentrations in the transition zone and shallow bedrock at location 1 are shown in Figure 6-13.

6.4 Hybrid Design Scenario

The hybrid design simulations begin in 2022 using the boron distributions from the decanted basin simulations described earlier. The hybrid design is based on the 2018 closure options evaluation summary report (Duke, 2018). Post decanting, this design, involves complete excavation of the ash from the northern part of the active ash basin, the southern fingers of the active ash basin, and the ash storage area. This ash would be placed in the southern part of the

active ash basin, forming a higher mound or stack than in the final cover design. The hybrid design results in a maximum ash stack elevation of 815 ft., and an overall footprint of about 63 acres. The hybrid design calls for the downstream active ash basin dam is to be completely removed. In the model the upstream dam was lowered approximately 15 feet to keep Suck Creek dammed to the west of the active ash basin. The Unit 5 inactive ash basin has the same design plan simulated in the final cover scenario.

The regraded ash in the active ash basin would be covered with an impermeable geomembrane, soil, and a grass surface. A drainage system was incorporated on the southern and eastern perimeter of the active ash basin stack to collect water around the edge of the capped ash stack. The drainage feature is along the southern active ash basin perimeter and flows north towards the northeast perimeter of the active ash basin stack. The elevation of the perimeter ditch around the ash stack ranges from about 764 ft. on the southern side of the stack to about 745 ft. on the northeast side of the stack (Figure 6-14). The northeast drain is connected to a shallow swale that follows the former footprint of Suck Creek to the Broad River (Figure 6-14).

The ash in the remaining part of the active ash basin would be graded to maintain slopes of at least 1% towards the perimeter ditch around the ash stack. Shallow swales are built into the southern fingers of the active ash basin to direct the surface water towards the perimeter ditch described above ultimately discharging to the Broad River.

The cover system over the ash is simulated by setting the recharge rate to 0.00054 inches per year as in the final cover system simulation. The excavated part of the active ash basin is simulated by increasing the hydraulic conductivity of the ash to a very high value, by restoring the recharge to the background level of 7.5 inches per year, and by adding a drain network along the base of the excavation in former valleys. This drain network is intended to simulate springs and streams that will form in the excavated area (Figure 6-14) and may require collection, treatment and discharge per NPDES permit for a period of time. Boron concentrations in the excavated part of the ash layers are set to zero, while initial boron concentrations in the deeper layers come from the decanted active ash basin pond simulation.

The boron initial conditions in the remaining ash also come from the decanted ash basin pond simulation. The boron concentrations in the ash are variable in time, and the K_d value in

the ash is set to the value measured in ash leaching tests performed with ash from the basin (0.53 mL/g).

The steady-state hydraulic heads in the transition zone are shown in Figure 6-15. The heads in the southern part of the active ash basin are similar to the final cover simulation, while those in the northern part are lower, due to the excavated area and dam removal.

The simulated boron concentrations in the transition zone (model layer 15) are shown for the years 2050, 2150, and 2450 for the hybrid case in Figure 6-16. The predicted boron concentrations in the shallow bedrock (model layer 17) are shown for the years 2050, 2150, and 2450 in Figure 6-17. The red outline is the potential active ash basin compliance boundary, the blue line is the potential Former Units 1-4 ash basin and the Unit 5 inactive ash basin compliance boundary, and the gold outline is the waste boundaries. The hybrid design simulations suggest that boron may continue to migrate beyond the new potential compliance boundary at north of the active ash basin dam at low concentrations for approximately 400 years.

As in the earlier simulations, one location was chosen to produce boron concentration versus time (time-series) plots (Figure 6-7). Location 1 is located at the compliance boundary north of the active ash basin. No other locations were chosen because the model simulation did not predict boron crossing the potential compliance boundary above 2L standard. The predicted concentrations in the transition zone and shallow bedrock at location 1 are shown in Figure 6-18. These time series concentrations take longer to reach 2L than the excavation and shorter than the final cover system. The concentrations are predicted to gradually decrease over time; however it takes approximately 400 years to achieve compliance with the 2L standard.

6.5 Conclusions Drawn from the Predictive Simulations

- Active ash basin pond decanting will have a significant effect on the groundwater flow field, resulting in lower heads near the active ash basin dam
- Predicted future boron concentrations at and beyond the current compliance boundary vary for the excavation, final cover system, and hybrid design closure simulations. In each case a low concentration (but above 2L) plume of boron is predicted to migrate north towards the Broad River in the ash storage area. A comparison of the

groundwater concentrations over time for the three conceptual closure design simulations are simulations similar as shown on Figures 6-19 through 6-22.

- These simulations do not include any active form of groundwater remediation. The relative benefits of various groundwater remediation alternatives will be addressed in the CAP. It is expected that engineered measures could control the boron plume
- In the absence of remedial measures associated with corrective action, boron is predicted to exceed the 2L standard at the current northern compliance boundary for approximately 100 years in the excavation scenario, 500 years for the final cover scenario, and 400 years for the hybrid scenario.
- In all three closure scenario modeling simulations no private wells are expected to be impacted.
- Evaluation and inclusion of ash basin pump test data and the installation of deep bedrock wells near the ash active basin dams will reduce model uncertainty, and results will be incorporated into the next version of this model.

7.0 REFERENCES

AECOM, 2018, Ash Basin Closure Plan 60% Draft, Final Grades - Active Ash Basin. Drawing Number CLS.C901.002.042, 8/14/2018.

AECOM, 2018, Ash Basin Closure Plan 60% Draft, Final Grades - Unit 5 Inactive Ash Basin. Drawing Number CLS.C901.002.040, 8/14/2018.

Daniel, C.C., Douglas G. Smith, and Jo Leslie Eimers, 1997, Hydrogeology and Simulation of Ground-Water Flow in the Thick Regolith-Fractured Crystalline Rock Aquifer System of Indian Creek Basin, North Carolina, USGS Water-Supply 2341.

Duke Energy, 2018 Rogers Energy Complex – Cliffside Steam Station Active Ash Basin Closure Options Evaluation Summary Report

Haven, W. T. 2003. Introduction to the North Carolina Groundwater Recharge Map. Groundwater Circular Number 19. North Carolina Department of Environment and Natural Resources. Division of Water Quality, 8 p.

HDR, 2015a. Comprehensive Site Assessment Report, Cliffside Steam Station Ash Basin, September, 2015.

HDR, 2015b. Corrective Action Plan Part 1. Cliffside Steam Station Ash Basin. December, 2015.

HDR, 2016. Comprehensive Site Assessment (CSA) Supplement 2, Cliffside Steam Station Ash Basin, August 11, 2016.

McDonald, M.G. and A.W. Harbaugh, 1988, A Modular Three-Dimensional Finite-Difference Ground-Water Flow Model, U.S. Geological Survey Techniques of Water Resources Investigations, book 6, 586 p.

Niswonger, R.G.,S. Panday, and I. Motomu, 2011, MODFLOW-NWT, A Newton formulation for MODFLOW-2005, U.S. Geological Survey Techniques and Methods 6-A37, 44-.

North Carolina Water Supply and Use, in “National Water Summary 1987 - Hydrologic Events and Water Supply and Use”. USGS Water-Supply Paper 2350, p. 393-400.

North Carolina; Estimated Water Use in North Carolina, 1995, USGS Fact Sheet FS-087-97

Radcliffe, D.E., L.T. West, L.A. Morris, and T. C. Rasmussen. 2006. Onsite Wastewater and Land Application Systems: Consumptive Use and Water Quality, University of Georgia.

SynTerra, 2018, 2018 Comprehensive Site Assessment Update, January 31, 2018.

Treece, M.W, Jr., Bales, J.D., and Moreau, D.H., 1990, North Carolina water supply and use, in National water summary 1987 Hydrologic events and water supply and use: U.S. Geological Survey Water-Supply Paper 2350, p. 393-400.

Zheng, C. and P.P. Wang, 1999, MT3DMS: A Modular Three-Dimensional Multi-Species Model for Simulation of Advection, Dispersion and Chemical Reactions of Contaminants in Groundwater Systems: Documentation and User’s Guide, SERDP-99-1, U.S. Army Engineer Research and Development Center, Vicksburg, MS.

TABLES

Table 5-1. Comparison of observed and computed heads for the calibrated flow model.

Well ID	Observed Head	Computed Head	Residuals
AB-01D	711.35	717.69	-6.34
AB-01S	734.02	727.59	6.43
AB-02D	734.29	735.97	-1.68
AB-02S	743.64	736.34	7.30
AB-03BRUA	758.12	760.94	-2.82
AB-03I	762.86	761.14	1.72
AB-03S	762.68	761.53	1.15
AB-03SL	762.59	761.16	1.43
AB-04BR	757.46	763.07	-5.61
AB-04D	762.29	763.14	-0.85
AB-04S	761.83	763.39	-1.56
AB-04SL	762.06	763.22	-1.16
AB-05BR	763.15	762.61	0.54
AB-05BRU	764.34	762.39	1.95
AB-05S	763.73	762.25	1.48
AB-06BR	759.1	762.89	-3.79
AB-06D	764.86	762.59	2.27
AB-06S	764.46	762.45	2.01
AS-01D	728.58	727.68	0.90
AS-01SB	729.45	727.75	1.70
AS-02BR	657.46	670.99	-13.53
AS-02D	666.43	670.66	-4.23
AS-02S	672.99	671.69	1.30
AS-03BRU	704.12	707.09	-2.97
AS-04D	744.61	738.27	6.34
AS-05BR	702.24	701.26	0.98
AS-05BRU	699.65	701.64	-1.99
AS-05S	701.54	701.30	0.24
AS-06BRA	714.08	716.85	-2.77
AS-06D	721.42	716.51	4.91
AS-06S	721.6	716.09	5.51
AS-07BR	701.76	703.57	-1.81
AS-07BRA	696.23	701.81	-5.58
AS-07D	705.49	704.65	0.84
AS-07S	709.69	704.38	5.31
BG-01D	775.23	780.17	-4.94
BG-01S	775	780.03	-5.03
CCPMW-01D	837.02	835.98	1.04
CCPMW-01S	838.62	836.14	2.48

CCPMW-02D	802.62	803.66	-1.04
CCPMW-02S	804.39	803.62	0.77
CCPMW-03D	796.25	797.65	-1.40
CCPMW-03S	798.13	797.72	0.41
CCPMW-04	818.09	822.47	-4.38
CCPMW-05	815.24	815.64	-0.40
CCPMW-06D	815.52	808.75	6.77
CCPMW-06S	815.46	808.60	6.86
CCPTW-01D	808.1	802.08	6.02
CCPTW-01S	809.69	802.27	7.42
CCPTW-02	800.13	797.72	2.41
CCR-03BR	725.74	728.61	-2.87
CCR-04D	758.58	758.04	0.54
CCR-05D	759.84	757.33	2.51
CCR-06D	758.89	757.68	1.21
CCR-06S	758.96	757.75	1.21
CCR-07D	751.71	747.66	4.05
CCR-07S	750.14	747.99	2.15
CCR-08D	761.42	756.18	5.24
CCR-09D	731.68	728.67	3.01
CCR-11D	730.75	727.35	3.40
CCR-11S	730.31	727.48	2.83
CCR-12D	738.72	736.74	1.98
CCR-12S	737.81	737.01	0.80
CCR-13D	762.02	755.48	6.54
CCR-14D	760.02	759.44	0.58
CCR-15D	763.84	764.16	-0.32
CCR-16D	763.51	762.48	1.03
CCR-16S	763.49	762.49	1.00
CCR-CCP-01D	824.92	831.00	-6.08
CCR-CCP-02D	820.07	814.53	5.54
CCR-CCP-03D	808.35	806.48	1.87
CCR-CCP-03DA	802.09	805.73	-3.64
CCR-CCP-03S	806.09	806.18	-0.09
CCR-CCP-04D	802.13	802.03	0.10
CCR-CCP-05D	799.45	799.94	-0.49
CCR-CCP-05S	798.87	799.90	-1.03
CCR-CCP-06D	801.64	801.37	0.27
CCR-CCP-06S	805.55	801.15	4.40
CCR-CCP-07D	814.54	810.12	4.42
CCR-CCP-09D	811.22	812.41	-1.19
CCR-CCP-09S	810.41	812.42	-2.01
CCR-CCP-10D	807.96	805.97	1.99

CCR-CCP-10DA	811.78	807.86	3.92
CCR-CCP-10S	814.06	806.19	7.87
CCR-CCP-11BR	809.15	811.08	-1.93
CCR-CCP-12D	814.46	810.02	4.44
CCR-CCP-12S	814.8	810.05	4.75
CCR-CCP-13D	822.64	815.60	7.04
CCR-CCP-14D	818.45	819.76	-1.31
CCR-CCP-15D	829.51	824.33	5.18
CCR-CCP-15S	833.05	824.31	8.74
CCR-IB-01D	659.49	661.60	-2.11
CCR-IB-01S	659.72	661.39	-1.67
CCR-IB-03D	659.65	659.64	0.01
CCR-IB-03S	660	659.69	0.31
CCR-U5-01D	729.95	736.86	-6.91
CCR-U5-02D	709.49	703.38	6.11
CCR-U5-03D	683.03	680.90	2.13
CCR-U5-03S	682.72	682.91	-0.19
CCR-U5-04D	678.15	679.41	-1.26
CCR-U5-04S	678.18	678.78	-0.60
CCR-U5-05D	705.94	707.70	-1.76
CCR-U5-06DA	708.41	710.53	-2.12
CCR-U5-06S	708.23	709.81	-1.58
CCR-U5-08D	749.1	753.51	-4.41
CCR-U5-08S	750.69	753.78	-3.09
CCR-U5-09S	756.2	758.81	-2.61
CCR-U5-10D	760.61	764.69	-4.08
CCR-U5-10S	760.63	764.75	-4.12
CLMW-01	751.85	748.63	3.22
CLMW-02	689.42	687.23	2.19
CLMW-03D	726.59	725.62	0.97
CLMW-03S	727.2	725.08	2.12
CLMW-04	655.56	662.10	-6.54
CLMW-05S	737.72	727.70	10.02
CLMW-06	766.14	767.82	-1.68
GWA-01BRU	767.59	764.07	3.52
GWA-02BR	669.84	671.32	-1.48
GWA-02BRU	670.04	671.98	-1.94
GWA-02S	671.52	671.63	-0.11
GWA-03D	698.56	699.00	-0.44
GWA-04D	705.9	707.48	-1.58
GWA-04S	707.13	707.33	-0.20
GWA-05BRU	754.61	755.52	-0.91
GWA-05S	755.68	755.46	0.22

GWA-06D	767.39	768.66	-1.27
GWA-10D	659.86	659.69	0.17
GWA-10S	659.84	659.90	-0.06
GWA-11BRU	657.99	661.57	-3.58
GWA-11S	658.64	661.47	-2.83
GWA-12BRU	681.31	690.65	-9.34
GWA-12S	690.82	690.75	0.07
GWA-13BR	697.59	706.04	-8.45
GWA-14BR	674.09	684.98	-10.89
GWA-14D	673.71	684.34	-10.63
GWA-14S	676.62	684.40	-7.78
GWA-20BR	728.45	727.35	1.10
GWA-20D	723.31	727.35	-4.04
GWA-20S	727.36	727.37	-0.01
GWA-21BR	670.72	666.82	3.90
GWA-21BRU	659.52	665.74	-6.22
GWA-21S	662.69	665.63	-2.94
GWA-22BRU	654.43	659.50	-5.07
GWA-22S	657.19	659.18	-1.99
GWA-23D	761.2	764.84	-3.64
GWA-24BR	776.39	772.50	3.89
GWA-24D	774.24	773.23	1.01
GWA-24S	775.03	772.73	2.30
GWA-25D	769.5	774.39	-4.89
GWA-25S	769.29	774.35	-5.06
GWA-26D	764.78	763.38	1.40
GWA-26S	763.61	763.37	0.24
GWA-27BR	757.74	754.33	3.41
GWA-27DA	756.46	756.17	0.29
GWA-28BR	711.01	715.81	-4.80
GWA-28S	725	716.87	8.13
GWA-28BRU	717.24	717.19	0.05
GWA-29BRA	663.01	660.14	2.87
GWA-29D	656.8	660.43	-3.63
GWA-30BR	771.9	782.02	-10.12
GWA-30BRU	779.02	783.47	-4.45
GWA-30S	780.73	784.12	-3.39
GWA-31BRA	Well not used		
GWA-31D	737.78	733.53	4.25
GWA-32BR	667.73	669.70	-1.97
GWA-32D	668.44	670.94	-2.50
GWA-33BR	697.55	716.54	-18.99
GWA-33D	716.78	717.80	-1.02

GWA-33S	717.43	717.87	-0.44
GWA-34S	707.08	698.59	8.49
GWA-35D	669.28	669.32	-0.04
GWA-35S	669.65	669.56	0.09
GWA-36D	702	695.52	6.48
GWA-36S	700.26	696.40	3.86
GWA-37D	672.54	673.27	-0.73
GWA-37S	668.78	673.15	-4.37
GWA-38D	701.64	697.79	3.85
GWA-39S	717.98	721.30	-3.32
GWA-40S	717.1	721.40	-4.30
GWA-42S	716.89	716.58	0.31
GWA-43D	705.7	717.49	-11.79
GWA-43S	716.71	717.69	-0.98
GWA-44BR	733.53	728.87	4.66
GWA-44D	726.01	728.97	-2.96
GWA-44S	723.83	728.85	-5.02
GWA-45D	752.58	759.12	-6.54
GWA-45S	760.68	759.28	1.40
GWA-46D	Well not used - DRY		
GWA-47D	755.14	759.16	-4.02
GWA-48BR	774.67	771.57	3.10
GWA-51D	738.45	738.30	0.15
GWA-54BRO	718.13	711.06	7.07
GWA-54D	719.07	712.05	7.02
GWA-54S	717.41	711.62	5.79
GWA-56D	676.75	680.65	-3.90
GWA-56S	678.67	681.18	-2.51
MW-02DA	693.97	688.17	5.80
MW-07D	766.29	756.06	10.23
MW-08D	727.24	727.19	0.05
MW-08S	730.19	726.93	3.26
MW-10D	758.87	756.98	1.89
MW-10S	758.42	756.87	1.55
MW-11DA	732.6	730.05	2.55
MW-11S	737.07	733.45	3.62
MW-20D	659.4	663.87	-4.47
MW-20DR	669.76	664.17	5.59
MW-21BR	763.04	763.07	-0.03
MW-21D	770.65	764.23	6.42
MW-22BR	780.21	780.44	-0.23
MW-22DR	782.1	780.87	1.23
MW-23D	716.89	719.68	-2.79

MW-23DR	717.8	719.55	-1.75
MW-23S	717.12	719.75	-2.63
MW-24D	796.98	797.62	-0.64
MW-24DR	800.81	797.97	2.84
MW-25DR	655.66	660.97	-5.31
MW-30D	789.16	789.94	-0.78
MW-30DA	787.52	789.86	-2.34
MW-30S	790.23	789.93	0.30
MW-32BR	807.1	804.86	2.24
MW-32D	805.89	804.91	0.98
MW-32S	806.56	804.74	1.82
MW-34BRU	719.79	719.14	0.65
MW-34S	724.49	719.58	4.91
MW-36BRU	666.72	667.36	-0.64
MW-36S	667	667.23	-0.23
MW-38BR	667.34	671.64	-4.30
MW-38D	668.52	671.29	-2.77
MW-38S	667.63	671.04	-3.41
MW-40BRU	704.69	705.04	-0.35
MW-40S	702.37	704.92	-2.55
MW-42DA	774.1	767.59	6.51
MW-42S	773.9	767.53	6.37
U5-01D	752.97	756.56	-3.59
U5-01S	752.87	757.15	-4.28
U5-02BR	723.42	728.79	-5.37
U5-02D	726.02	727.89	-1.87
U5-2S-SLA	732.41	728.27	4.14
U5-4BR	Well not used		
U5-4BRA	Well not used		
U5-04D	701.39	699.21	2.18
U5-04S	698.55	698.99	-0.44
U5-05BR	698.71	704.43	-5.72
U5-05D	703.75	705.13	-1.38
U5-06D	714.13	718.03	-3.90
U5-6S	713.84	717.73	-3.89
U5-08BR	762.9	764.00	-1.10
U5-08D	761.89	763.96	-2.07
U5-08S	763	764.10	-1.10

Table 5-2. Calibrated hydraulic parameters.

Hydrostratigraphic Unit	Model Layers	Spatial Zones (number corresponds to Figures 5-1 through 5-7)	Horizontal Hydraulic Conductivity, ft/d	Anisotropy ratio, K_h:K_v
Ash Basin	1-8	#1 coal ash	2.0	10
Ash Basin (pond or excavated)	1-8	#2 ponds in ash basins	200	1
Ash Basin Dam	1-8	#3 ash basin dam	0.1	2
Saprolite	9-13	#1	0.1	1
	9-13	#2	0.2	1
	9-13	#3	0.5	1
	9-13	#4	0.8	1
	9-13	#5	1.0	1
	9-13	#6	2.0	1
	9-13	#7	3.0	1
	9-13	#8	4.0	1
	9-13	#9	5.0	1
Transition zone	14-15	#1	0.04	1
	14-15	#2	0.08	1
	14-15	#3	0.1	1
	14-15	#4	0.2	1
	14-15	#5	0.5	1
	14-15	#6	0.8	1
	14-15	#7	1.0	1
	14-15	#8	1.5	1
	14-15	#9	2.0	1
	14-15	#10	3.0	1
	14-15	#11	4.0	1
Fractured Bedrock	16-22	#1	0.006	1
	16-22	#2	0.04	1
	16-22	#3	0.1	1
	16-22	#4	0.3	1
	16-22	#5	0.5	1
	16-22	#6	0.6	1
	16-22	#7	0.8	1
	16-22	#8	1.0	1
	16-22	#9	2.0	1
	16-22	#10	3.0	1
	16-22	#11	4.0	1
	16-22	#12	8.0	1
Bedrock (lower)	21-27	#1 main model	0.006	1

Table 5-3. Flow model sensitivity. The normalized root mean square error (NRMSE) is shown.

Parameter	Decreased by 1/2	Calibrated	Increased by 2
Regional Recharge (7.5 in/yr)	3.22%	2.29%	3.71%
Ash Kh (2.0 ft/d)	2.31%	2.29%	2.28%
Saprolite Kh (1-3 ft/d)	2.48%	2.29%	2.31%
TZ Kh (1.0 ft/d)	2.31%	2.29%	2.65%
Upper Bedrock Kh (0.04 ft/d)	2.27%	2.29%	2.45%
Lower Bedrock Kh (0.006 ft/d)	2.26%	2.29%	2.36%

Table 5-4. Ash basin boron source concentrations (ug/L) used in historical transport model.

Date	Former Unit 1-4 Ash Basin	Unit 5 Inactive Ash Basin	Ash Storage North	Ash Storage Center	Ash Storage West	Ash Storage South	Active Ash Basin Center	Active Ash Basin North	Active Ash Basin West	Sluicing Channel	Active Ash Basin Sluicing Channel West	Active Ash Basin Pond SW	Active Ash Basin Pond South and East	Active Ash Basin Pond Southeast
1957-1975														
boron	400	0	0	0	0	0	0	0	0	0	0	0	0	0
1975-2018														
boron	400	400	400	2,000	800	1,500	2,280	700	1,050	1,050	7,650	7,000	2,280	5,000

Table 5-5. Comparison of observed and simulated boron concentrations (ug/L) in monitoring wells.

WELL	Observed Boron (µg/L)	Boron Model (µg/L)
AB-01D	551	661
AB-01S	0	274
AB-02D	234	742
AB-02S	170	1050
AB-03BRUA	54.1	130
AB-03I	39.3	246
AB-03S	2040	2280
AB-03SLA	948	2152
AB-04BR	43.2	7
AB-04D	0	886
AB-04S	2440	2280
AB-04SL	1630	2211
AB-05BR	0	26
AB-05BRU	0	525
AB-05S	4950	5000
AB-06BR	0	757
AB-06D	0	197
AB-06S	7650	7000
AS-01D	626	492
AS-01SB	1430	864
AS-02BR	374	63
AS-02D	305	222
AS-02S	801	782
AS-03BRU	0	48
AS-04D	0	3
AS-05BR	0	16
AS-05BRU	0	18
AS-05S	0	23
AS-06BRA	0	15
AS-06D	0	4
AS-06S	31.6	28
AS-07BRA	37.7	166
AS-07D	725	248
AS-07S	1400	2000
AS-08D	689	214
AS-08S	87.8	1233
BG-01BRA	0	0
BG-01D	0	0
BG-01S	0	0

CCPMW-01D	0	0
CCPMW-01S	0	0
CCR-12D	294	639
CCR-12S	1020	549
CCR-13D	45.3	1
CCR-15D	117	418
CCR-IB-01D	0	39
CCR-IB-01S	134	78
CCR-IB-03D	66.2	64
CCR-IB-03S	263	122
CLMW-01	1310	1557
CLMW-02	434	655
CLMW-03D	720	1
CLMW-03S	745	215
CLMW-05S	0	376
CLMW-06	0	0
GWA-01BRU	0	0
GWA-02BR	78.1	275
GWA-02BRU	118	200
GWA-02S	116	272
GWA-03D	370	247
GWA-04D	153	209
GWA-04S	140	314
GWA-05BRU	28.9	75
GWA-05S	0	123
GWA-10D	0	26
GWA-10S	102	98
GWA-11BRU	325	192
GWA-11S	360	281
GWA-12BRU	0	0
GWA-12S	0	0
GWA-13BR	73.4	0
GWA-14BR	0	0
GWA-14D	110	0
GWA-20BR	223	627
GWA-20D	784	731
GWA-20S	247	522
GWA-21BR	102	338
GWA-21BRU	133	462
GWA-21S	179	313
GWA-22BRU	0	213
GWA-22S	232	194
GWA-23D	0	4

GWA-24BR	0	0
GWA-24D	0	0
GWA-24S	27.3	0
GWA-25D	0	0
GWA-25S	0	0
GWA-26S	0	0
GWA-27BR	177	540
GWA-27DA	910	633
GWA-28BR	0	331
GWA-28BRU	0	241
GWA-28S	0	36
GWA-29BRA	0	0
GWA-29D	0	0
GWA-30BR	0	0
GWA-30S	0	0
GWA-31BRA	25.6	101
GWA-31D	38.8	179
GWA-32D	0	0
GWA-33BR	138	0
GWA-33D	0	0
GWA-33S	0	0
GWA-34S	0	3
GWA-35D	123	172
GWA-35S	106	161
GWA-36D	162	66
GWA-36S	55.7	93
GWA-37D	52.6	51
GWA-37S	71.6	97
GWA-43D	26.6	0
GWA-43S	62.5	0
GWA-44BR	43.3	0
GWA-44D	32	0
GWA-44S	30.3	0
GWA-47D	333	0
GWA-48BR	0	0
GWA-51D	720	57
GWA-54BRO	84.7	0
GWA-54D	54	0
GWA-54S	57.1	0
GWA-56D	0	0
GWA-56S	32.2	0
MW-02DA	0	49
MW-08D	128	819

MW-08S	134	331
MW-10D	150	99
MW-10S	208	35
MW-11DA	66.1	140
MW-11S	700	135
MW-20D	360	455
MW-20DR	161	458
MW-21BR	0	0
MW-21D	0	0
MW-22BR	0	0
MW-22DR	0	0
MW-23D	30.7	0
MW-23DR	0	0
MW-23S	0	0
MW-24D	0	0
MW-24DR	0	0
MW-25DR	0	0
MW-30D	0	0
MW-30DA	0	0
MW-30S	0	0
MW-32BR	0	0
MW-32D	0	0
MW-34S	0	2
MW-36BRU	0	15
MW-36S	40.2	3
MW-38BR	47.7	165
MW-38D	210	107
MW-38S	124	79
MW-40BRU	0	0
MW-40S	0	0
MW-42DA	0	0
MW-42S	0	0
U5-01D	0	115
U5-01S	0	219
U5-02BR	125	204
U5-02D	115	274
U5-4BRA	0	8
U5-04D	0	39
U5-04S	65.1	157
U5-05BR	386	323
U5-05D	231	387
U5-06D	116	369
U5-08BR	26.1	0

U5-08D	38.1	14
U5-08S	29.6	400

Table 5-6. Transport model sensitivity to the boron K_d values. The calibrated model has a normalized root mean square error (NRMSE) of 6.43%. Boron concentrations are shown for the calibrated model, and for models where the K_d is increased and decreased by a factor of 5.

WELL	Observed Boron (µg/L)	Boron Model (µg/L)	Model, low Kd	Model, high Kd
	NRMSE	**3.49%**	**5.28%**	**3.39%**
AB-01D	551	661	664	657
AB-01S	0	274	274	273
AB-02D	234	742	997	579
AB-02S	170	1050	1050	1050
AB-03BRUA	54.1	130	867	41
AB-03I	39.3	246	1205	91
AB-03S	2040	2280	2280	2280
AB-03SLA	948	2152	2257	2044
AB-04BR	43.2	7	182	1
AB-04D	0	886	1754	558
AB-04S	2440	2280	2280	2280
AB-04SL	1630	2211	2269	2150
AB-05BR	0	26	257	7
AB-05BRU	0	525	1454	289
AB-05S	4950	5000	5000	5000
AB-06BR	0	757	1656	451
AB-06D	0	197	958	76
AB-06S	7650	7000	7000	7000
AS-01D	626	492	1585	179
AS-01SB	1430	864	1738	467
AS-02BR	374	63	587	23
AS-02D	305	222	951	124
AS-02S	801	782	879	747
AS-03BRU	0	48	124	20
AS-04D	0	3	21	1
AS-05BR	0	16	94	4
AS-05BRU	0	18	86	5
AS-05S	0	23	57	17
AS-06BRA	0	15	86	4
AS-06D	0	4	59	1
AS-06S	31.6	28	94	10
AS-07BRA	37.7	166	998	51
AS-07D	725	248	1299	80
AS-07S	1400	2000	2000	2000
AS-08D	689	214	1104	92

AS-08S	87.8	1233	1334	1211
BG-01BRA	0	0	0	0
BG-01D	0	0	0	0
BG-01S	0	0	0	0
CCPMW-01D	0	0	0	0
CCPMW-01S	0	0	0	0
CCR-12D	294	639	907	435
CCR-12S	1020	549	647	438
CCR-13D	45.3	1	6	0
CCR-15D	117	418	572	321
CCR-IB-01D	0	39	40	37
CCR-IB-01S	134	78	79	77
CCR-IB-03D	66.2	64	68	58
CCR-IB-03S	263	122	125	118
CLMW-01	1310	1557	2110	1115
CLMW-02	434	655	1136	435
CLMW-03D	720	1	140	0
CLMW-03S	745	215	377	140
CLMW-05S	0	376	376	374
CLMW-06	0	0	0	0
GWA-01BRU	0	0	3	0
GWA-02BR	78.1	275	278	277
GWA-02BRU	118	200	222	192
GWA-02S	116	272	276	275
GWA-03D	370	247	272	245
GWA-04D	153	209	311	183
GWA-04S	140	314	337	309
GWA-05BRU	28.9	75	213	61
GWA-05S	0	123	140	126
GWA-10D	0	26	27	24
GWA-10S	102	98	99	96
GWA-11BRU	325	192	197	184
GWA-11S	360	281	283	278
GWA-12BRU	0	0	0	0
GWA-12S	0	0	0	0
GWA-13BR	73.4	0	0	0
GWA-14BR	0	0	0	0
GWA-14D	110	0	0	0
GWA-20BR	223	627	946	448
GWA-20D	784	731	776	695
GWA-20S	247	522	532	509
GWA-21BR	102	338	502	284
GWA-21BRU	133	462	466	457

GWA-21S	179	313	320	305
GWA-22BRU	0	213	240	182
GWA-22S	232	194	218	167
GWA-23D	0	4	4	4
GWA-24BR	0	0	0	0
GWA-24D	0	0	0	0
GWA-24S	27.3	0	0	0
GWA-25D	0	0	0	0
GWA-25S	0	0	0	0
GWA-26S	0	0	0	0
GWA-27BR	177	540	1550	220
GWA-27DA	910	633	1227	361
GWA-28BR	0	331	368	295
GWA-28BRU	0	241	292	187
GWA-28S	0	36	64	24
GWA-29BRA	0	0	3	0
GWA-29D	0	0	1	0
GWA-30BR	0	0	0	0
GWA-30S	0	0	0	0
GWA-31BRA	25.6	101	186	97
GWA-31D	38.8	179	184	204
GWA-32D	0	0	0	0
GWA-33BR	138	0	0	0
GWA-33D	0	0	0	0
GWA-33S	0	0	0	0
GWA-34S	0	3	27	4
GWA-35D	123	172	256	144
GWA-35S	106	161	170	165
GWA-36D	162	66	312	31
GWA-36S	55.7	93	137	87
GWA-37D	52.6	51	175	31
GWA-37S	71.6	97	175	77
GWA-43D	26.6	0	0	0
GWA-43S	62.5	0	0	0
GWA-44BR	43.3	0	0	0
GWA-44D	32	0	0	0
GWA-44S	30.3	0	0	0
GWA-47D	333	0	3	0
GWA-48BR	0	0	0	0
GWA-51D	720	57	159	22
GWA-54BRO	84.7	0	46	0
GWA-54D	54	0	16	0
GWA-54S	57.1	0	1	0

GWA-56D	0	0	4	0
GWA-56S	32.2	0	3	0
MW-02DA	0	49	303	18
MW-08D	128	819	919	756
MW-08S	134	331	339	320
MW-10D	150	99	145	73
MW-10S	208	35	62	23
MW-11DA	66.1	140	141	139
MW-11S	700	135	135	135
MW-20D	360	455	461	445
MW-20DR	161	458	502	424
MW-21BR	0	0	0	0
MW-21D	0	0	0	0
MW-22BR	0	0	0	0
MW-22DR	0	0	0	0
MW-23D	30.7	0	0	0
MW-23DR	0	0	0	0
MW-23S	0	0	0	0
MW-24D	0	0	0	0
MW-24DR	0	0	0	0
MW-25DR	0	0	0	0
MW-30D	0	0	0	0
MW-30DA	0	0	0	0
MW-30S	0	0	0	0
MW-32BR	0	0	0	0
MW-32D	0	0	0	0
MW-34S	0	2	17	3
MW-36BRU	0	15	94	11
MW-36S	40.2	3	19	2
MW-38BR	47.7	165	277	121
MW-38D	210	107	291	67
MW-38S	124	79	141	60
MW-40BRU	0	0	23	0
MW-40S	0	0	16	0
MW-42DA	0	0	0	0
MW-42S	0	0	0	0
U5-01D	0	115	113	119
U5-01S	0	219	217	221
U5-02BR	125	204	203	207
U5-02D	115	274	273	277
U5-4BRA	0	8	15	5
U5-04D	0	39	61	30
U5-04S	65.1	157	170	152

U5-05BR	386	323	343	314
U5-05D	231	387	391	385
U5-06D	116	369	383	363
U5-08BR	26.1	0	4	0
U5-08D	38.1	14	110	11
U5-08S	29.6	400	400	400

FIGURES

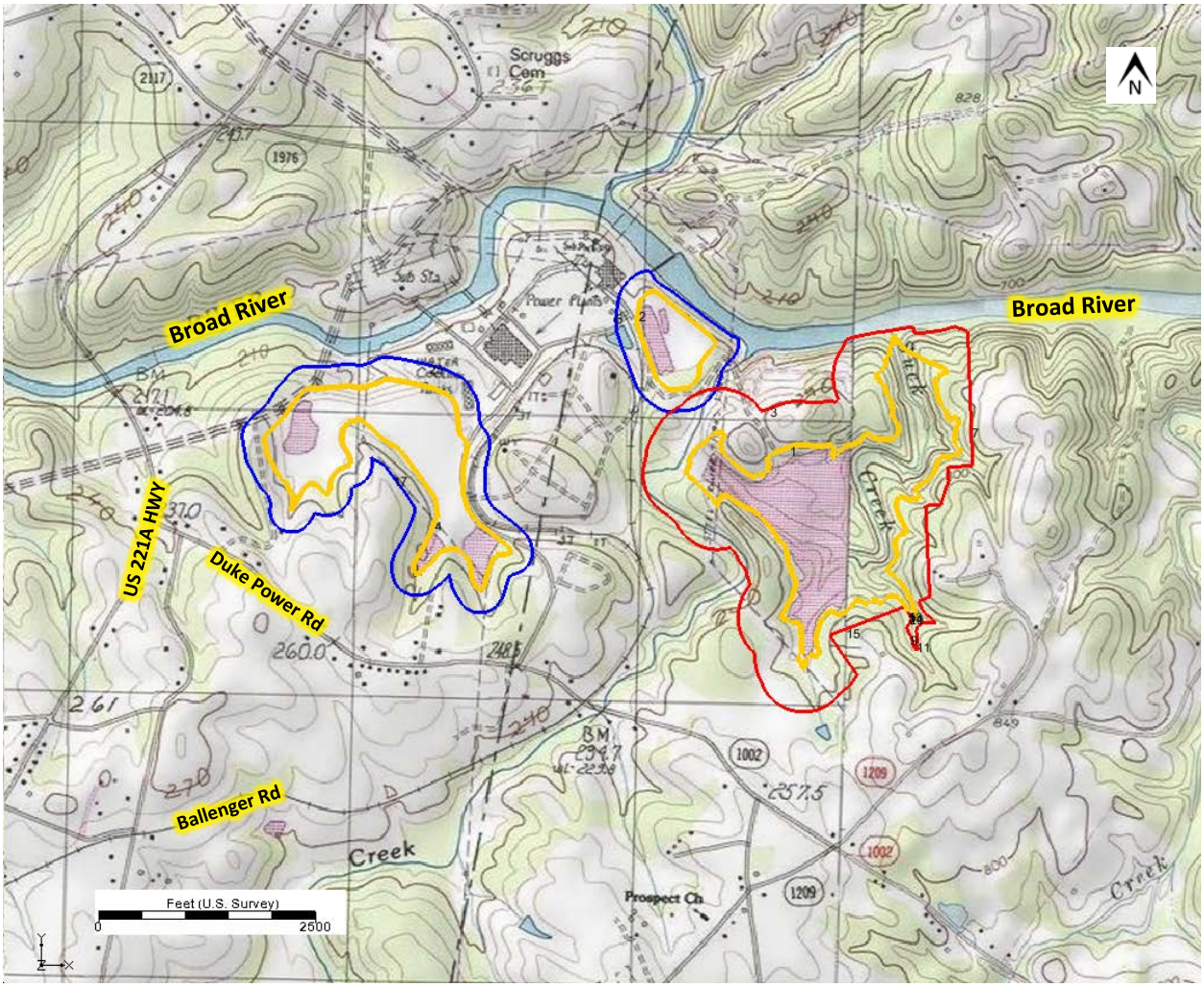

Figure 1-1 Site location map, Cliffside Steam Station, Cleveland County, NC. The red outline is the active ash basin compliance boundary, the blue outlines are the Former Units 1-4 and the Unit 5 inactive ash basin potential compliance boundaries, and the gold outlines are waste boundaries.

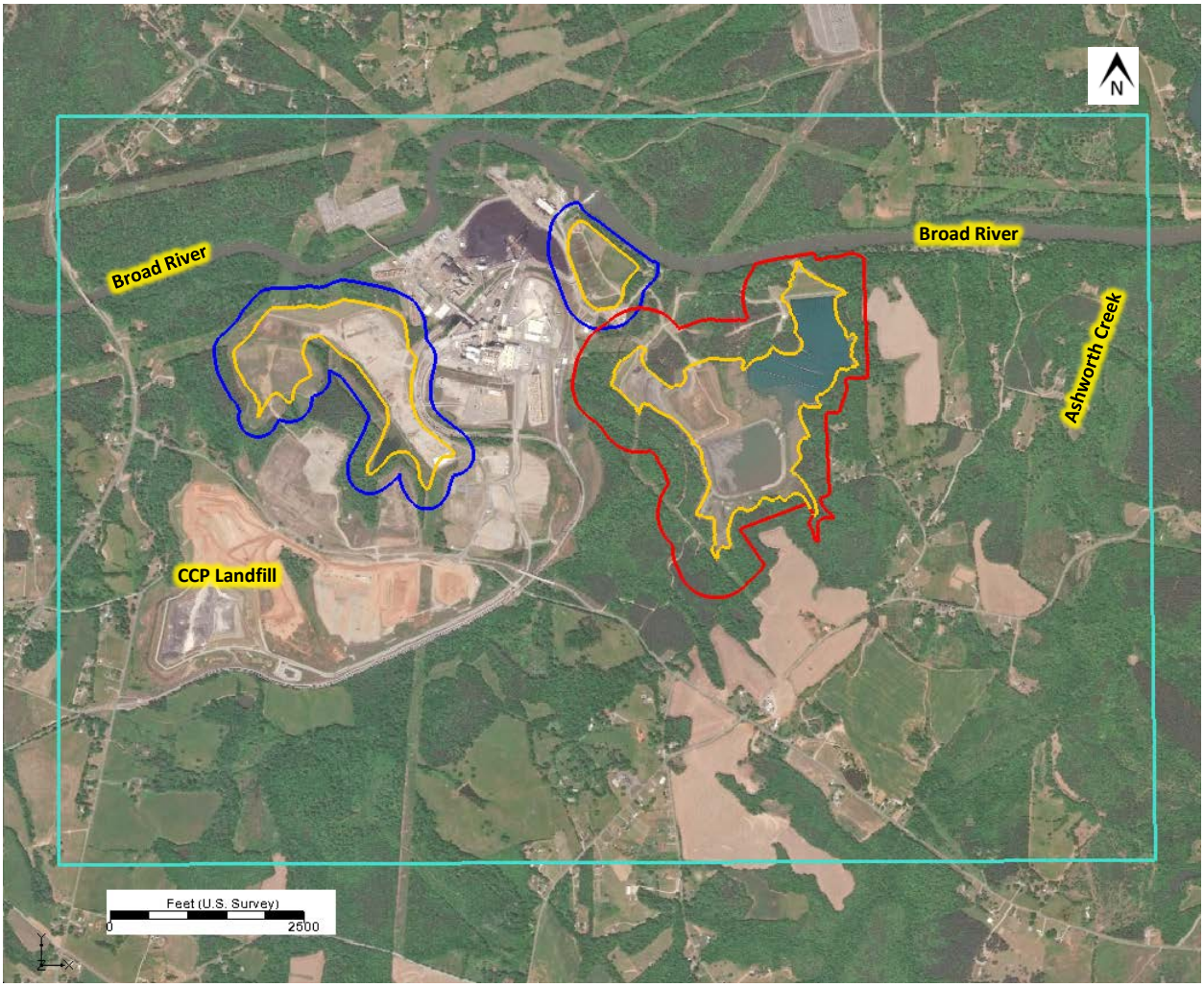

Figure 4-1. Numerical model domain. Domain is represented as the turquoise rectangle. The red outline is the active ash basin compliance boundary, the blue outlines are the Former Units 1-4 and the Unit 5 inactive ash basin compliance boundaries, and the gold outlines are waste boundaries.

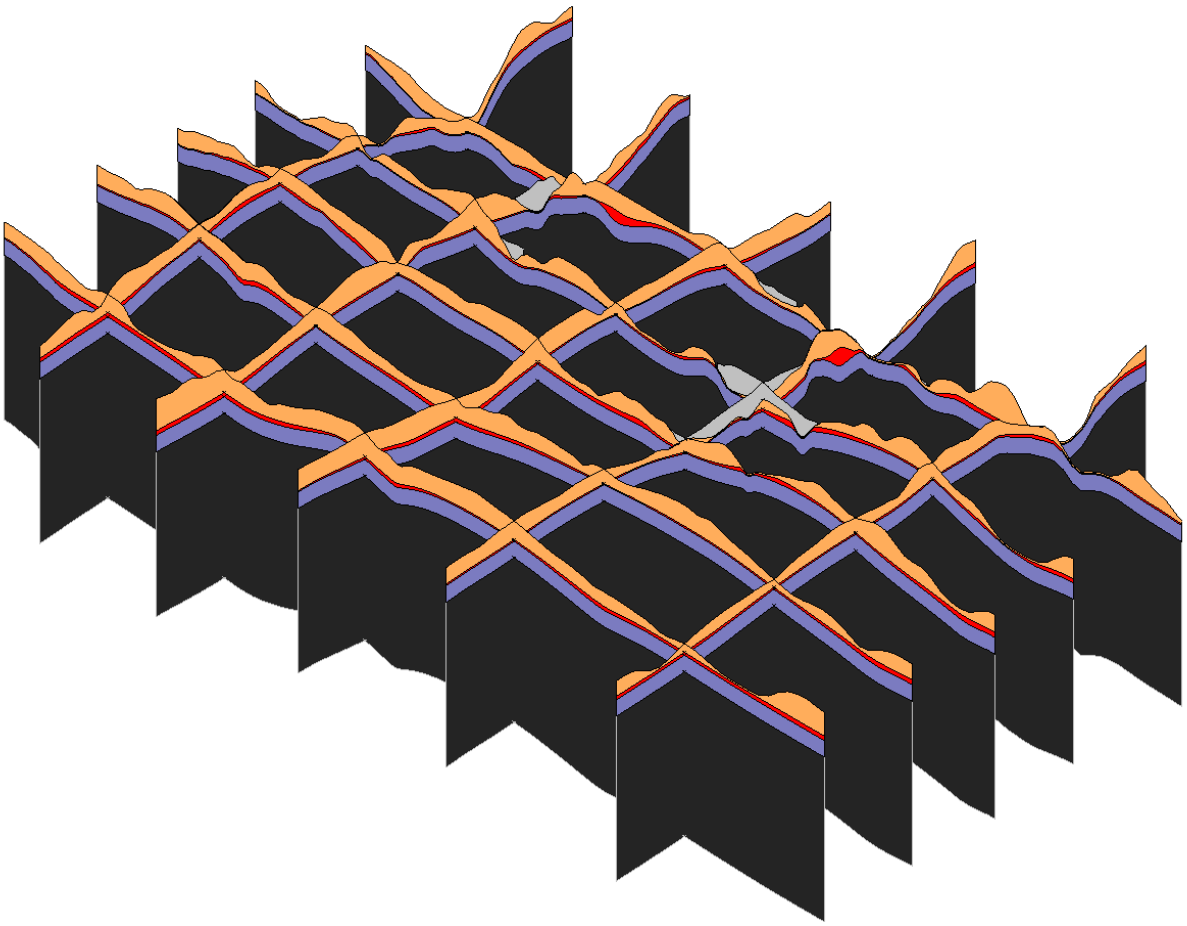

Figure 4-2. Fence diagram of the 3D hydrostratigraphic model used to construct the model grid. The view is to the northwest, with 5x vertical exaggeration. The light grey in the upper portion of the model represents ash, the orange layer is saprolite, red is the transition zone, purple is the fractured bedrock, and dark grey is competent bedrock.

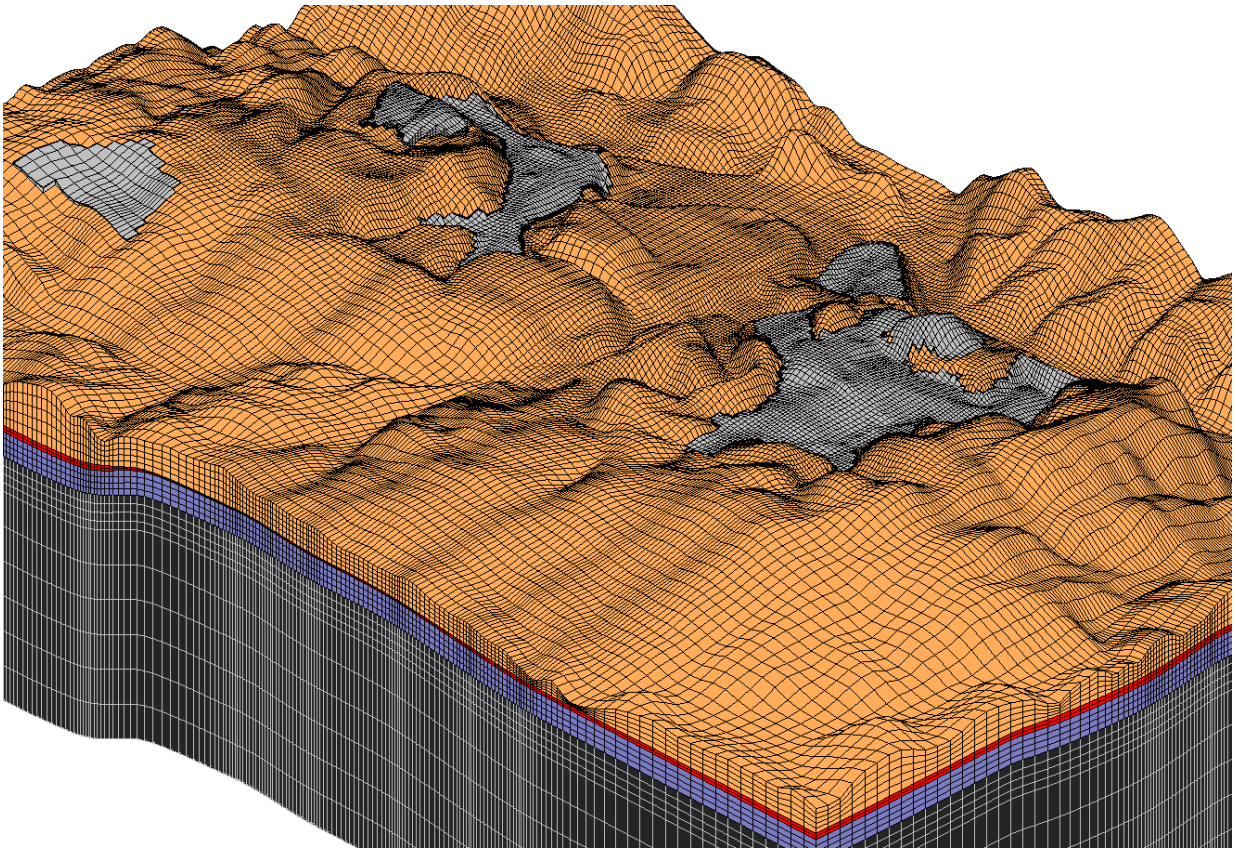

Figure 4-3. Numerical grid used for flow and transport modeling. Vertical exaggeration is 5x. Perspective of site looking northwest. Numerical grid used for flow and transport modeling. Grey represents ash, tan is saprolite, red is transition zone, purple is upper fractured bedrock, and dark grey is deep bedrock.

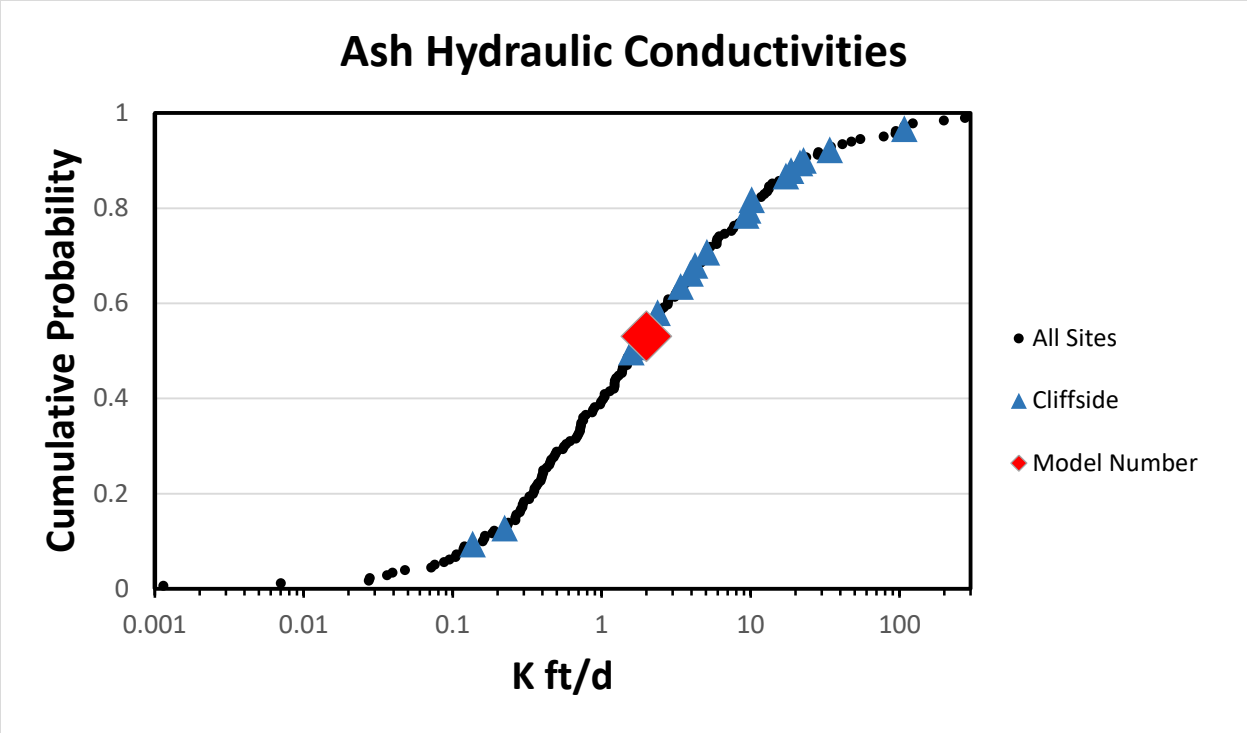

Figure 4-4. Hydraulic conductivity measured in slug tests performed in coal ash at 14 sites in North Carolina.

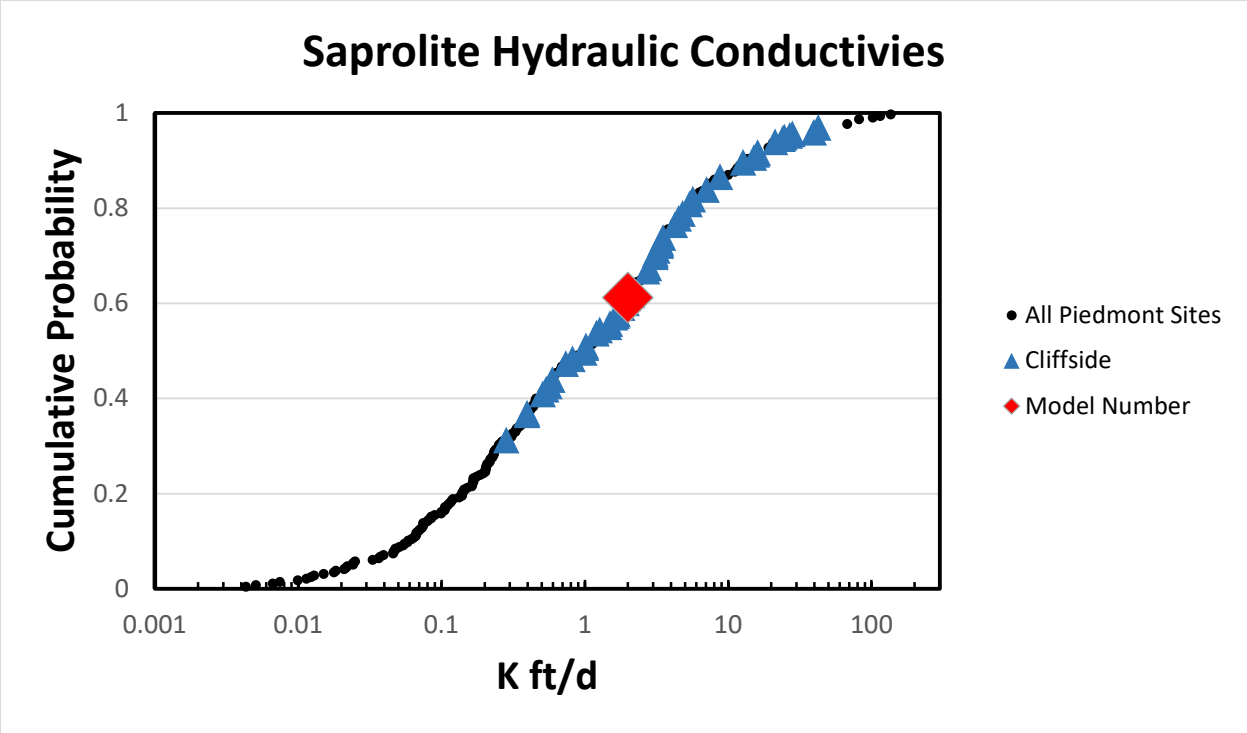

Figure 4-5. Hydraulic conductivity measured in slug tests performed in the transition zone at 10 Piedmont sites in North Carolina.

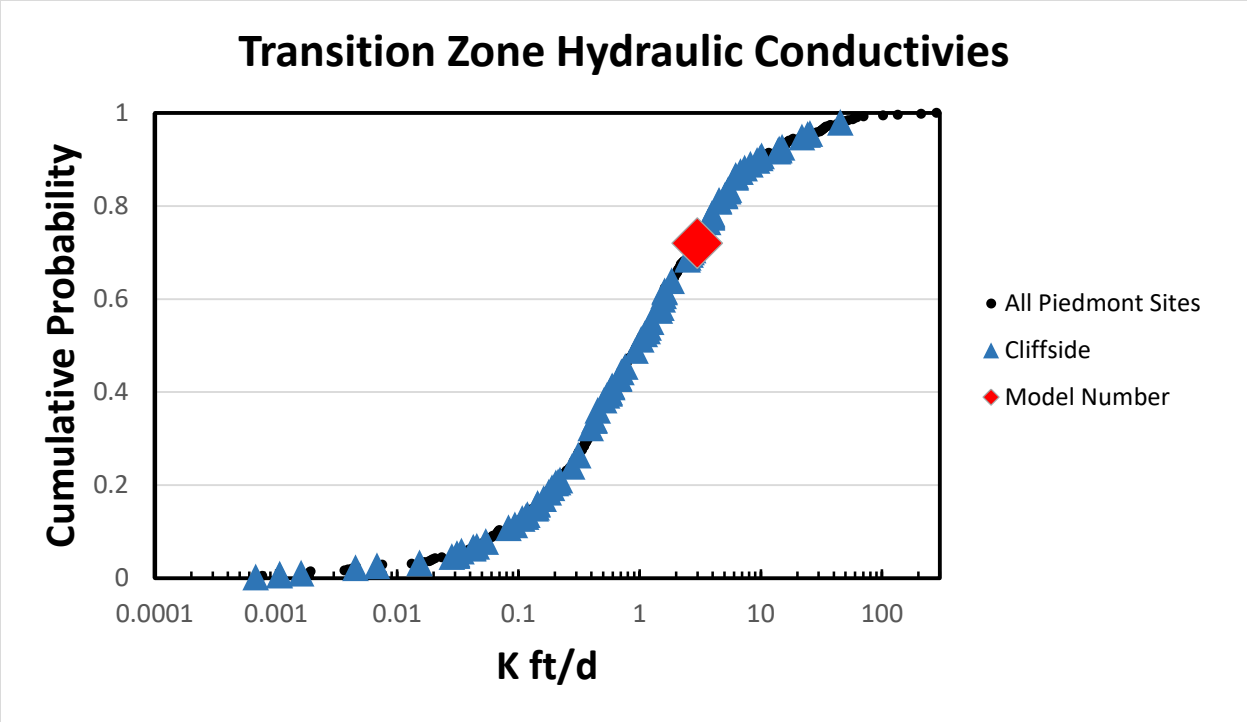

Figure 4-6. Hydraulic conductivity measured in slug tests performed in the transition zone at 10 Piedmont sites in North Carolina.

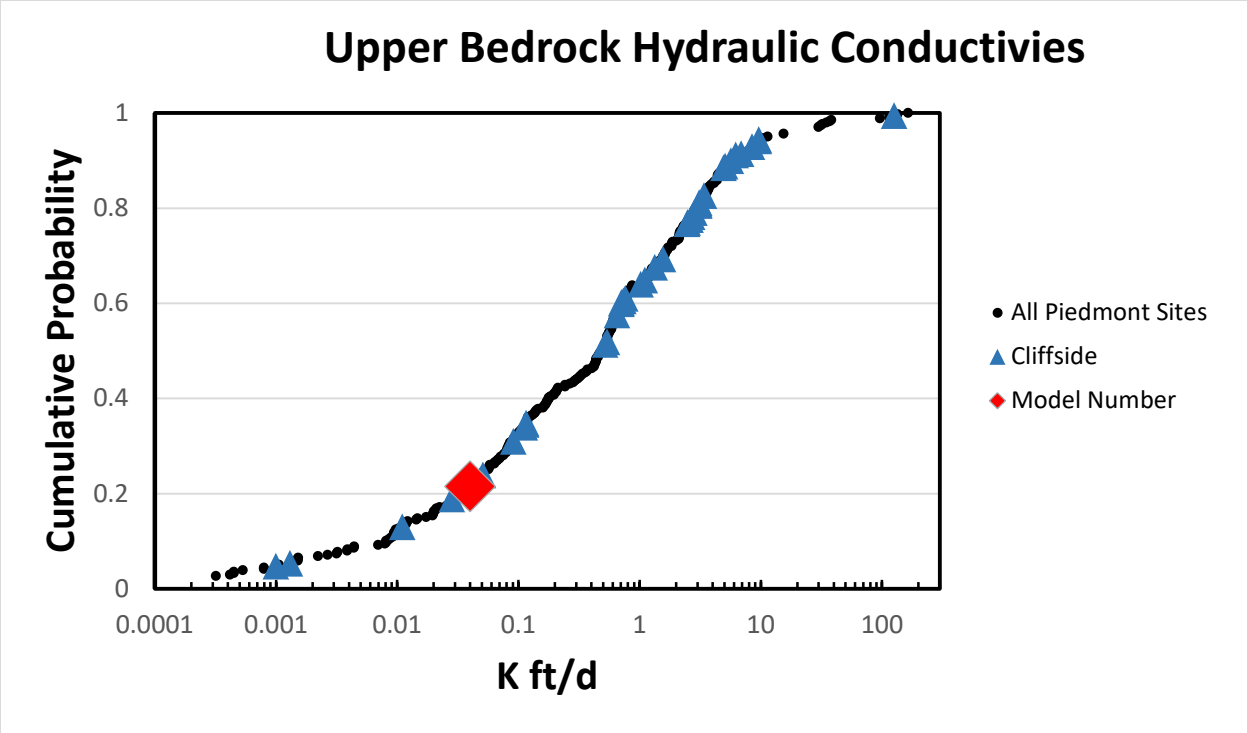

Figure 4-7. Hydraulic conductivity measured in slug tests performed in bedrock at 10 Piedmont sites in North Carolina.

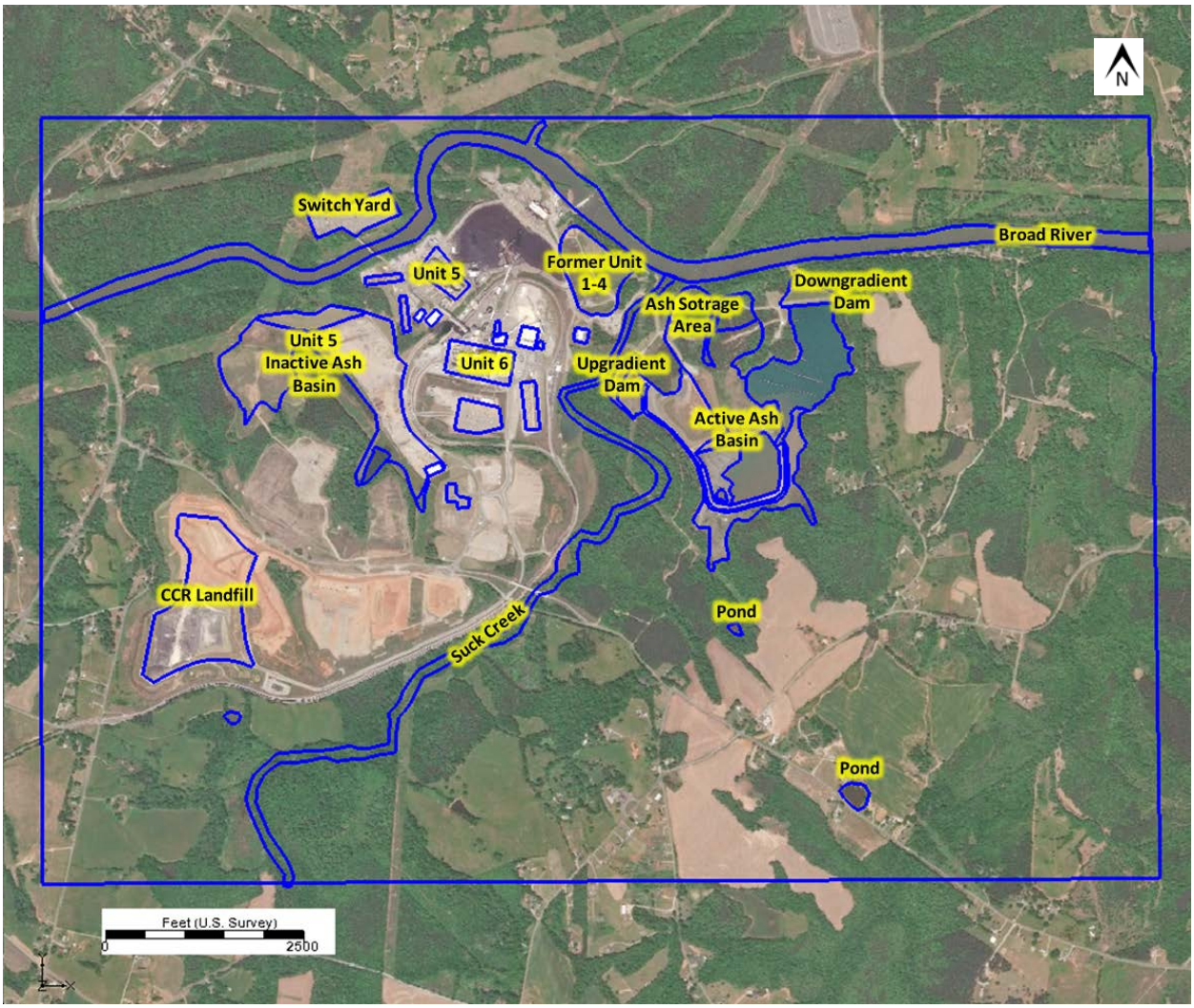

Figure 4-8. Distribution of recharge zones in the model. The background recharge rate is 7.5 inches/year. Blue lines represent different recharge zones.

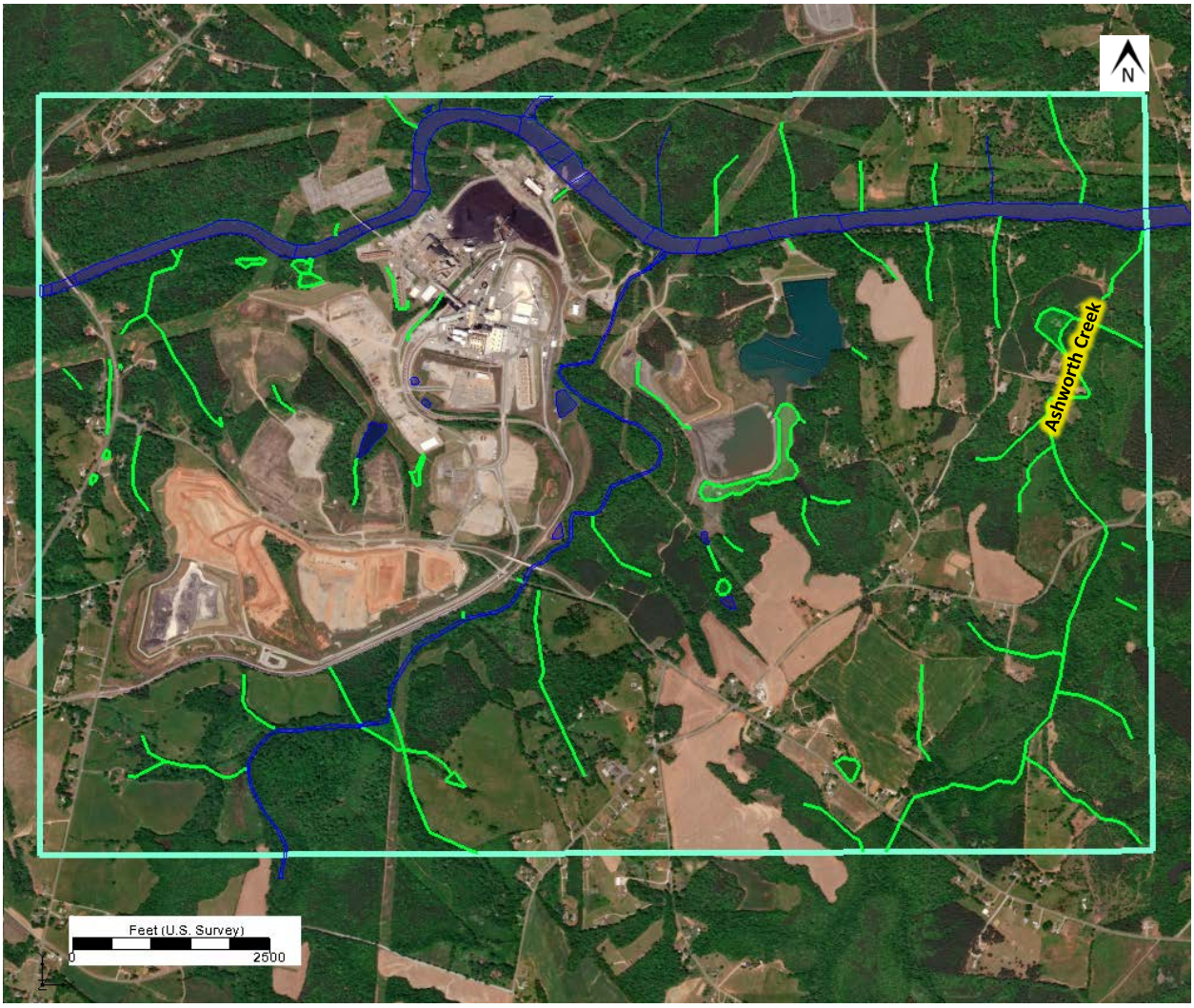

Figure 4-9. Surface water features included in the model outside of the ash basin area (the ash basin areas are shown in Figure 4.9). General heads such as the Broad River, Suck Creek and pond features are shown in blue and drains are shown in green. The outside turquoise line is the model boundary. The hydraulic features are in the uppermost active layer.

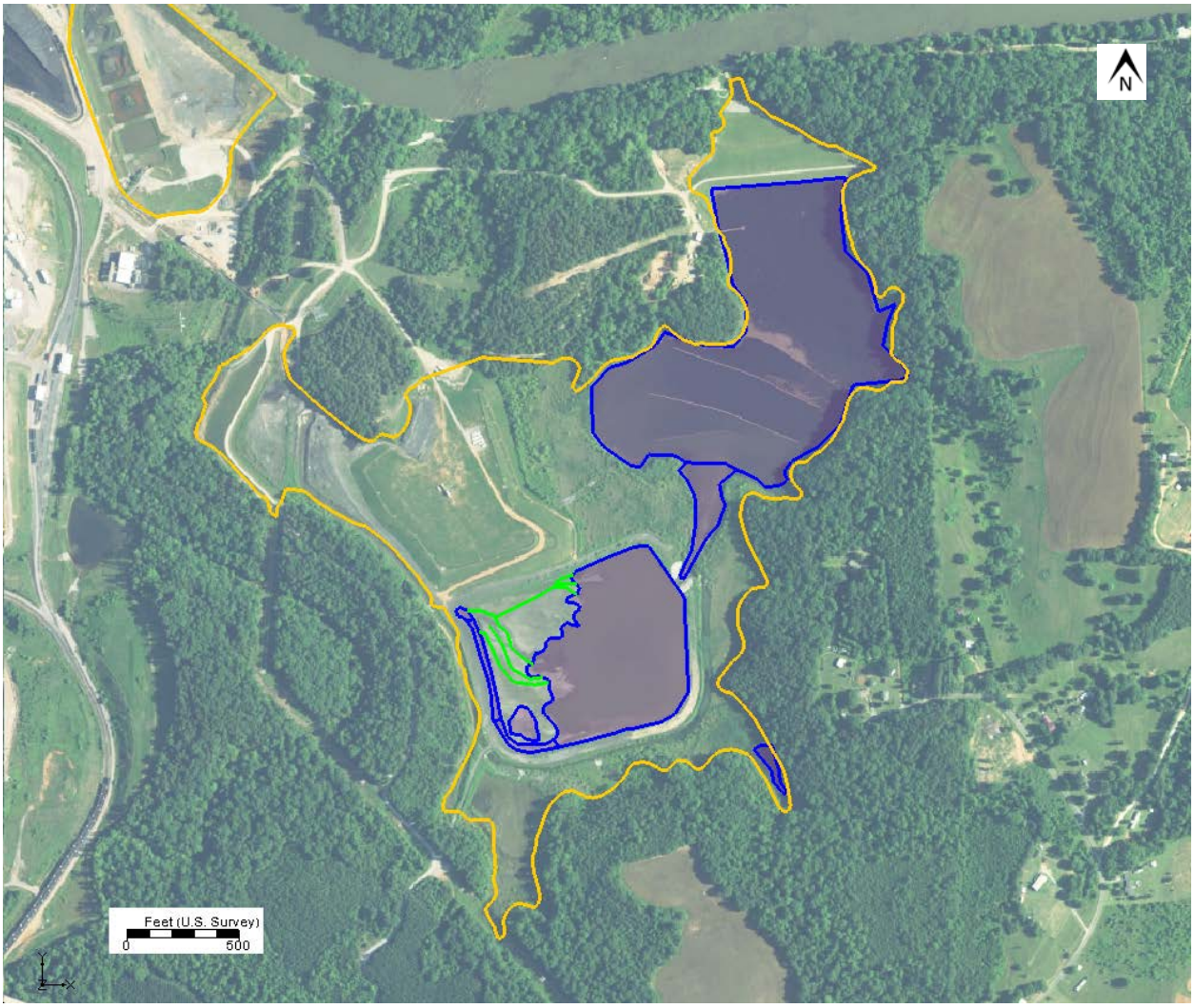

Figure 4-10. Surface water features included in the model in the active ash basin area. The area enclosed by dark blue represents the active ash basin pond, which is maintained at an elevation of approximately 759 feet in the northern portion and 765 feet in the southern portion. The gold lines represent the waste boundary for the active ash basin and Former Units 1-4 inactive ash basin.

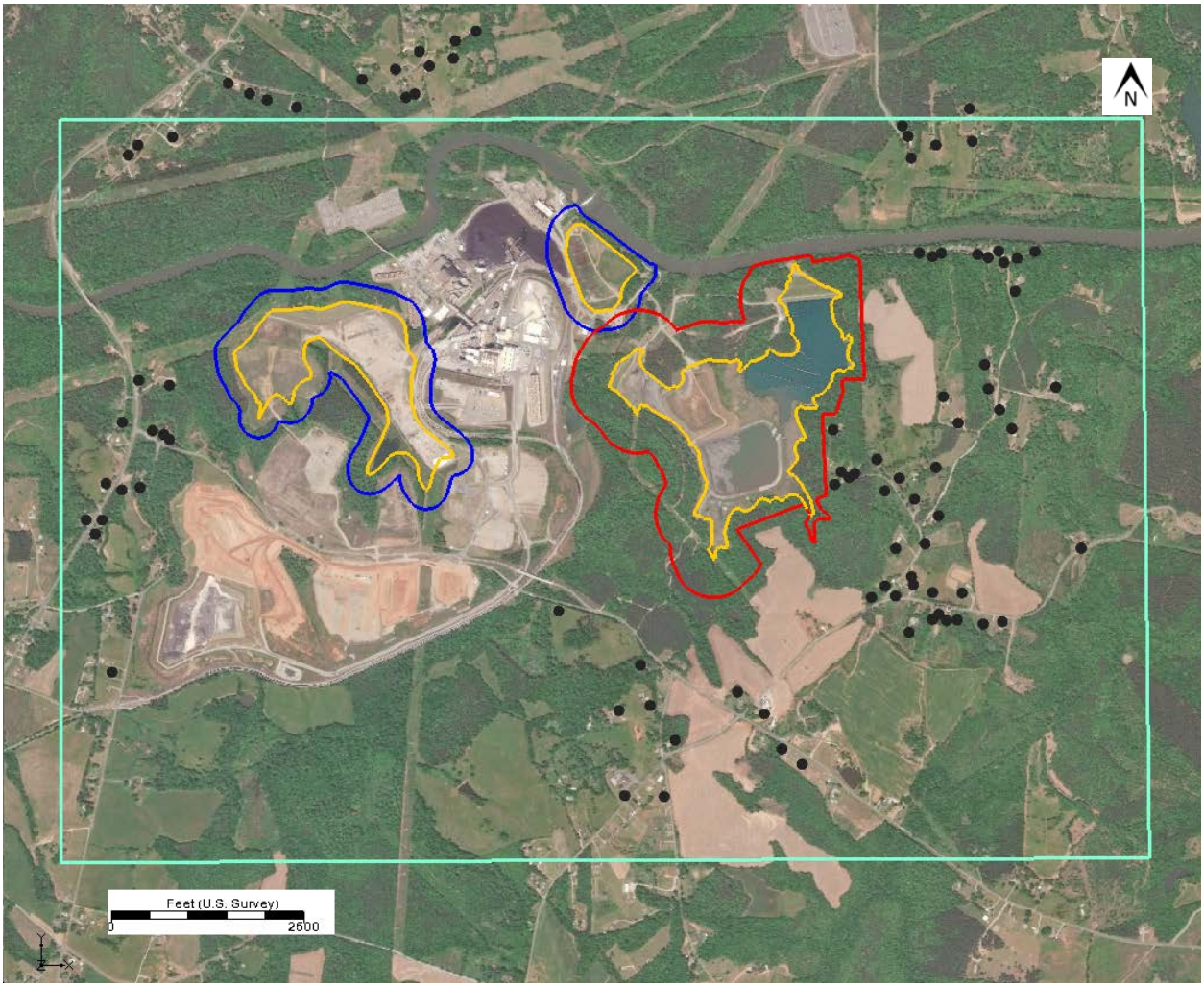

Figure 4-11. Location of water supply wells in the model area. Black symbols represent supply wells, the outside turquoise rectangle is the model domain. The red outline is the active ash basin compliance boundary, the blue outlines are the Former Units 1-4 and the Unit 5 inactive ash basin potential compliance boundaries, and the gold outlines are waste boundaries.

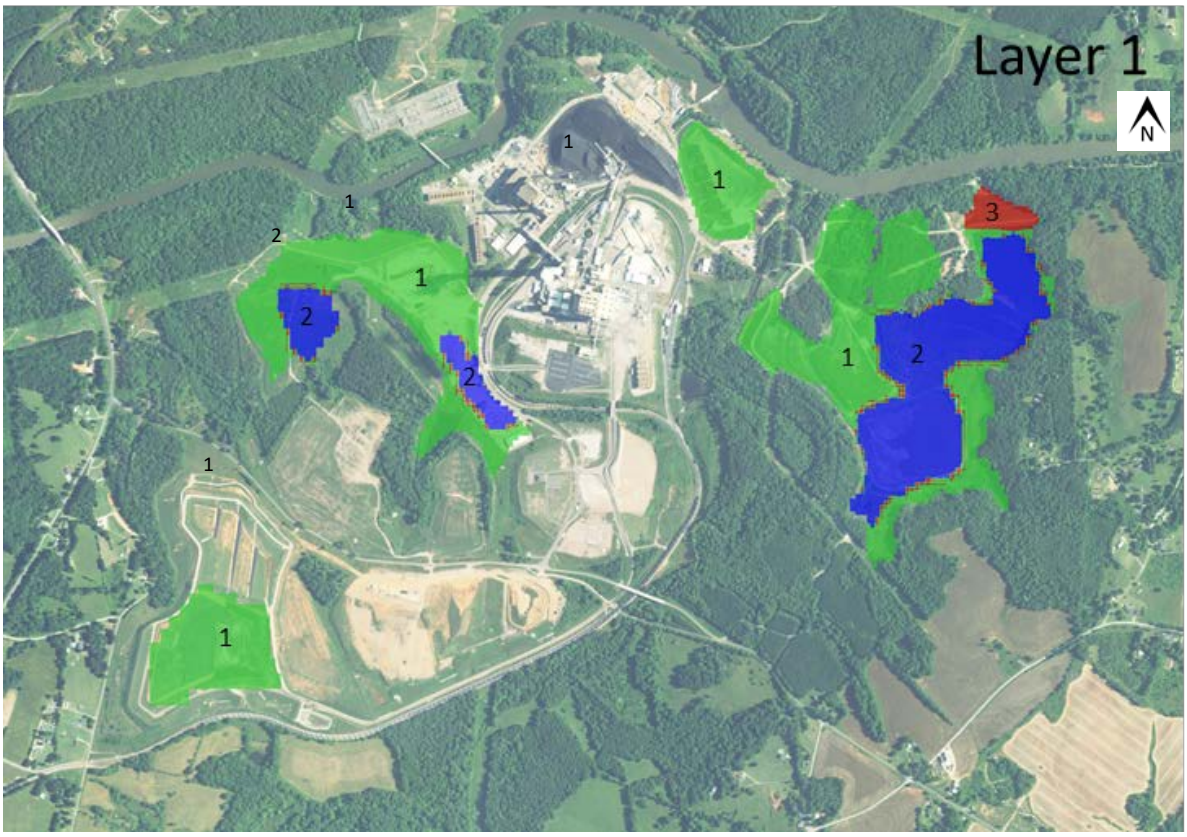

Figure 5-1a. Zones used to define horizontal hydraulic conductivity and horizontal to vertical anisotropy in the ash (model layer 1 shown). Blue regions are areas with high conductivity to represent future closure scenarios where ash would be stacked. The remainder of ash basins have conductivities of 2 ft/d.

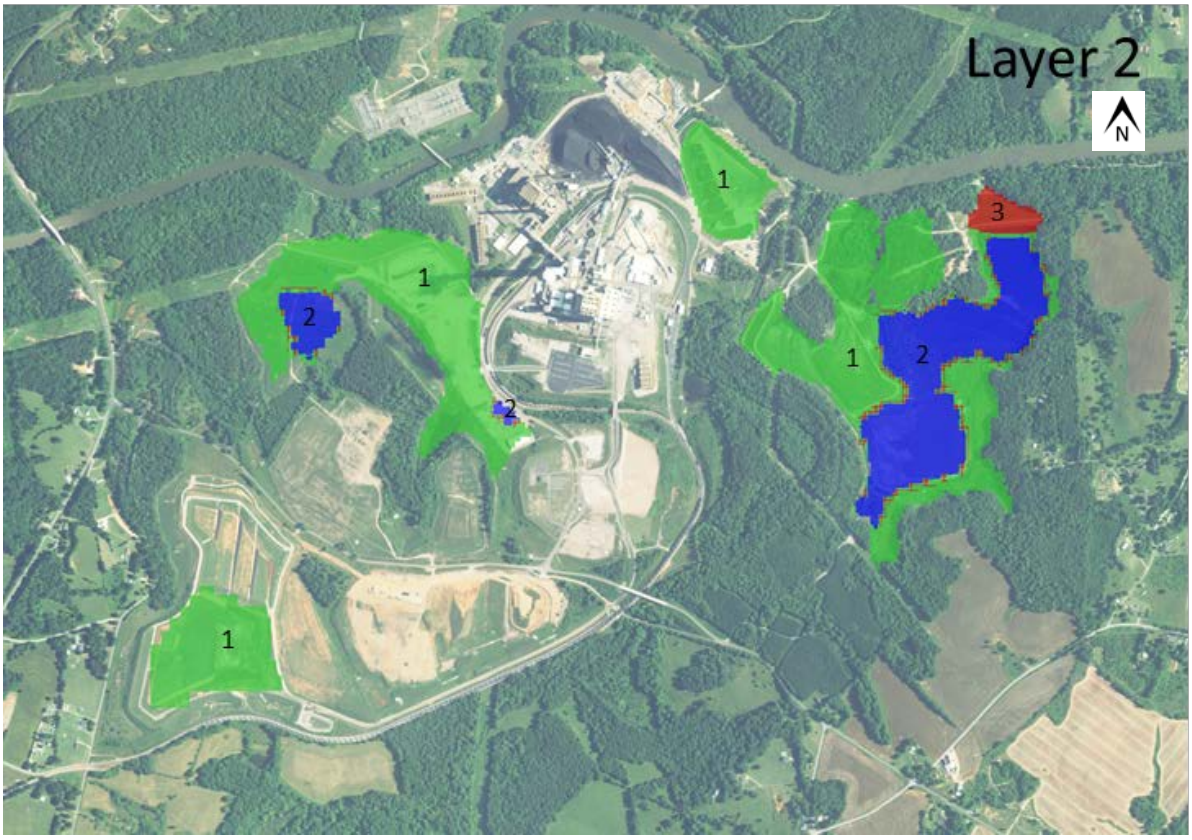

Figure 5-1b. Zones used to define horizontal hydraulic conductivity and horizontal to vertical anisotropy in the ash (model layer 2 shown). Blue regions are areas with high conductivity to represent future closure scenarios where ash would be stacked. The remainder of ash basins have conductivities of 2 ft/d.

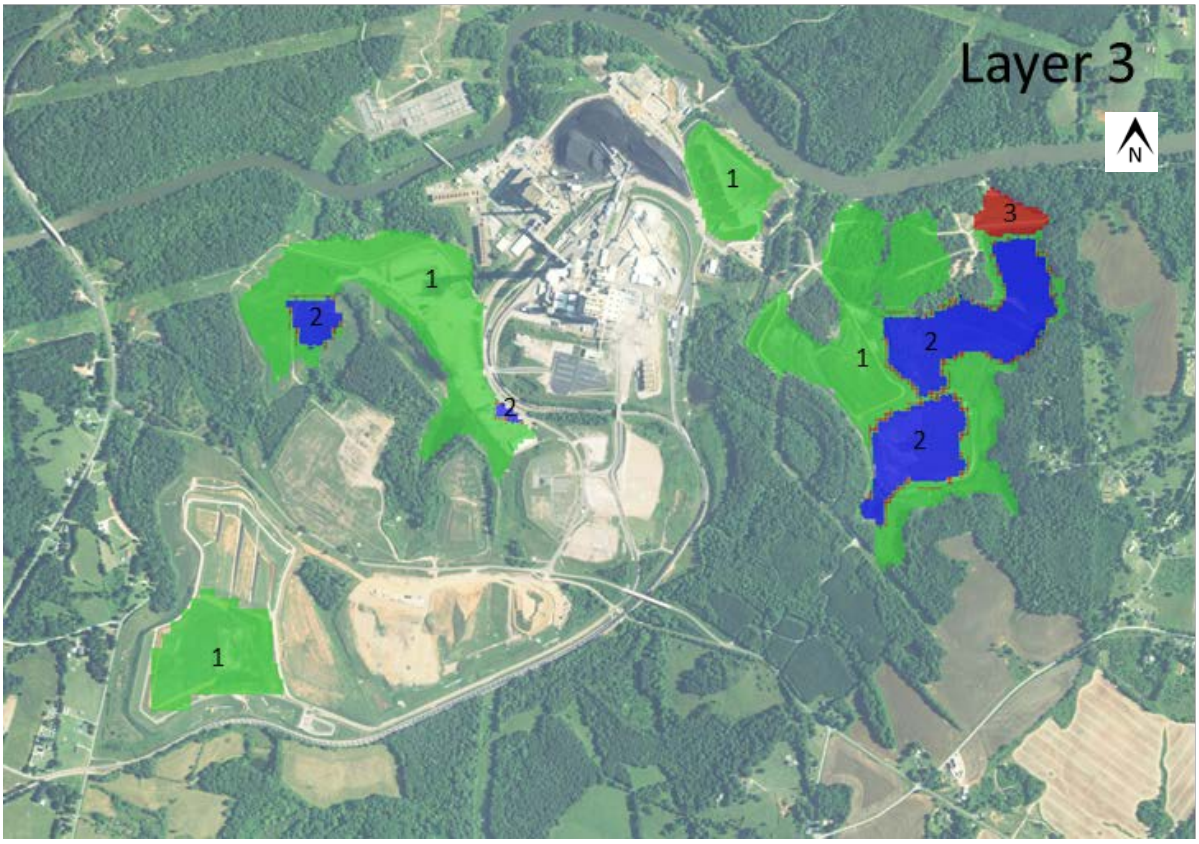

Figure 5-1c. Zones used to define horizontal hydraulic conductivity and horizontal to vertical anisotropy in the ash (model layer 3 shown). Blue regions are areas with high conductivity to represent future closure scenarios where ash would be stacked. The remainder of ash basins have conductivities of 2 ft/d.

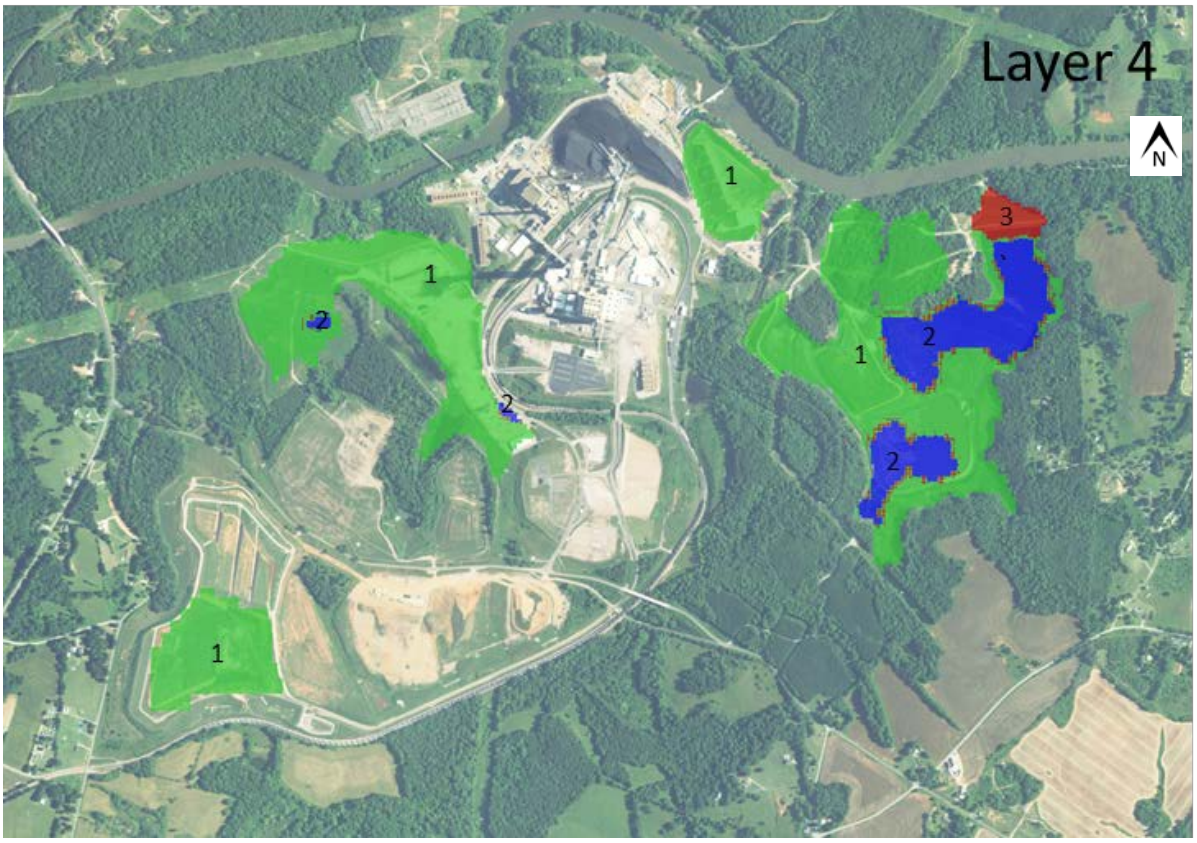

Figure 5-1d. Zones used to define horizontal hydraulic conductivity and horizontal to vertical anisotropy in the ash (model layer 4 shown). Blue regions are areas with high conductivity to represent future closure scenarios where ash would be stacked. The remainder of ash basins have conductivities of 2 ft/d.

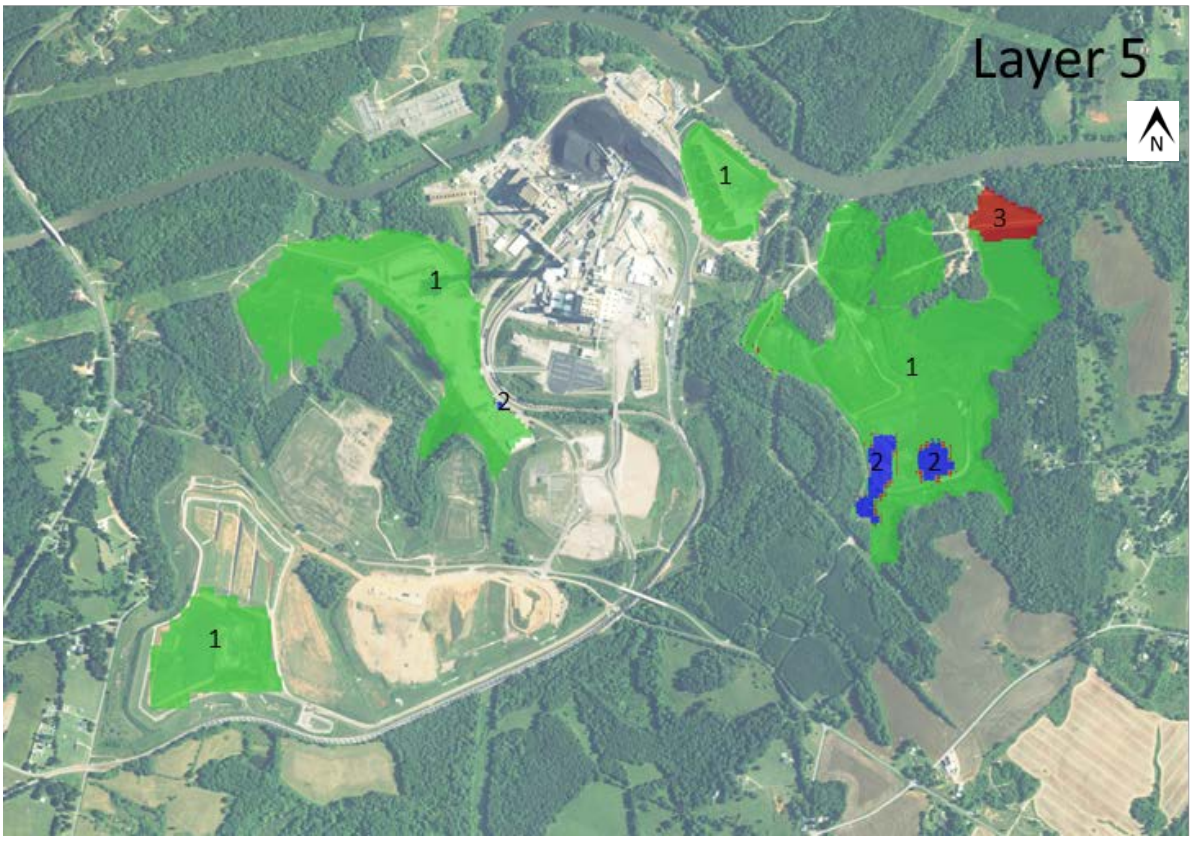

Figure 5-1e. Zones used to define horizontal hydraulic conductivity and horizontal to vertical anisotropy in the ash (model layer 5 shown). Blue regions are areas with high conductivity to represent future closure scenarios where ash would be stacked. The remainder of ash basins have conductivities of 2 ft/d.

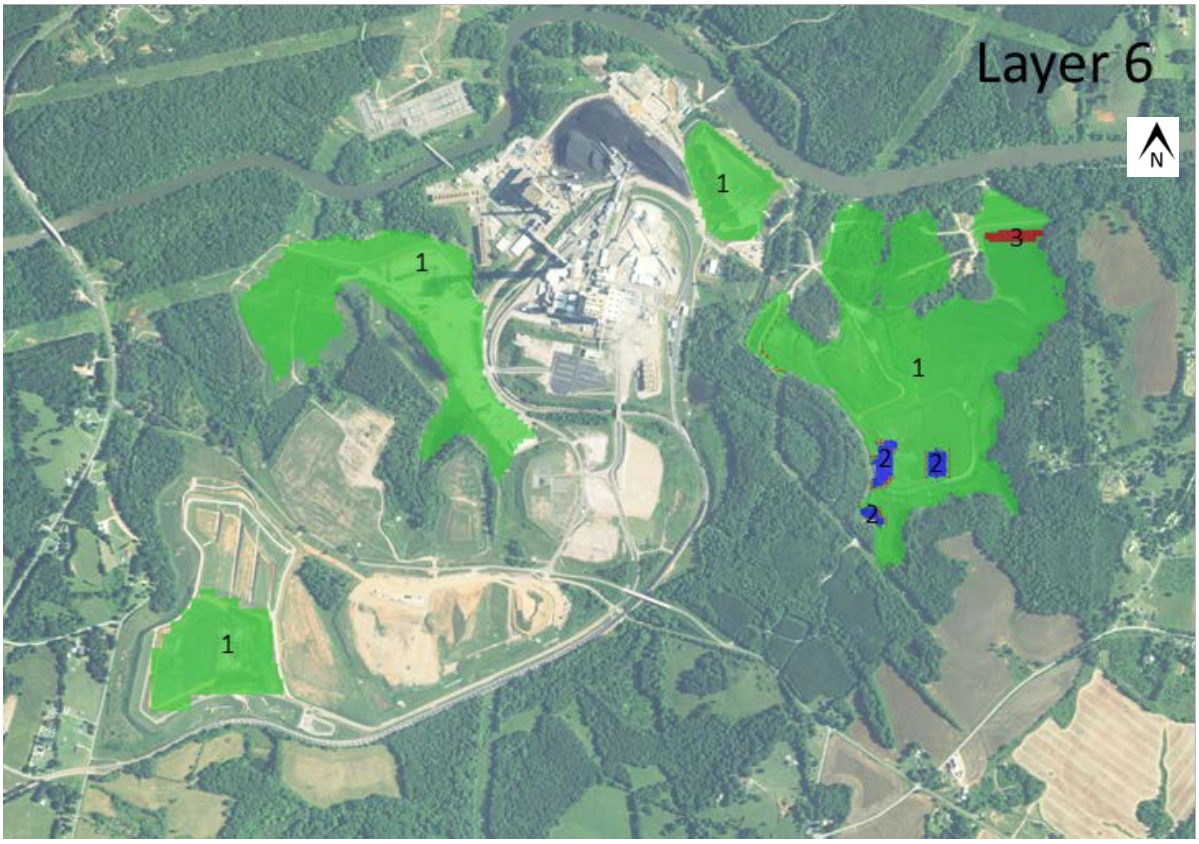

Figure 5-1f. Zones used to define horizontal hydraulic conductivity and horizontal to vertical anisotropy in the ash (model layer 6 shown). Blue regions are areas with high conductivity to represent future closure scenarios where ash would be stacked. The remainder of ash basins have conductivities of 2 ft/d.

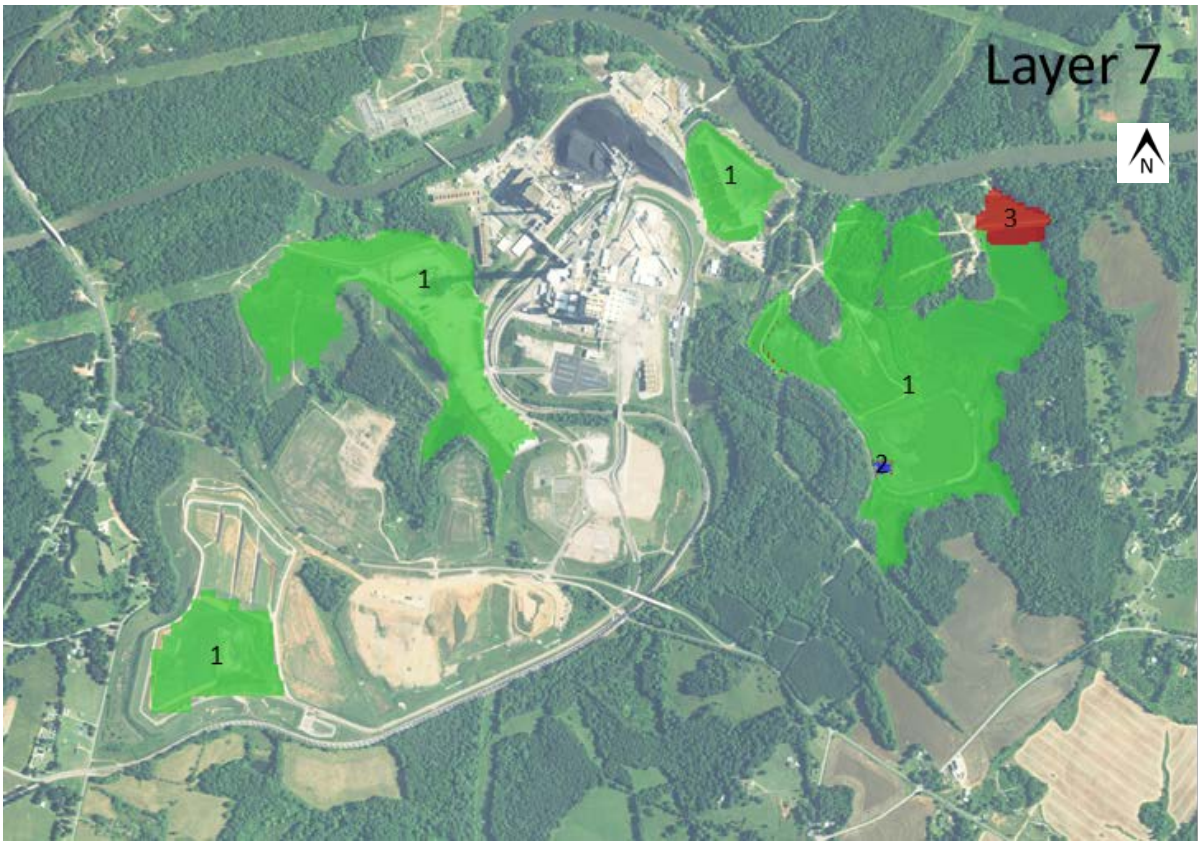

Figure 5-1g. Zones used to define horizontal hydraulic conductivity and horizontal to vertical anisotropy in the ash (model layer 7 shown). Blue regions are areas with high conductivity to represent future closure scenarios where ash would be stacked. The remainder of ash basins have conductivities of 2 ft/d.

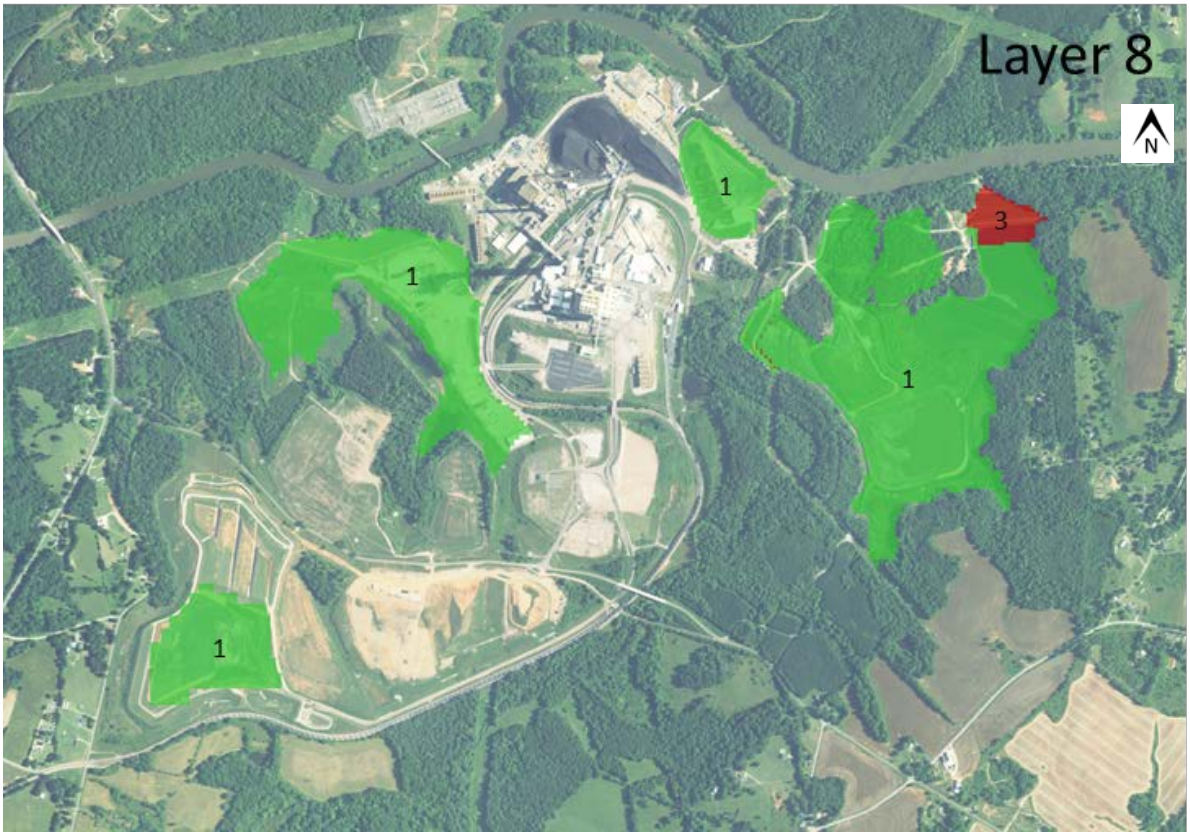

Figure 5-1h. Zones used to define horizontal hydraulic conductivity and horizontal to vertical anisotropy in the ash (model layer 8 shown). Blue regions are areas with high conductivity to represent future closure scenarios where ash would be stacked. The remainder of ash basins have conductivities of 2 ft/d.

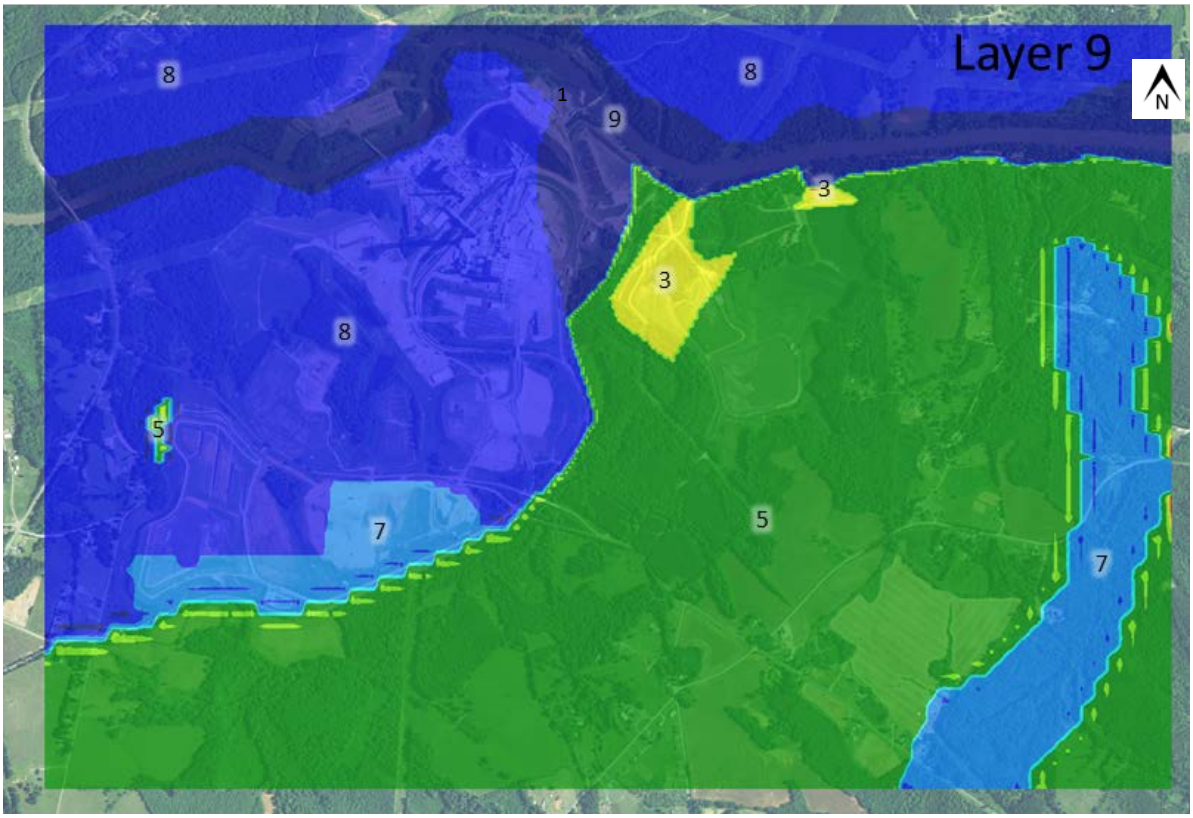

Figure 5-2a. Zones used to define horizontal hydraulic conductivity and horizontal to vertical anisotropy in the upper saprolite, model layer 9.

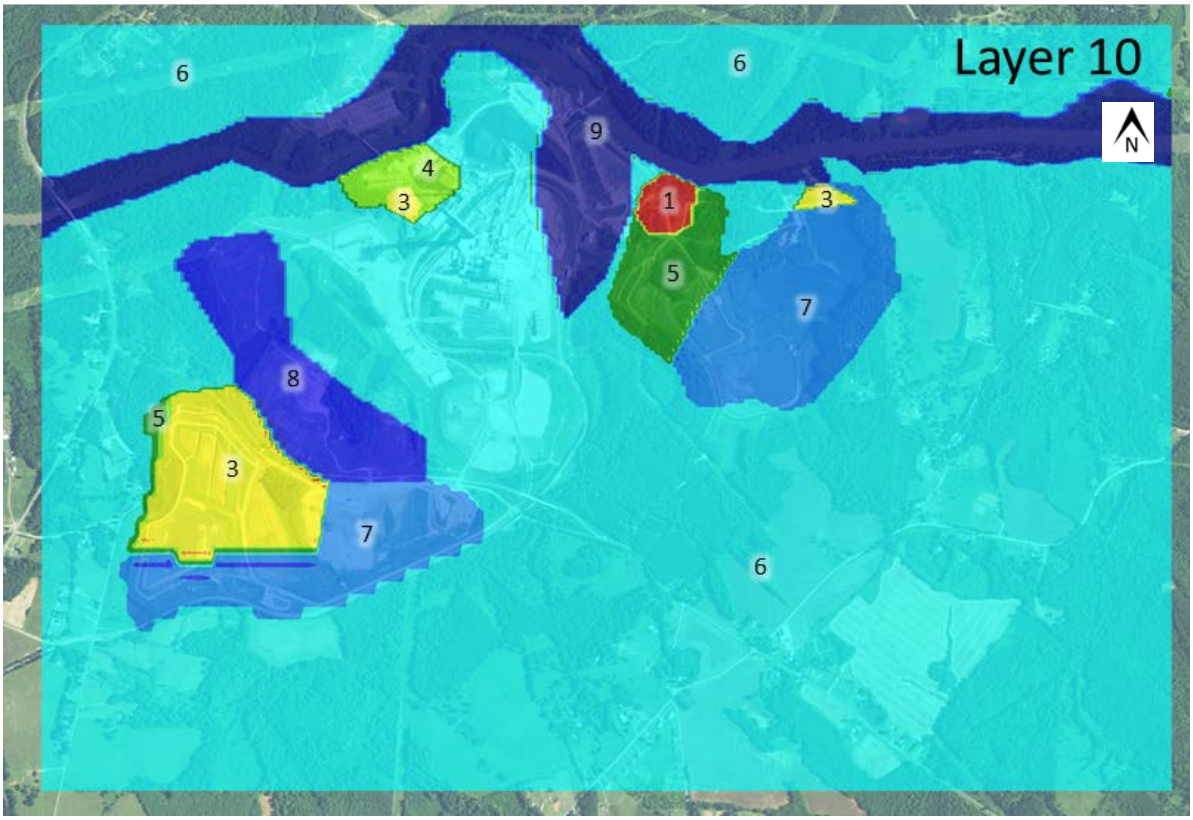

Figure 5-2b. Zones used to define horizontal hydraulic conductivity and horizontal to vertical anisotropy in the upper saprolite, model layer 10.

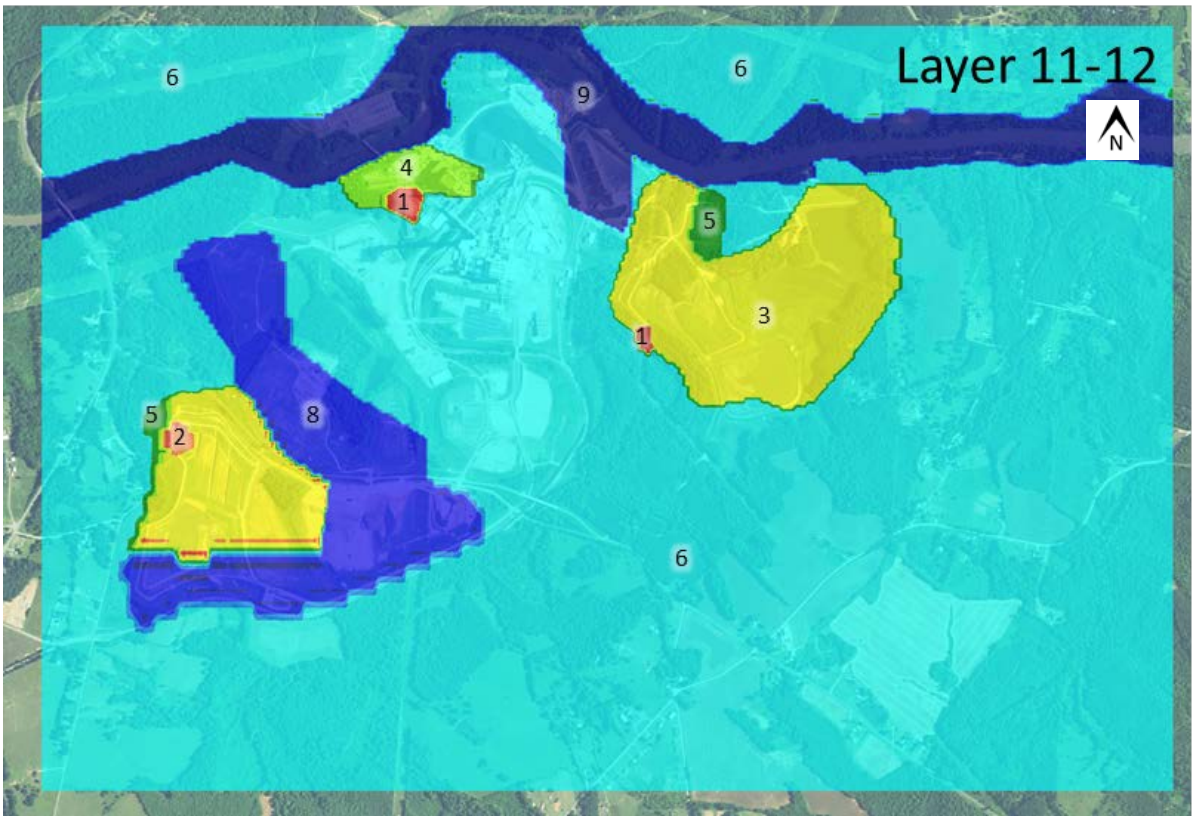

Figure 5-2c. Zones used to define horizontal hydraulic conductivity and horizontal to vertical anisotropy in the upper saprolite, model layer 11 and 12.

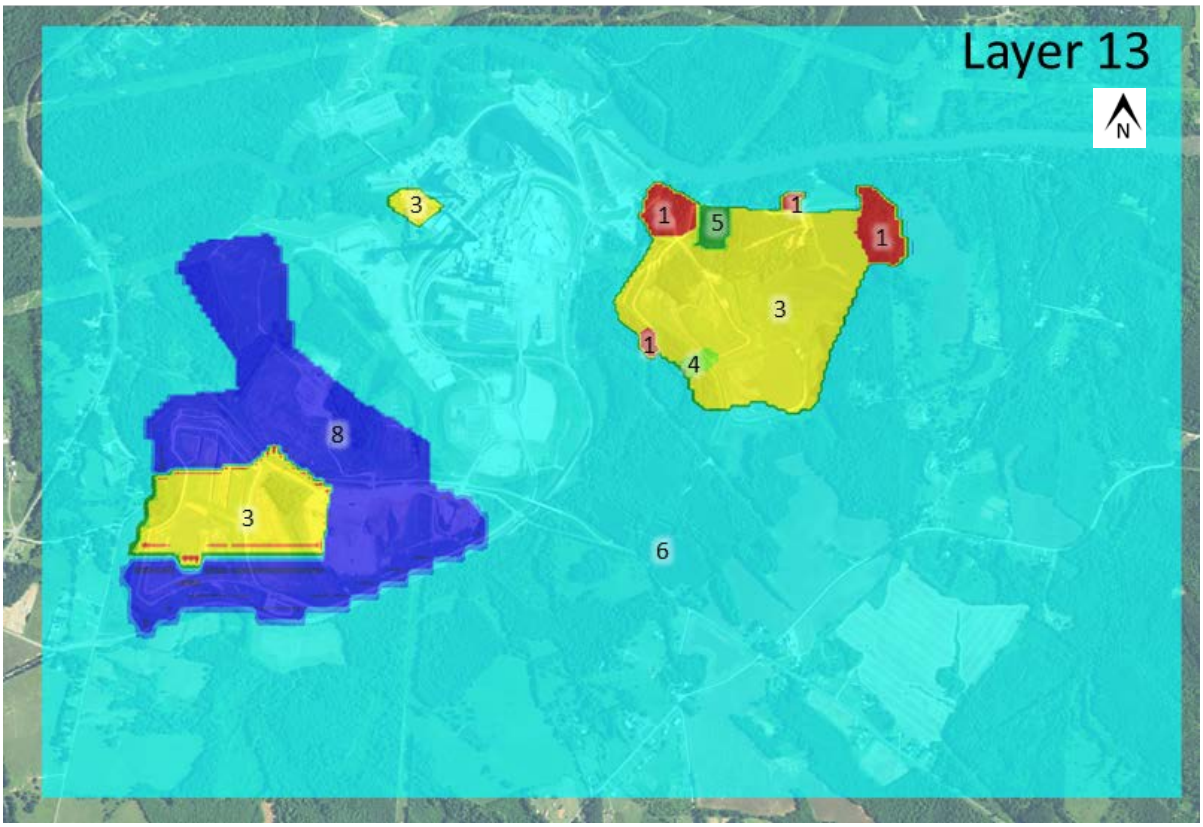

Figure 5-2d. Zones used to define horizontal hydraulic conductivity and horizontal to vertical anisotropy in the upper saprolite, model layer 13.

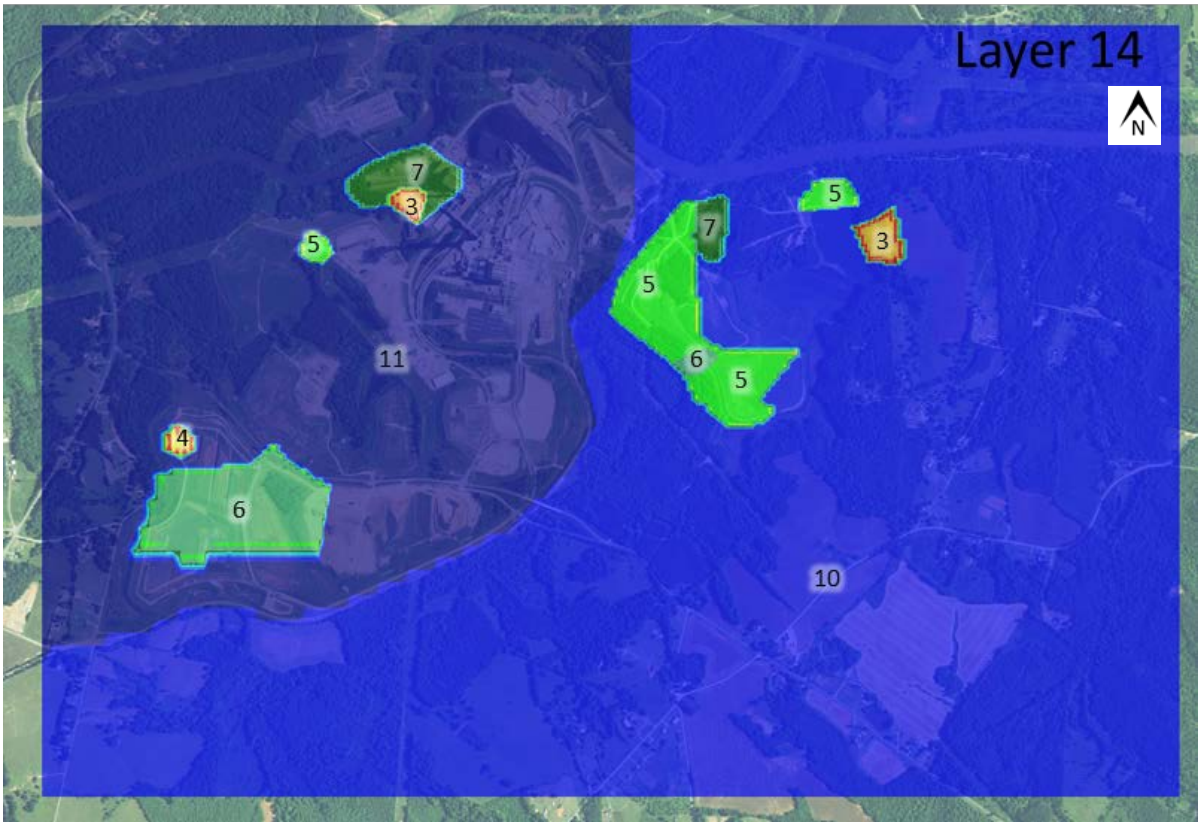

Figure 5-3a. Zones used to define horizontal hydraulic conductivity and horizontal to vertical anisotropy in the transition zone, model layer 14.

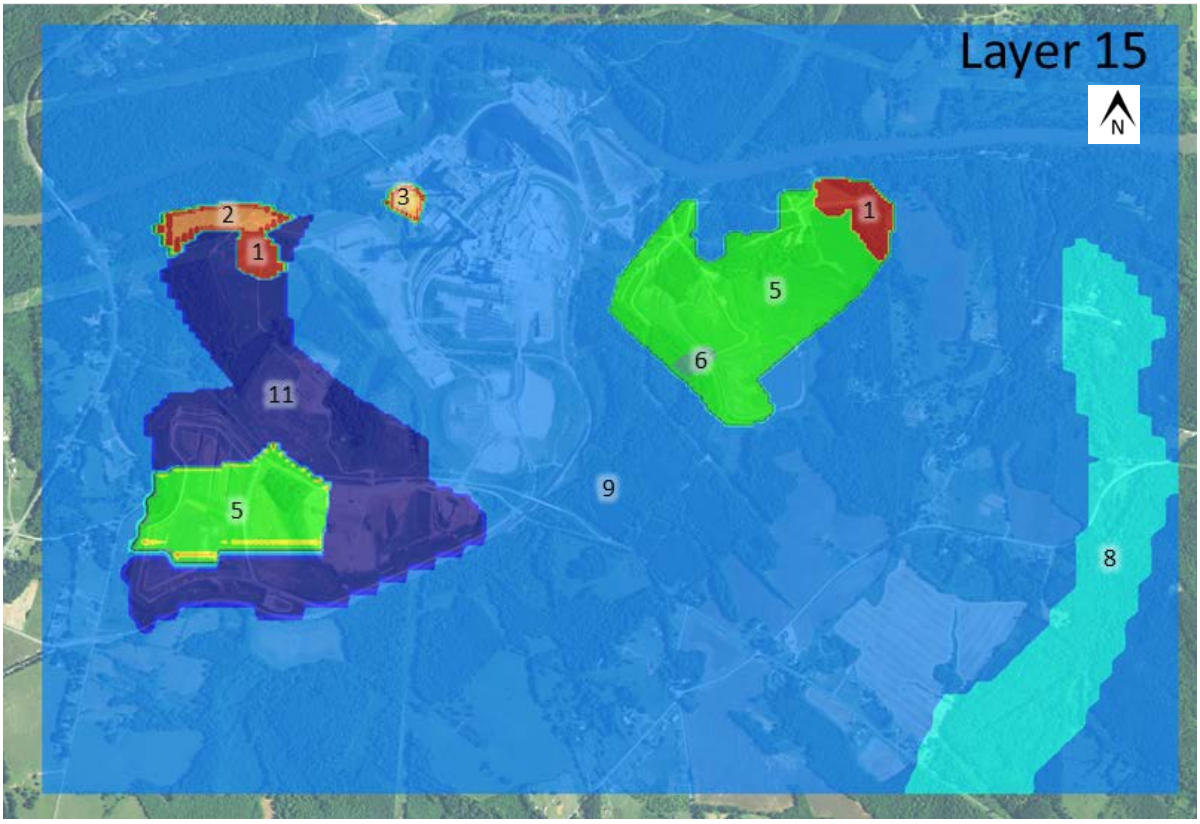

Figure 5-3b. Zones used to define horizontal hydraulic conductivity and horizontal to vertical anisotropy in the transition zone, model layer 15.

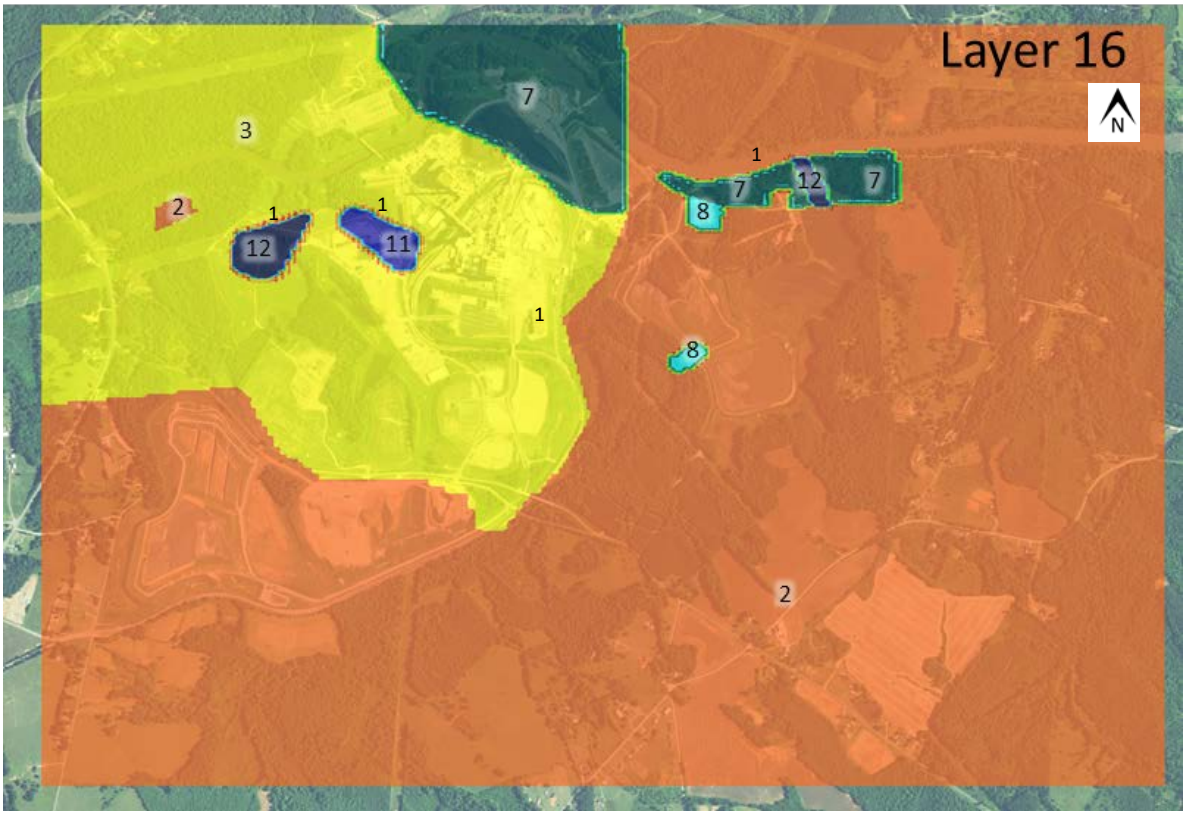

Figure 5-4. Zones used to define horizontal hydraulic conductivity and horizontal to vertical anisotropy in the transition zone/upper bedrock, model layer 16.

Figure 5-5a. Zones used to define horizontal hydraulic conductivity and horizontal to vertical anisotropy in the upper bedrock, model layer 17.

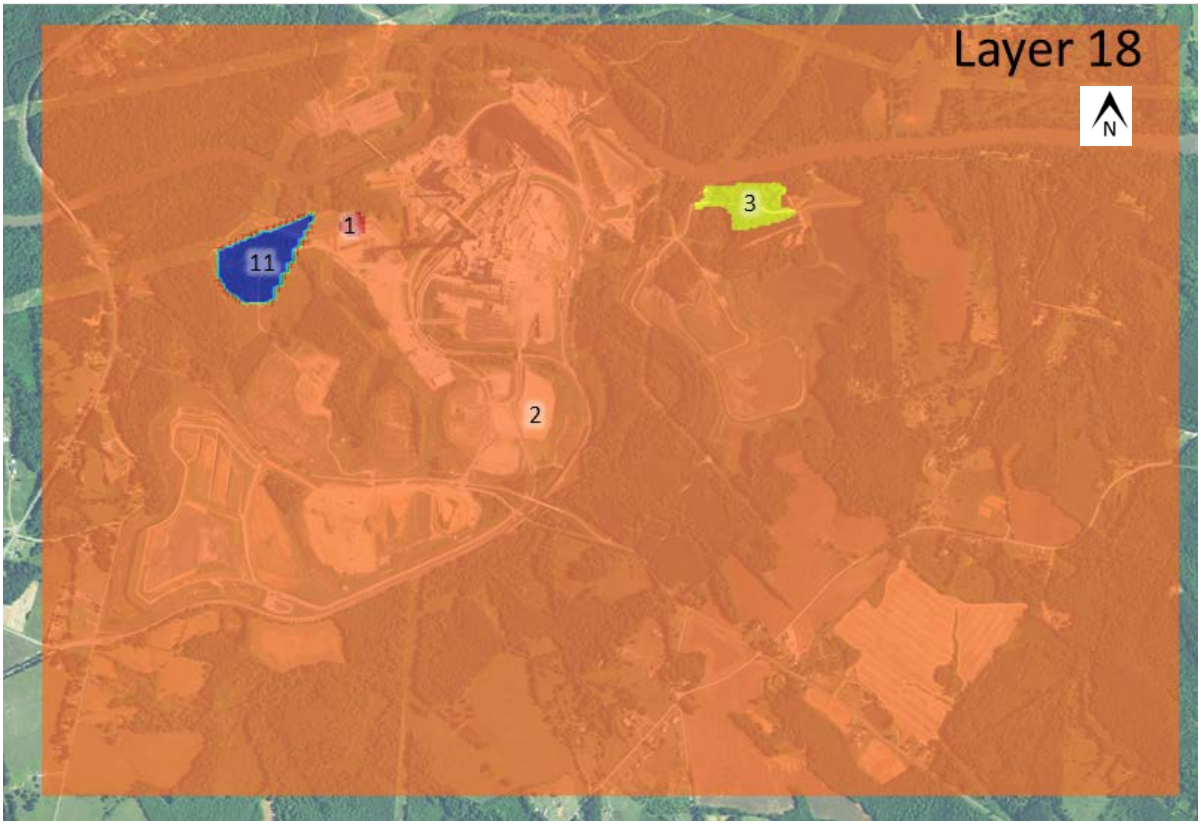

Figure 5-5b. Zones used to define horizontal hydraulic conductivity and horizontal to vertical anisotropy in the upper bedrock, model layer 18.

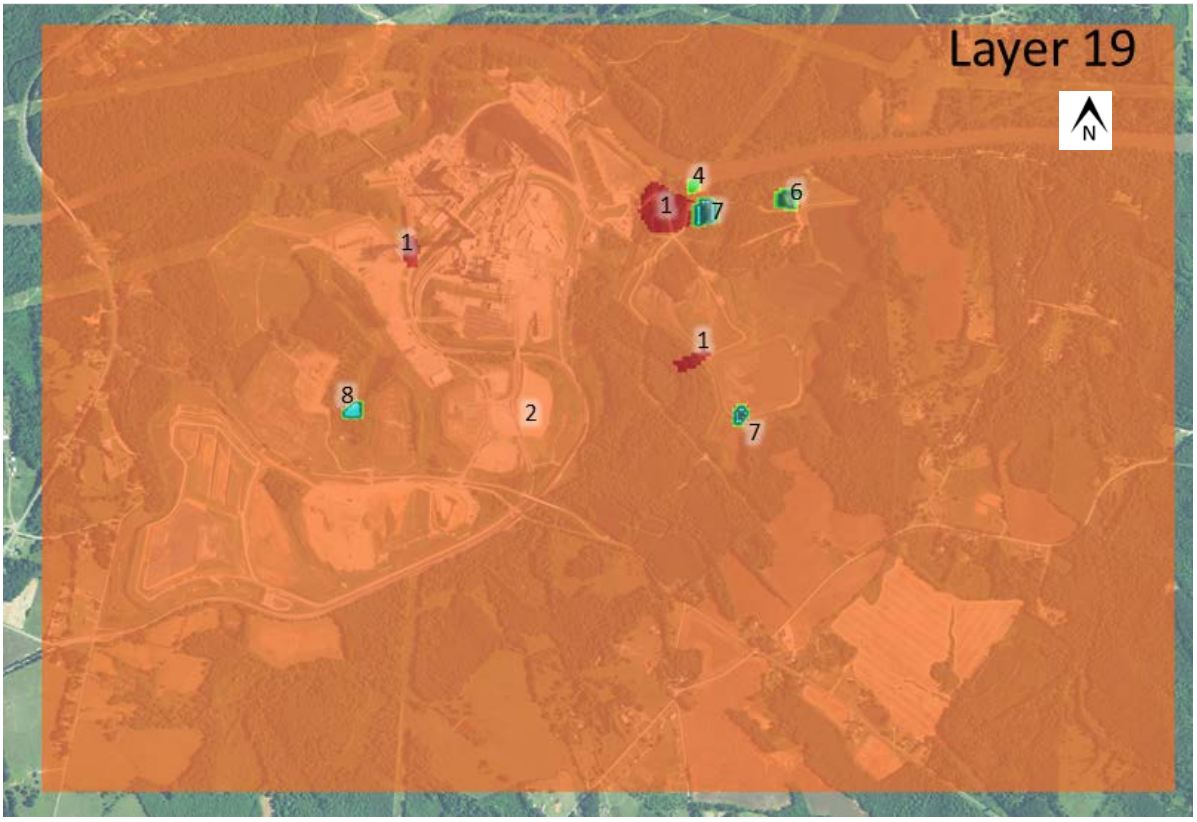

Figure 5-5c. Zones used to define horizontal hydraulic conductivity and horizontal to vertical anisotropy in the upper bedrock, model layer 19.

Figure 5-5d. Zones used to define horizontal hydraulic conductivity and horizontal to vertical anisotropy in the upper bedrock, model layer 20.

Figure 5-6a. Zones used to define horizontal hydraulic conductivity and horizontal to vertical anisotropy in the bedrock, model layer 21.

Figure 5-6b. Zones used to define horizontal hydraulic conductivity and horizontal to vertical anisotropy in the bedrock, model layer 22.

Figure 5-7. Zones used to define horizontal hydraulic conductivity and horizontal to vertical anisotropy in the deep bedrock, model layers 23-28.

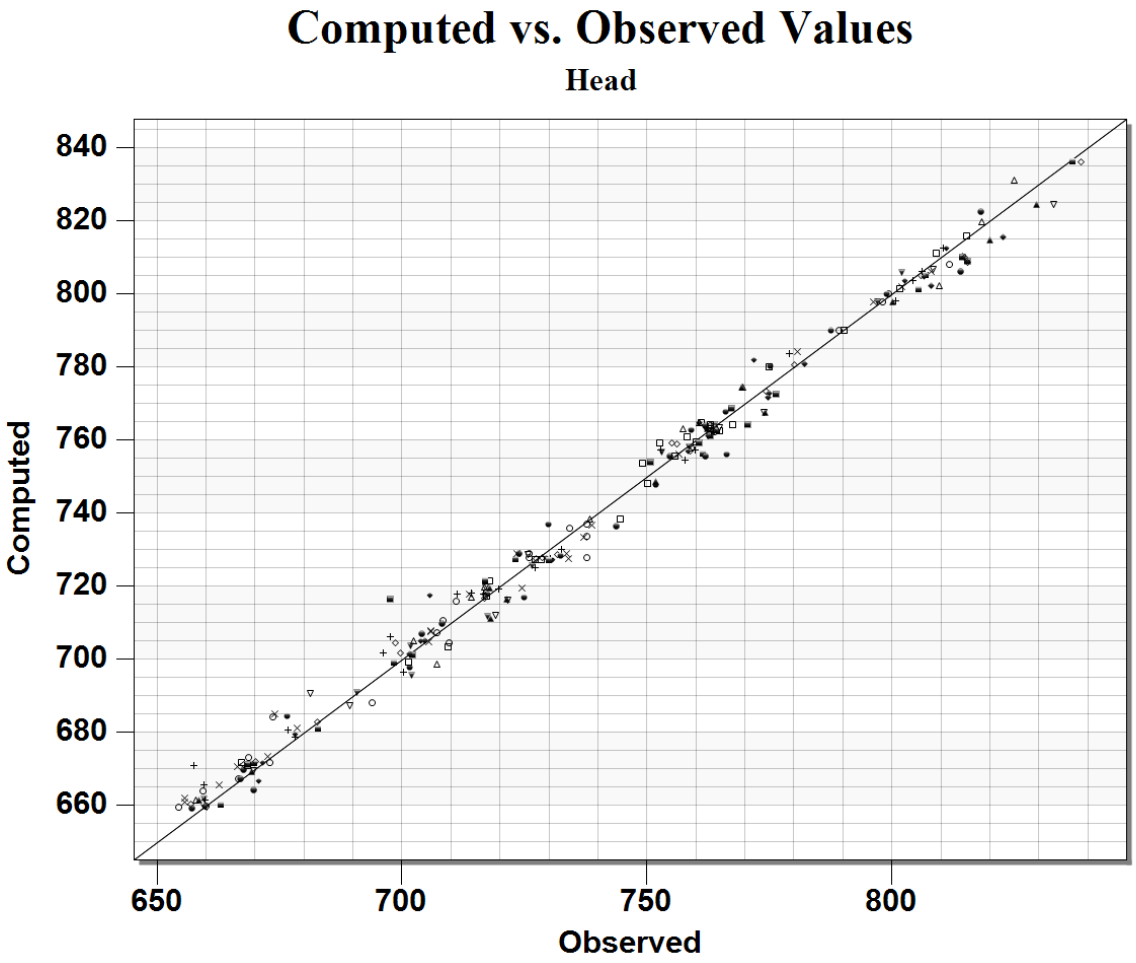

Figure 5-8. Comparison of observed and computed heads from the calibrated steady state flow model.

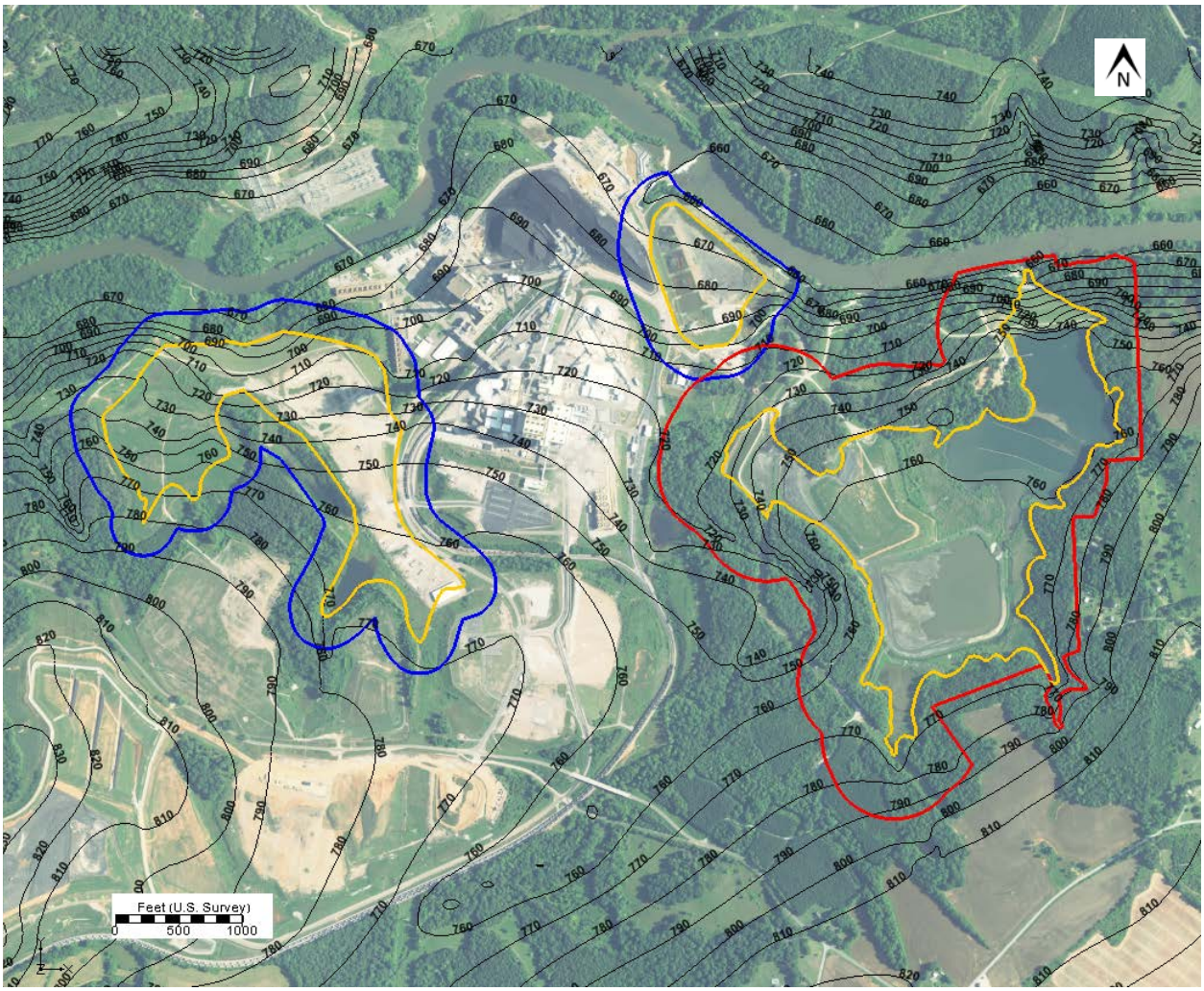

Figure 5-9. Simulated heads in the transition zone (model layer 15). The blue outline is the active ash basin compliance boundary, the red lines are the Former Units 1-4 and the Unit 5 inactive ash basin compliance boundaries, and the gold outlines are the waste boundaries.

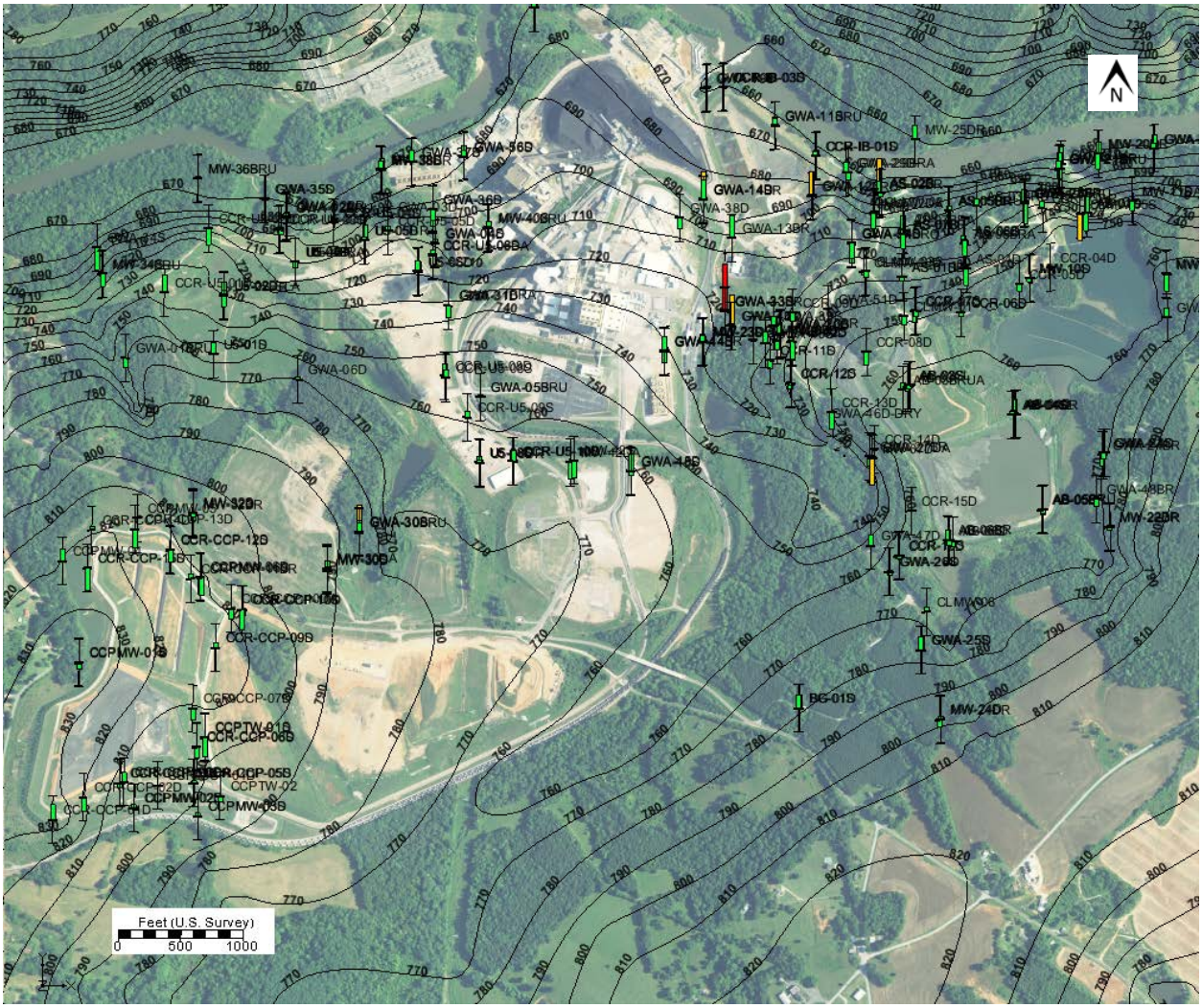

Figure 5-10. Simulated heads in the second fractured bedrock model layer (model layer 17).

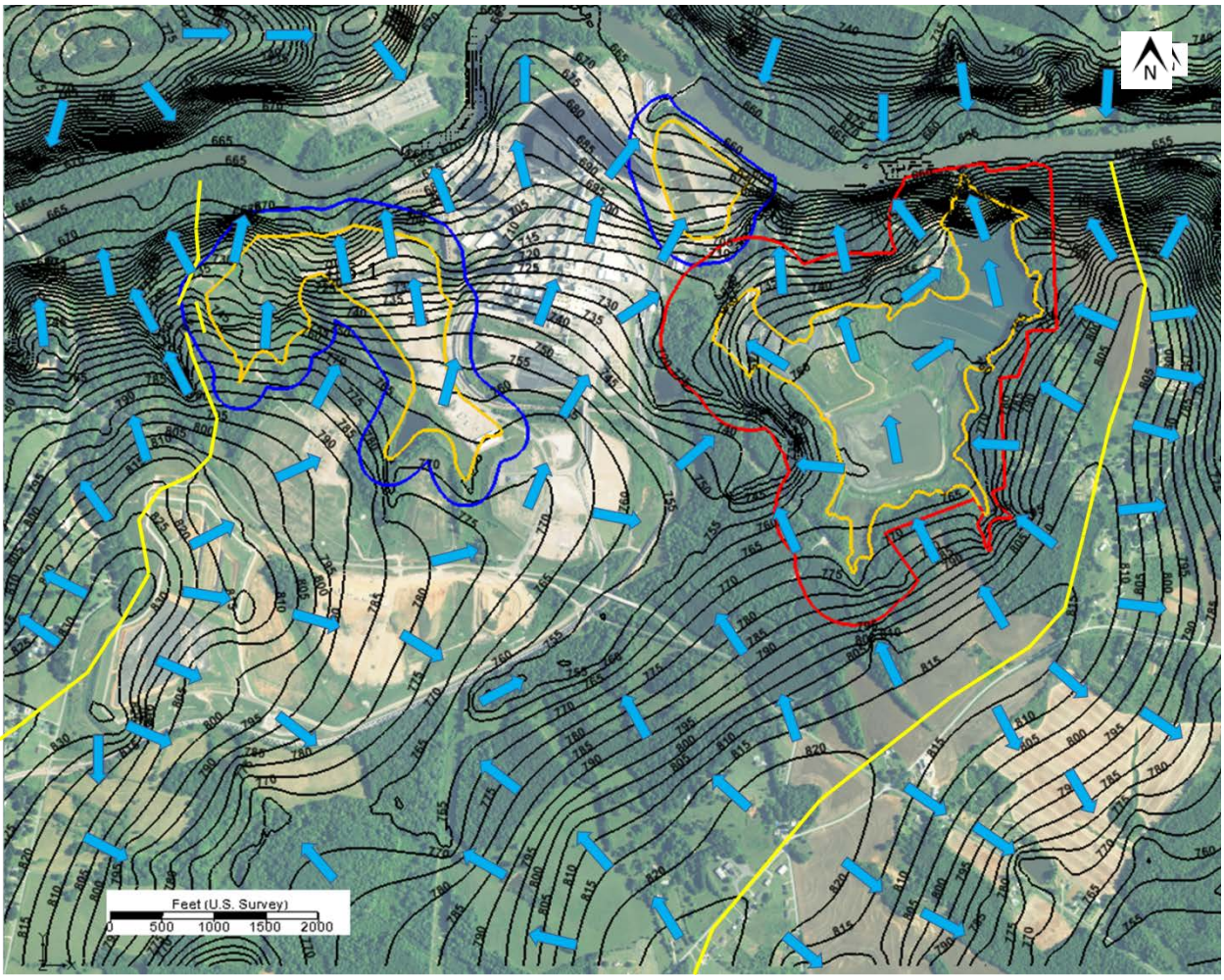

Figure 5-11. Groundwater divide and flow directions under current conditions at the CSS. The blue outline is the active ash basin compliance boundary, the red lines are the Former Units 1-4 and the Unit 5 inactive ash basin compliance boundaries, and the gold outlines are the waste boundaries. Approximate groundwater divides are yellow lines and approximate flow directions are light blue arrows.

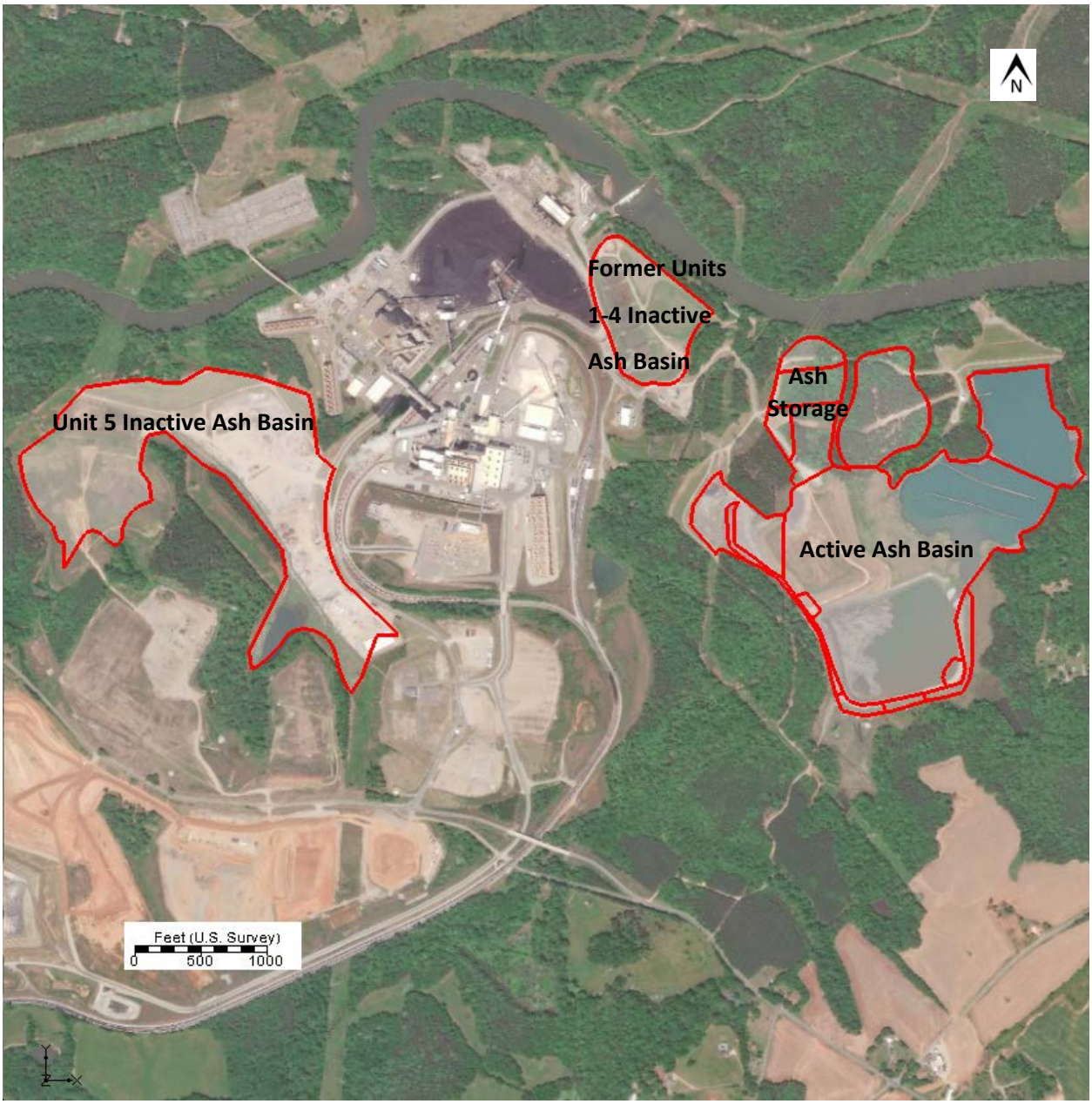

Figure 5-12. COI source zones for the historical transport model.

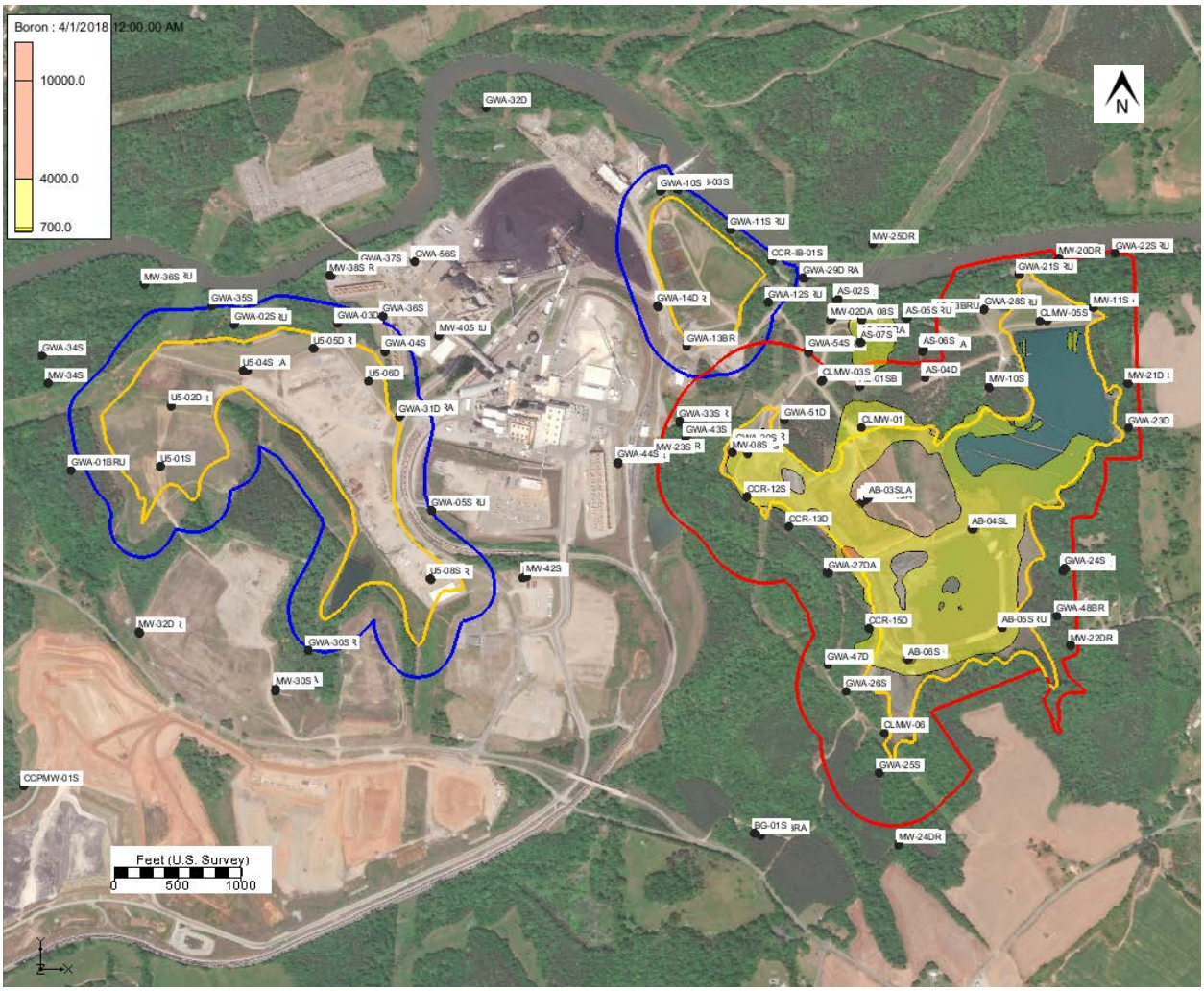

Figure 5-13a. Simulated April 2018 boron concentrations (µg/L) in the saprolite (layer 13). The red outline is the active ash basin compliance boundary, the blue outlines are the Former Units 1-4 and the Unit 5 inactive ash basin potential compliance boundaries, and the gold outlines are waste boundaries.

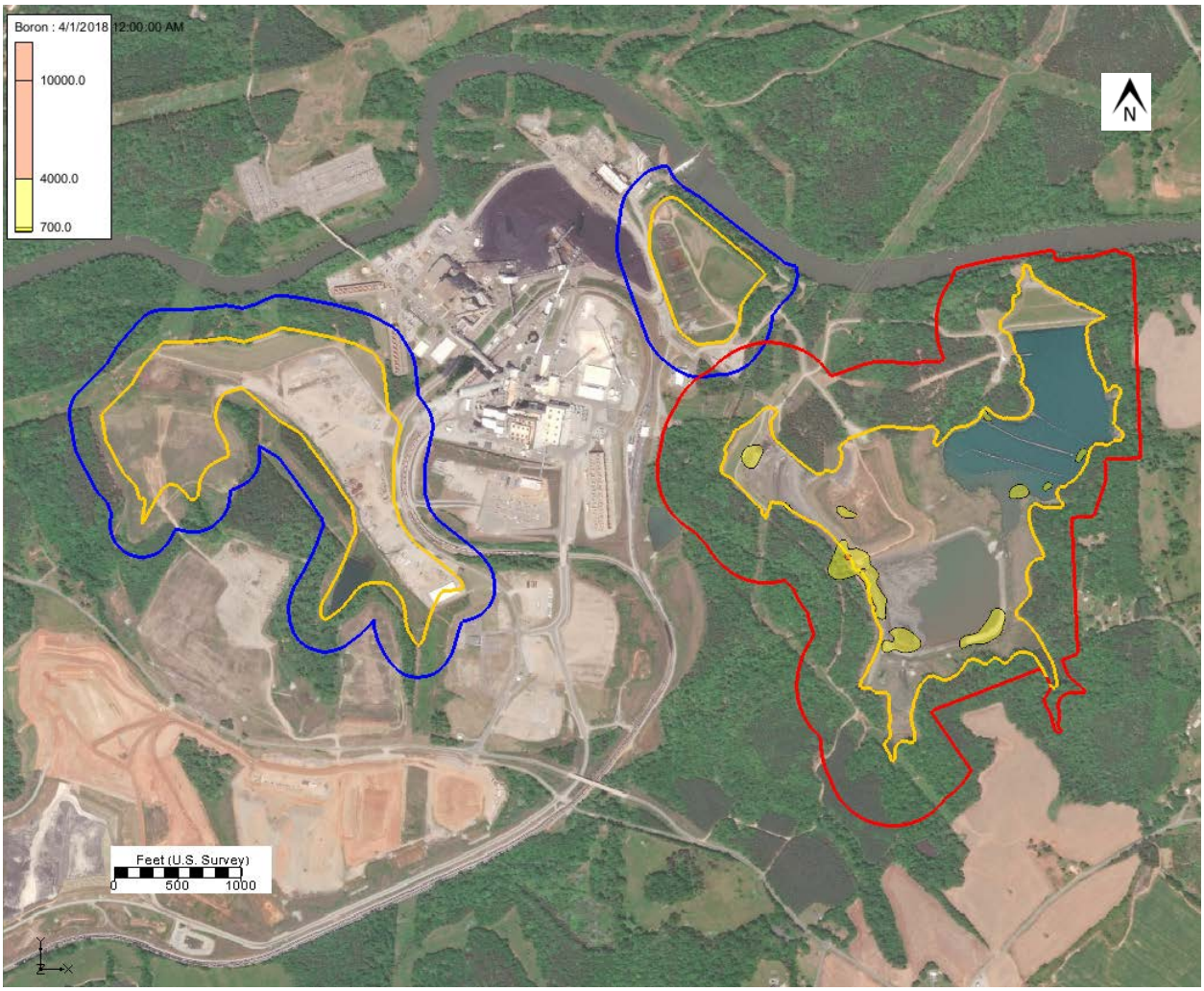

Figure 5-13b. Simulated April 2018 boron concentrations (µg/L) in the transition zone/upper bedrock (layer 16). The red outline is the active ash basin compliance boundary, the blue outlines are the Former Units 1-4 and the Unit 5 inactive ash basin potential compliance boundaries, and the gold outlines are waste boundaries.

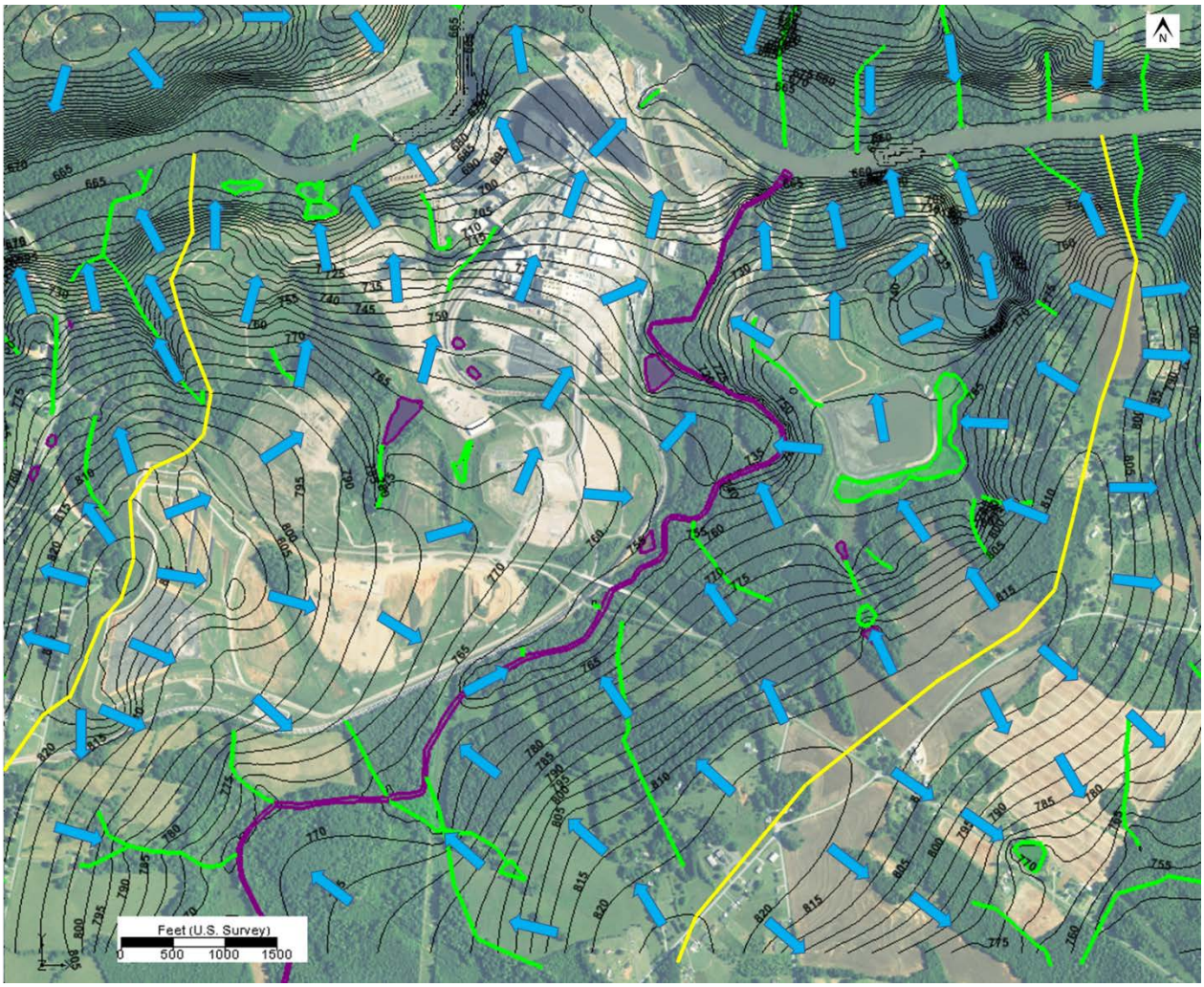

Figure 6-1. Simulated hydraulic heads in the saprolite zone (layer 9) after ash basin pond drainage. Drains are represented as green lines and general head is in purple. Approximate groundwater divides are yellow lines and approximate flow directions are light blue arrows.

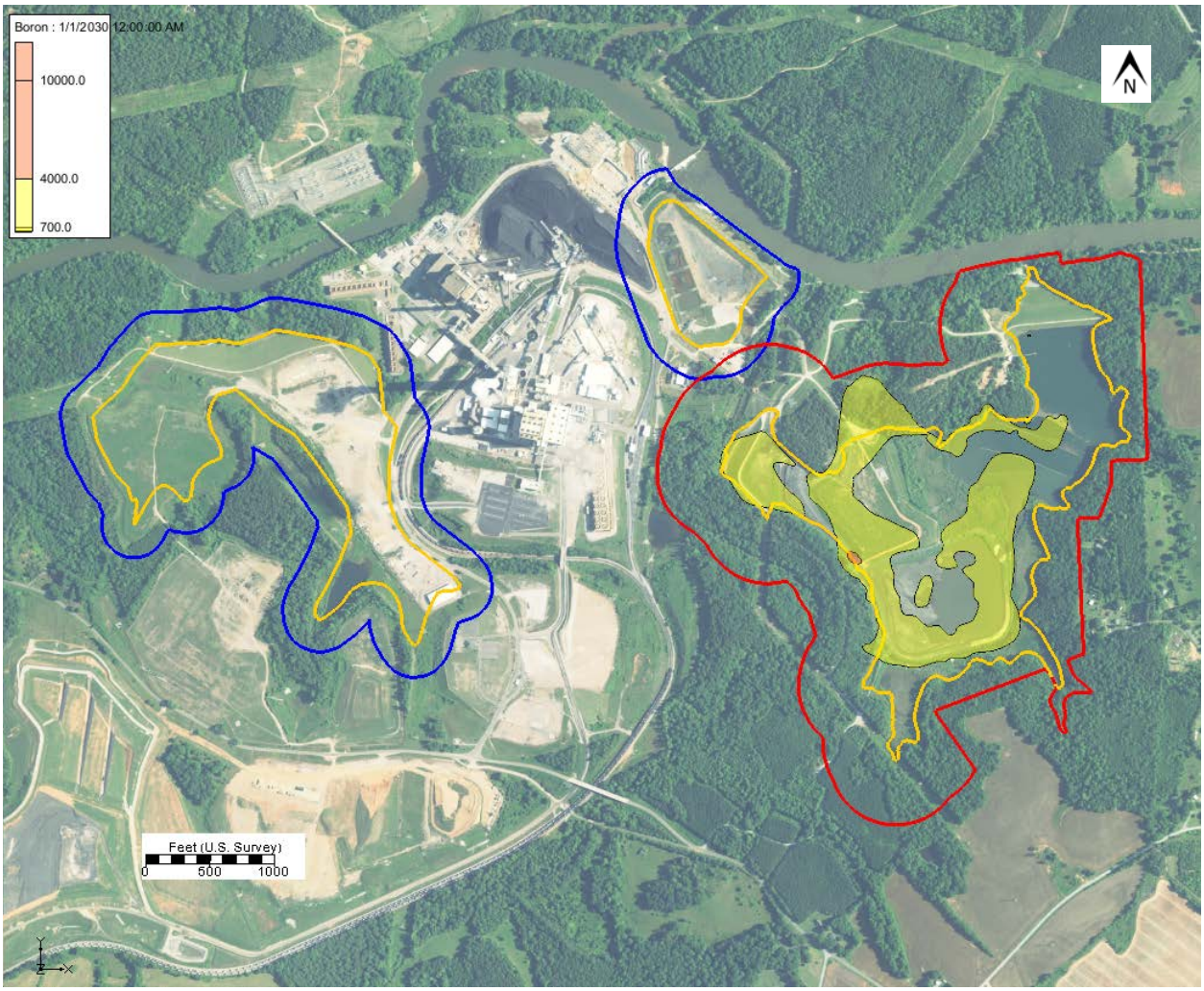

Figure 6-2. Simulated boron concentrations in the transition zone (layer 15) in 2030 for a simulation where the ash basin pond has been decanted. The red outline is the active ash basin compliance boundary, the blue outlines are the Former Units 1-4 and the Unit 5 inactive ash basin potential compliance boundaries, and the gold outlines are waste boundaries.

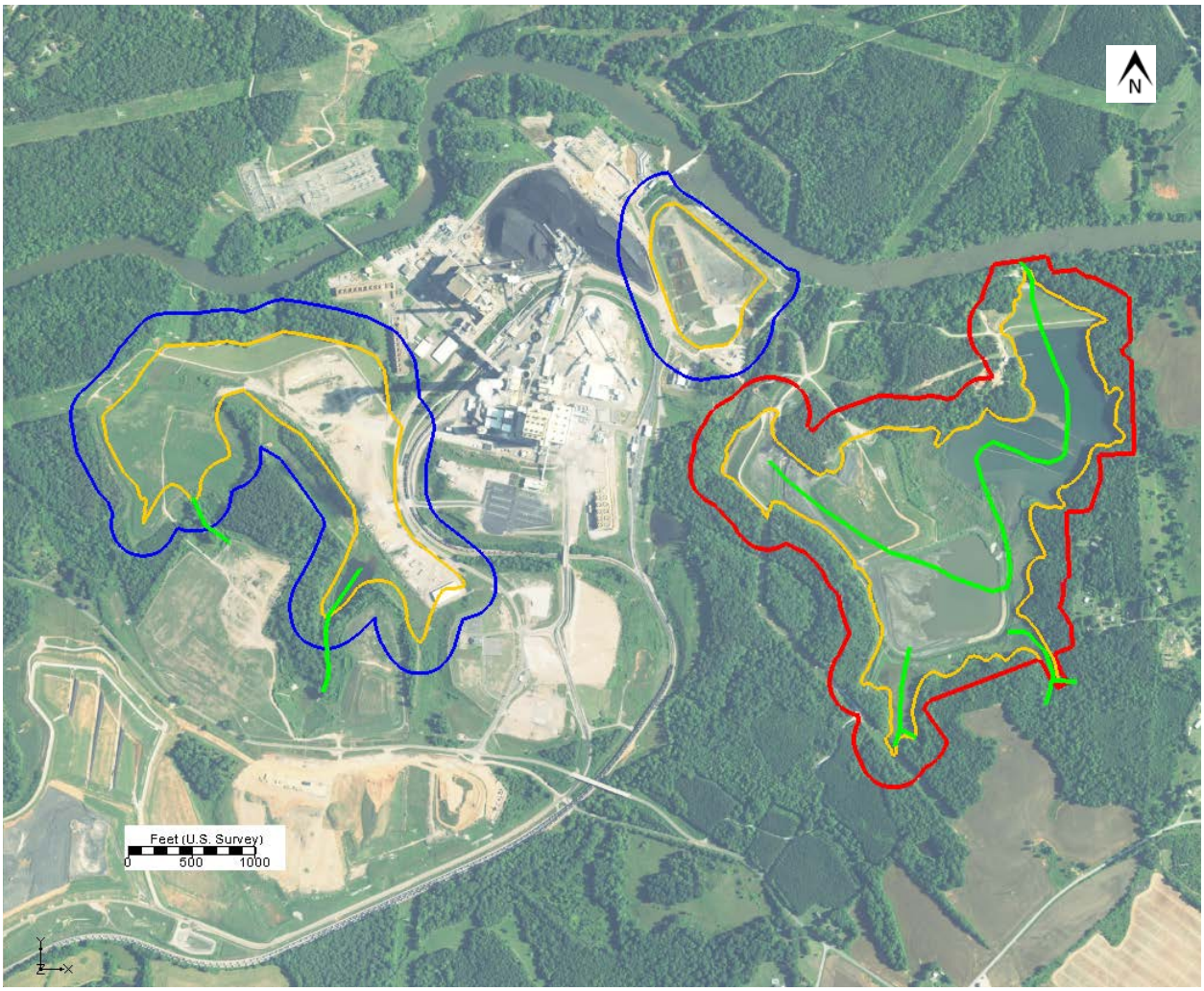

Figure 6-3. Drain network used in excavation simulations to represent springs and streams that may form. The elevations are set to the top of the saprolite surface, which approximately corresponds to the original ground surface. Drains are represented as green lines. The red outline is the active ash basin potential compliance boundary, the blue outlines are the Former Units 1-4 and the Unit 5 inactive ash basin potential compliance boundaries, and the gold outlines are waste boundaries.

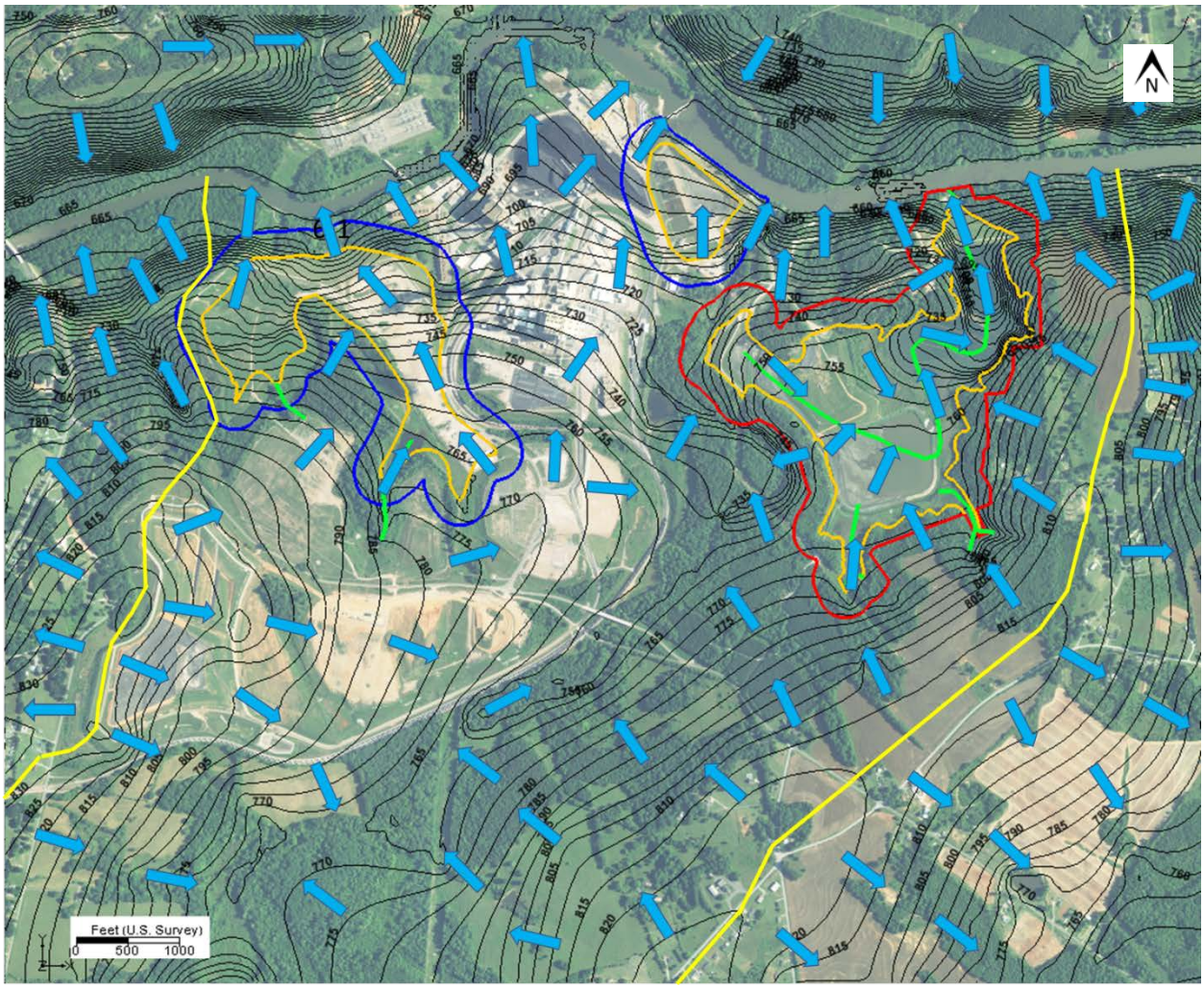

Figure 6-4. Simulated hydraulic heads for excavation scenario in the saprolite zone (layer 9). The red outline is the active ash basin potential compliance boundary, the blue outlines are the Former Units 1-4 and the Unit 5 inactive ash basin potential compliance boundaries, and the gold outlines are waste boundaries. Approximate groundwater divides are yellow lines and approximate flow directions are light blue arrows.

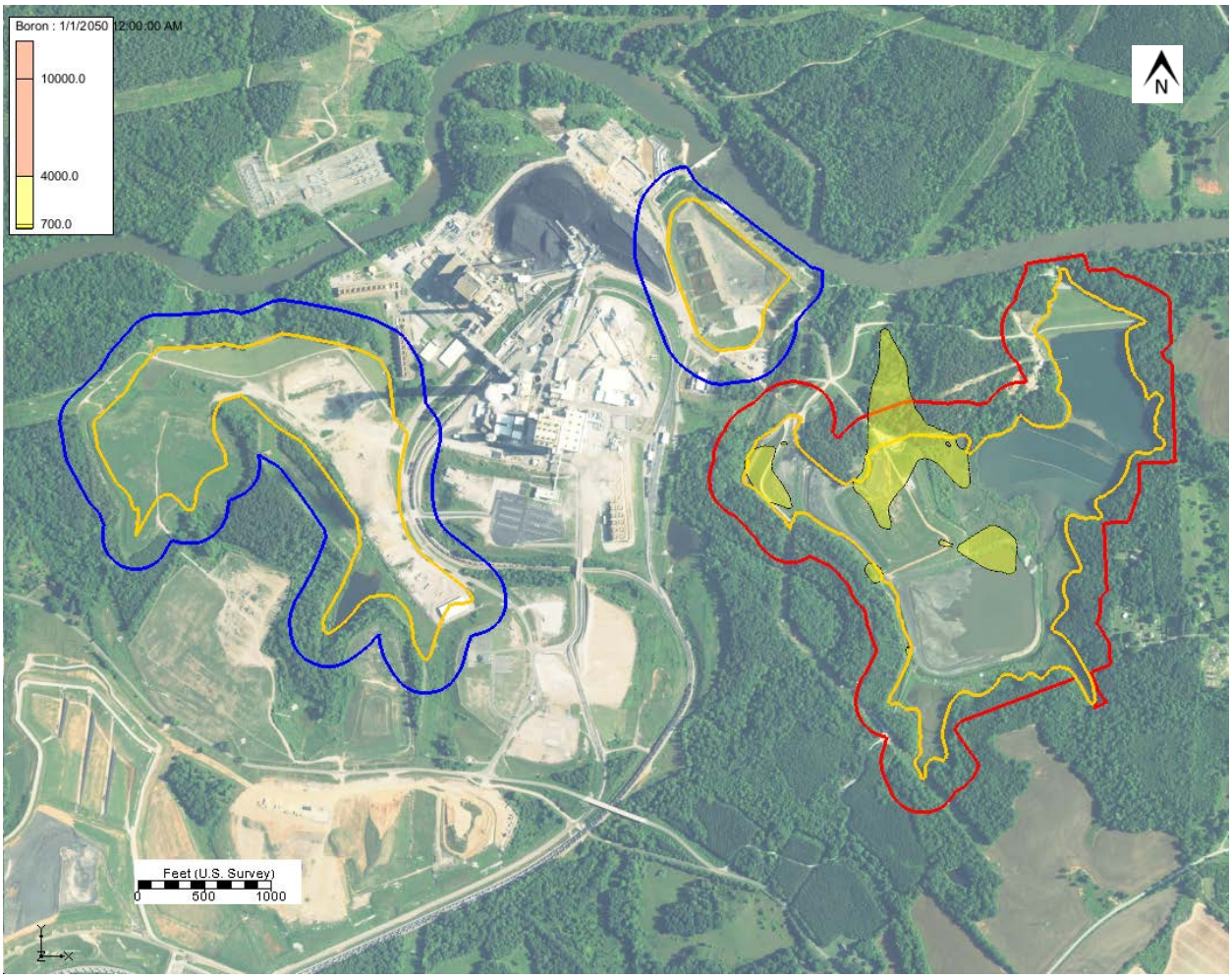

Figure 6-5a. Simulated boron concentrations in the transition zone (layer 15) in 2050 for the excavation scenario. The red outline is the active ash basin potential compliance boundary, the blue outlines are the Former Units 1-4 and the Unit 5 inactive ash basin potential compliance boundaries, and the gold outlines are waste boundaries.

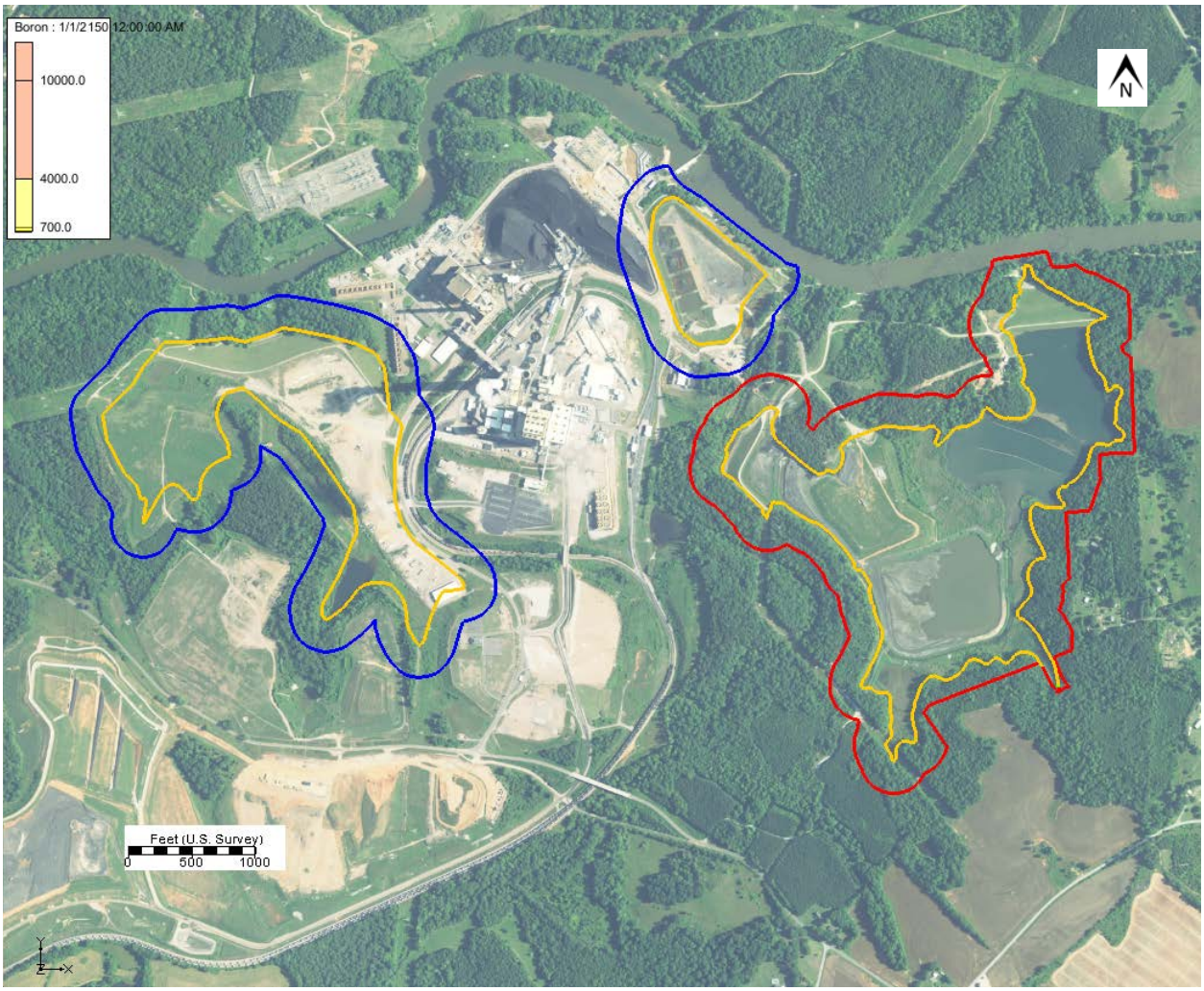

Figure 6-5b. Simulated boron concentrations in the transition zone (layer 15) in 2150 for the excavation scenario. The red outline is the active ash basin potential compliance boundary, the blue outlines are the Former Units 1-4 and the Unit 5 inactive ash basin potential compliance boundaries, and the gold outlines are waste boundaries.

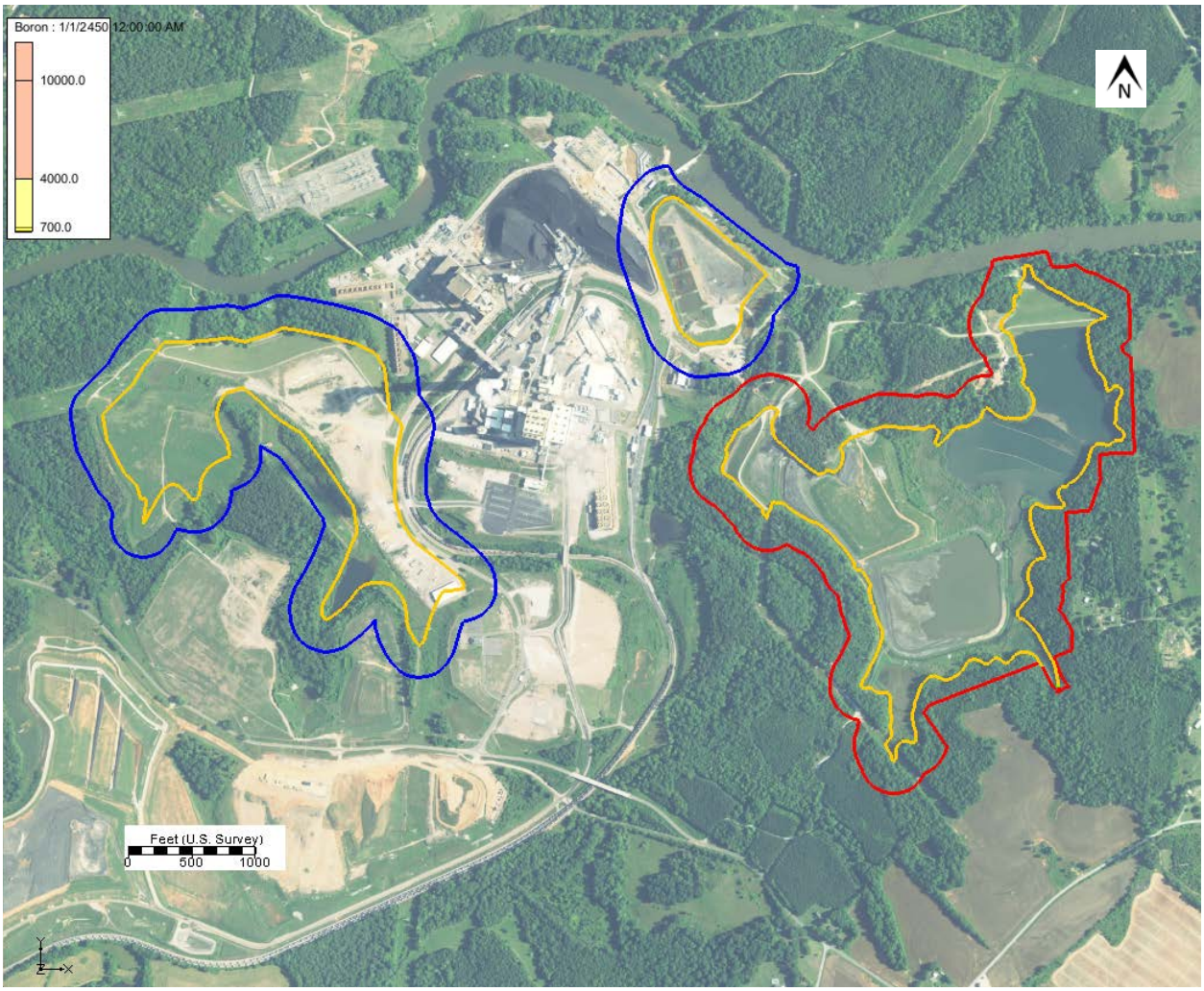

Figure 6-5c. Simulated boron concentrations in the transition zone (layer 15) in 2450 for the excavation scenario. The red outline is the active ash basin potential compliance boundary, the blue outlines are the Former Units 1-4 and the Unit 5 inactive ash basin potential compliance boundaries, and the gold outlines are waste boundaries.

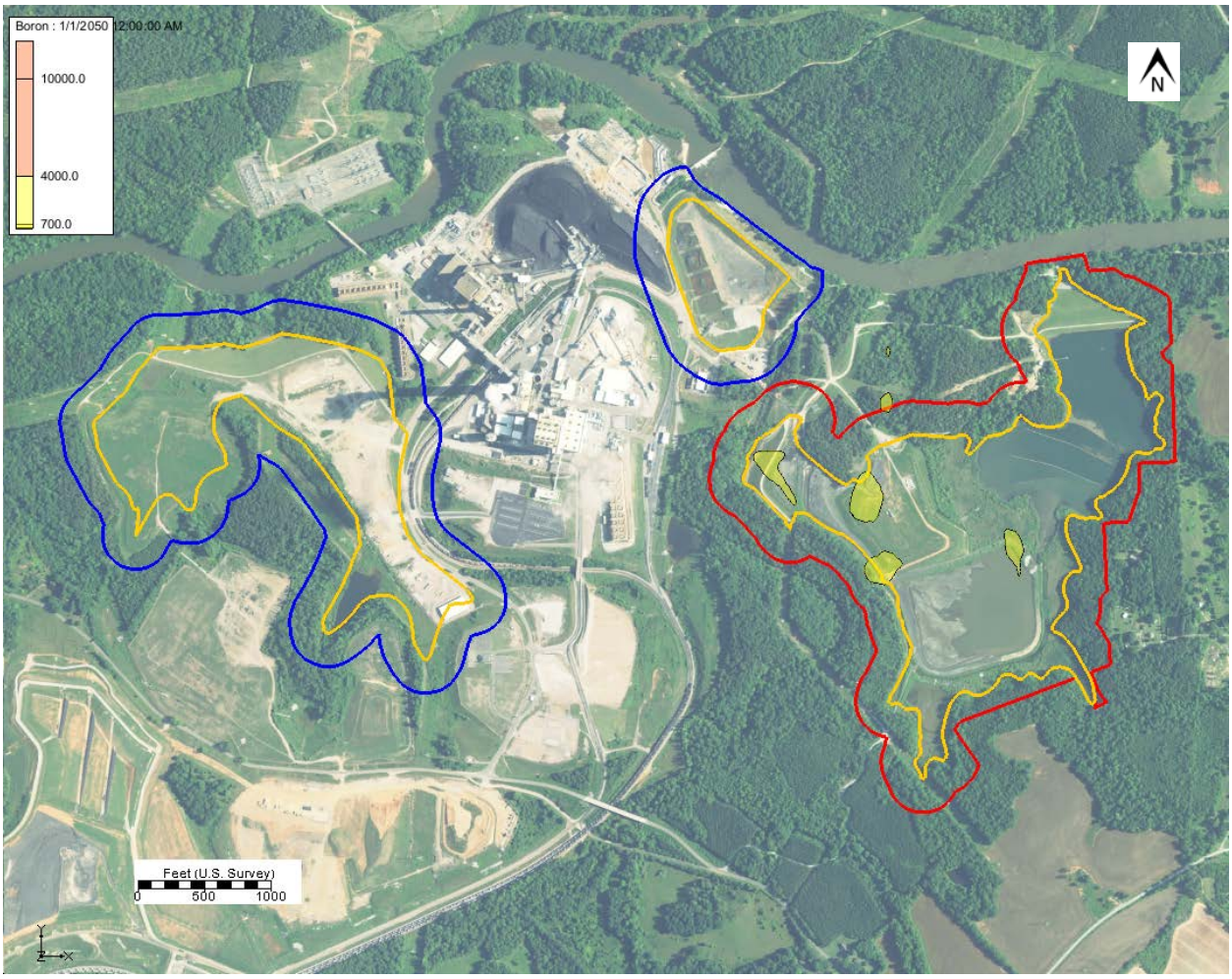

Figure 6-6a. Simulated boron concentrations in the upper bedrock (layer 17) in 2050 for the excavation scenario. The red outline is the active ash basin potential compliance boundary, the blue outlines are the Former Units 1-4 and the Unit 5 inactive ash basin potential compliance boundaries, and the gold outlines are waste boundaries.

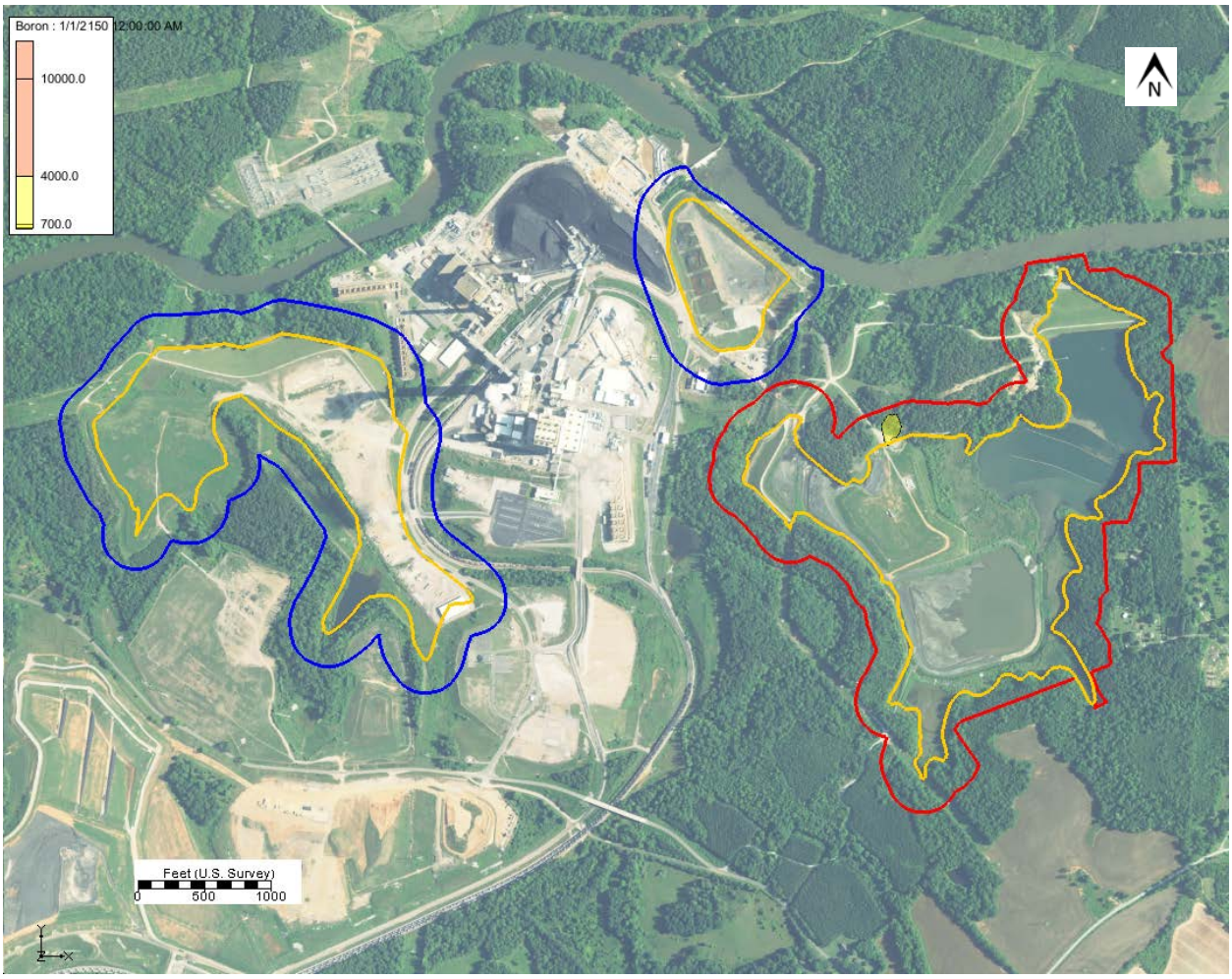

Figure 6-6b. Simulated boron concentrations in the upper bedrock (layer 17) in 2150 for the excavation scenario. The red outline is the active ash basin potential compliance boundary, the blue outlines are the Former Units 1-4 and the Unit 5 inactive ash basin potential compliance boundaries, and the gold outlines are waste boundaries.

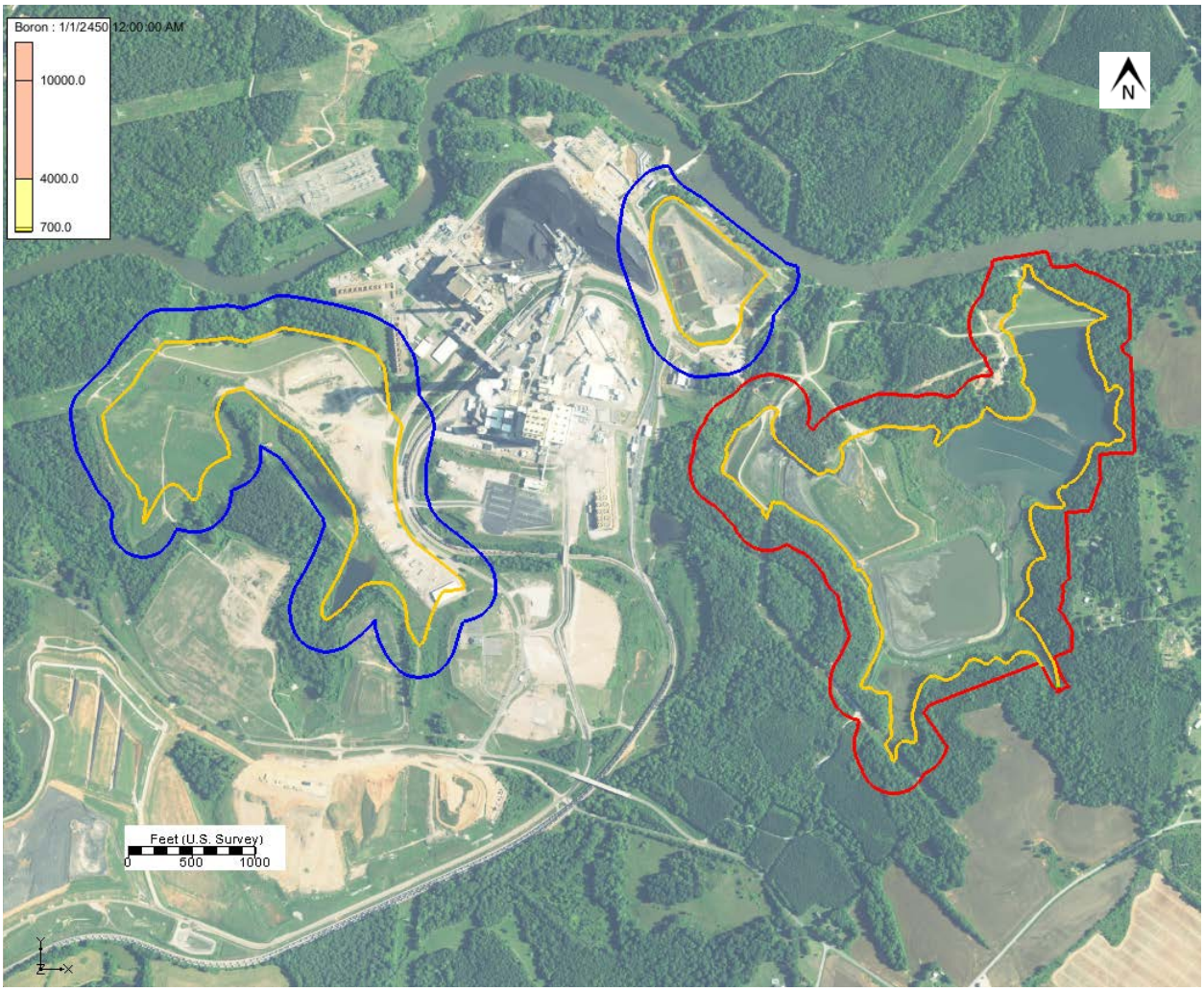

Figure 6-6c. Simulated boron concentrations in the upper bedrock (layer 17) in 2450 for the excavation scenario. The red outline is the active ash basin potential compliance boundary, the blue outlines are the Former Units 1-4 and the Unit 5 inactive ash basin potential compliance boundaries, and the gold outlines are waste boundaries.

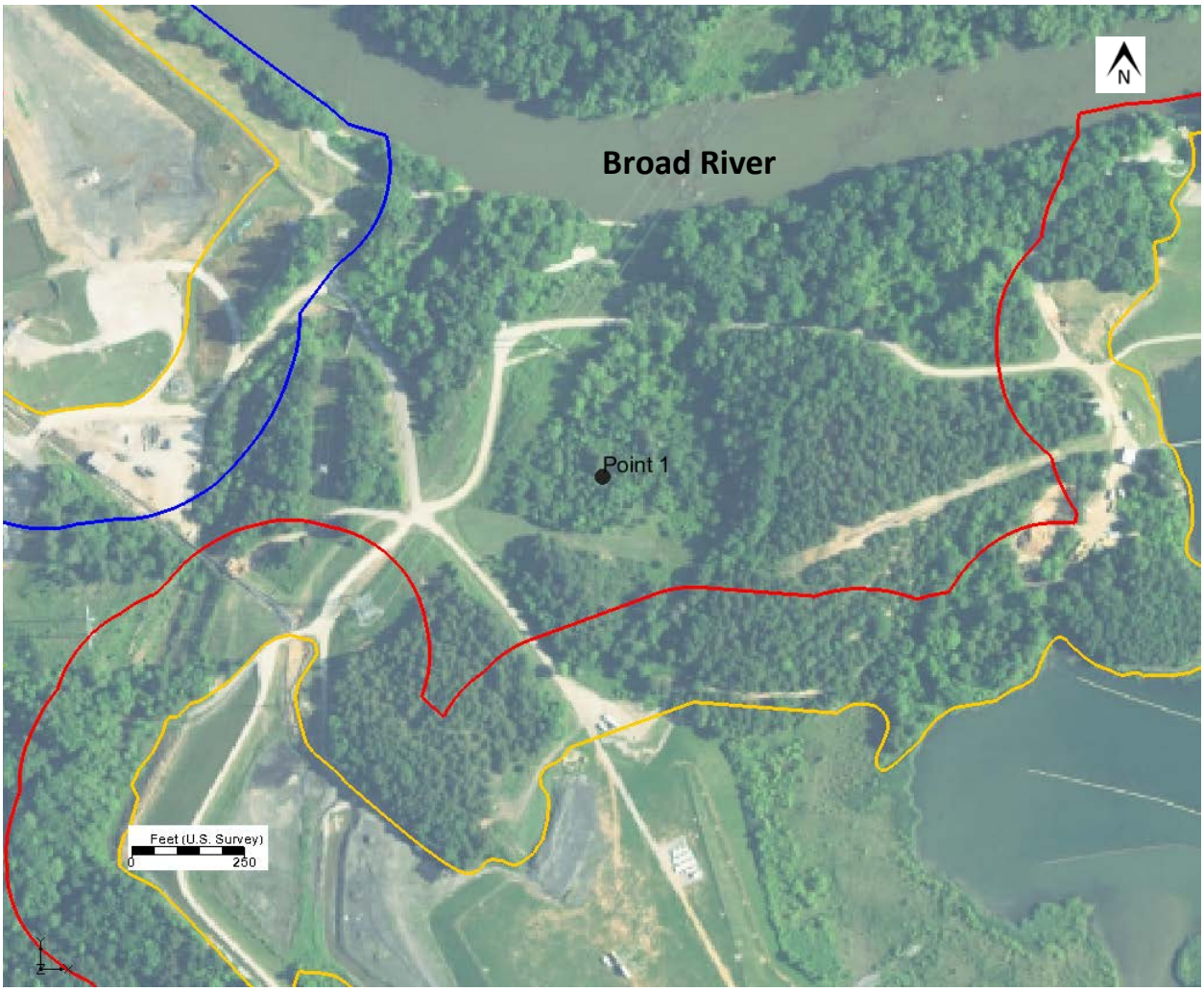

Figure 6-7. Point 1 represents the location of the boron time-series plot which is located north of the active ash basin compliance boundary. The red line is the current compliance boundary for the active ash basin, the blue line is the potential compliance boundary for Former Unit 1-4 inactive ash basin, and the gold lines are the waste boundaries.

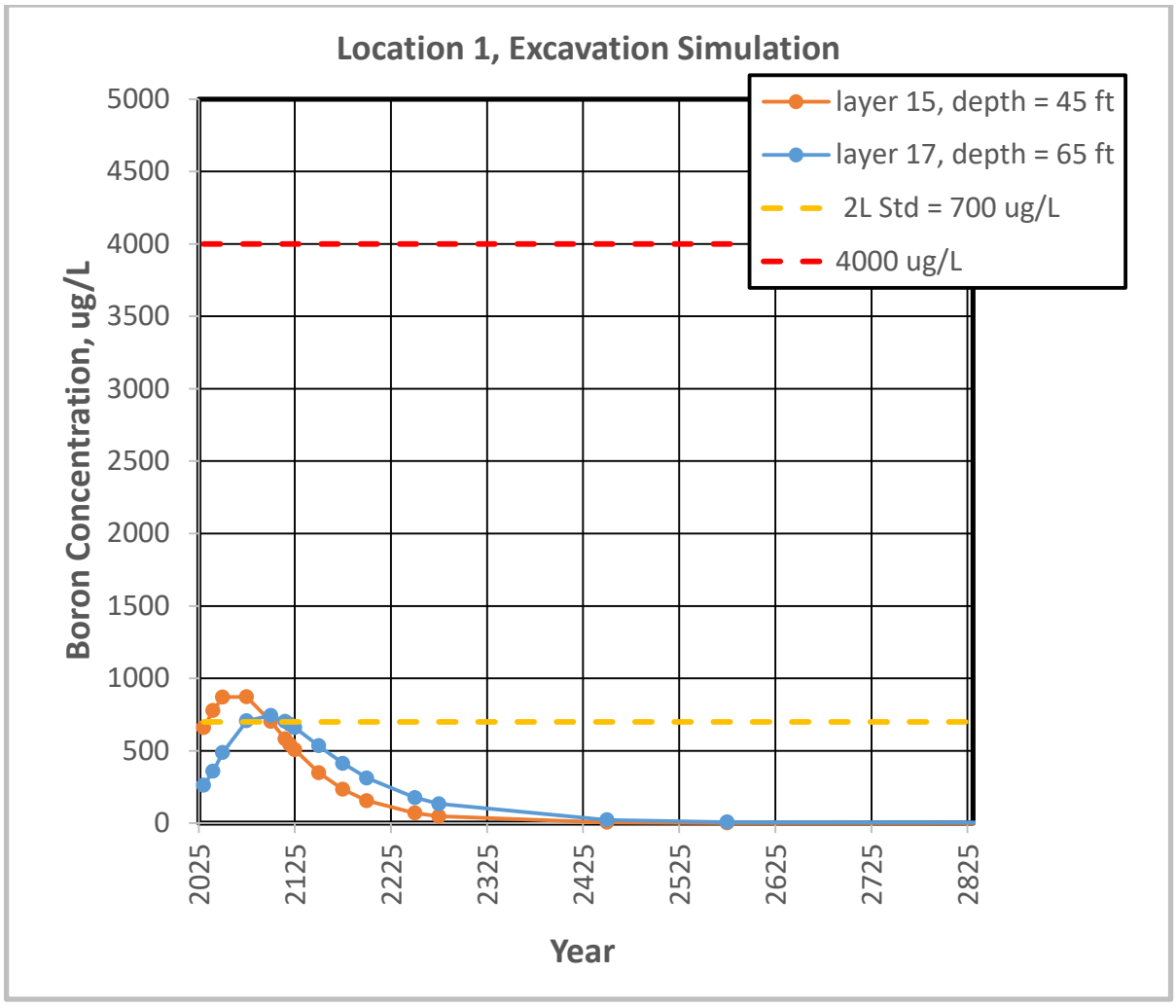

Figure 6-8. Predicted boron concentrations at Point 1 north of the active ash basin for the excavation scenario.

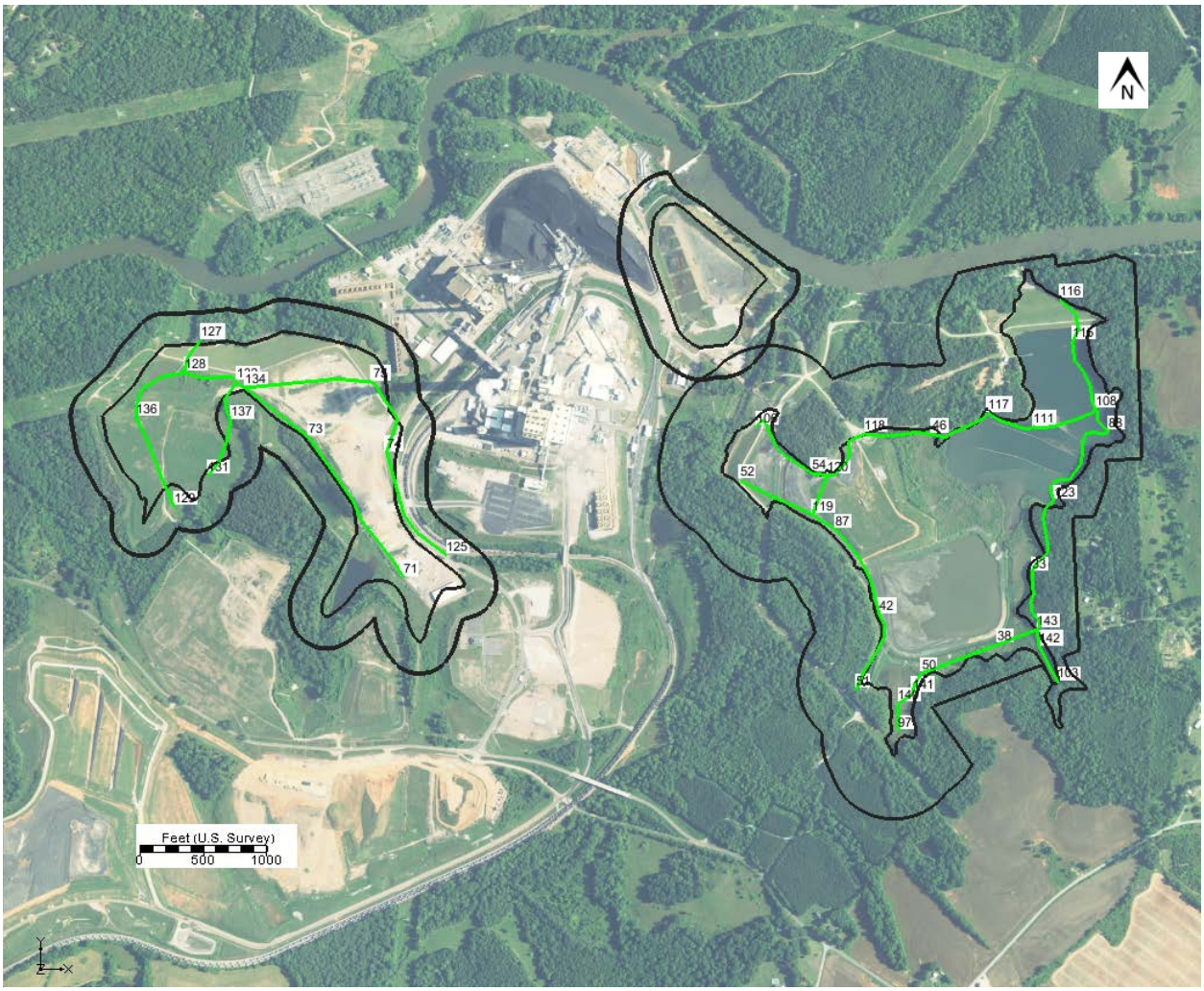

Figure 6-9. Proposed ash basin drain system for the final cover simulations. The numbered locations are nodes where the drain elevation was specified using the draft design from AECOM.

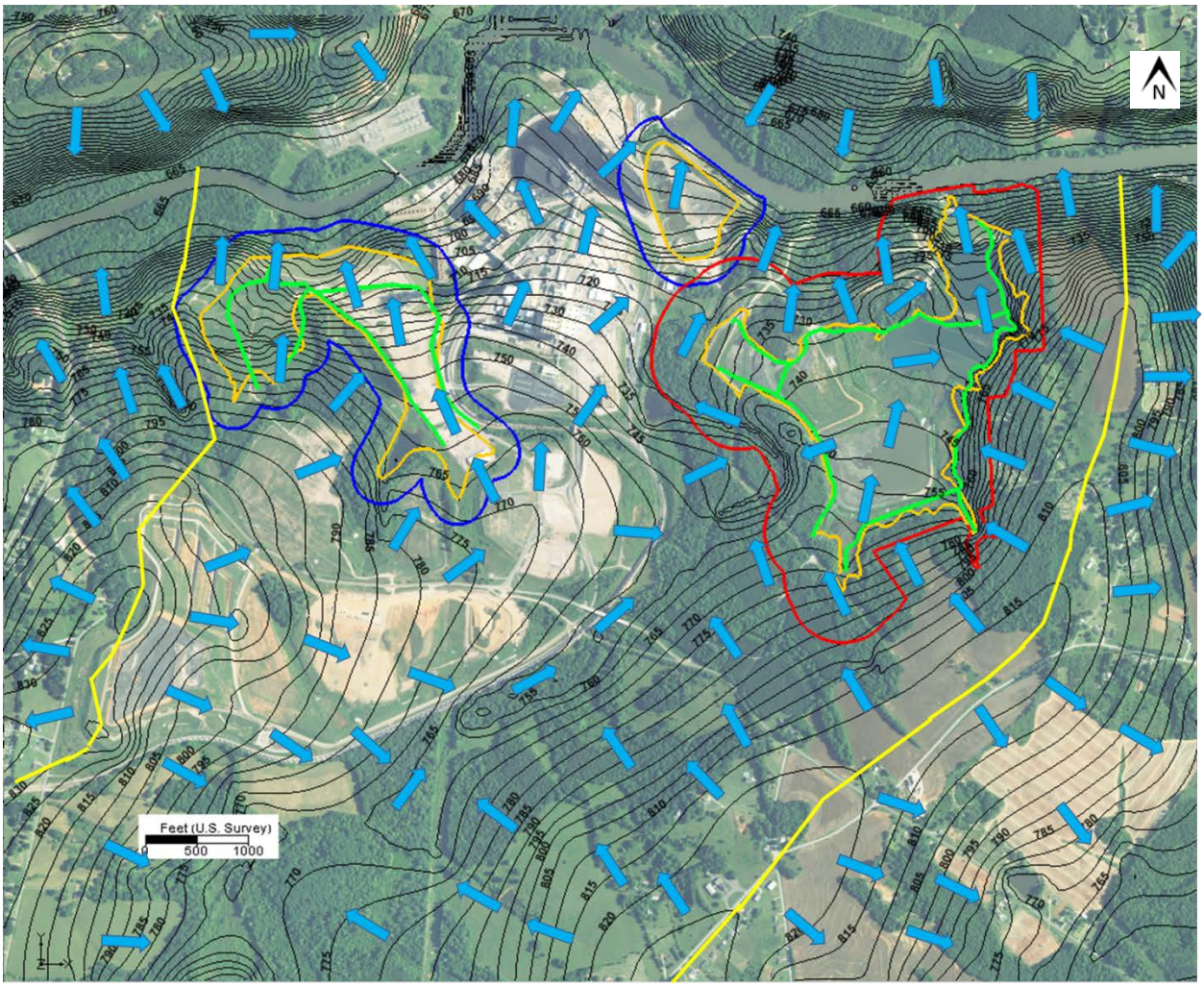

Figure 6-10. Simulated hydraulic heads for the final cover scenario within saprolite (layer 9). The red outline is the active ash basin compliance boundary, the blue outlines are the Former Units 1-4 and the Unit 5 inactive ash basin potential compliance boundaries, the gold outlines are waste boundaries, and the green lines are drains. Approximate groundwater divides are yellow lines and approximate flow directions are light blue arrows.

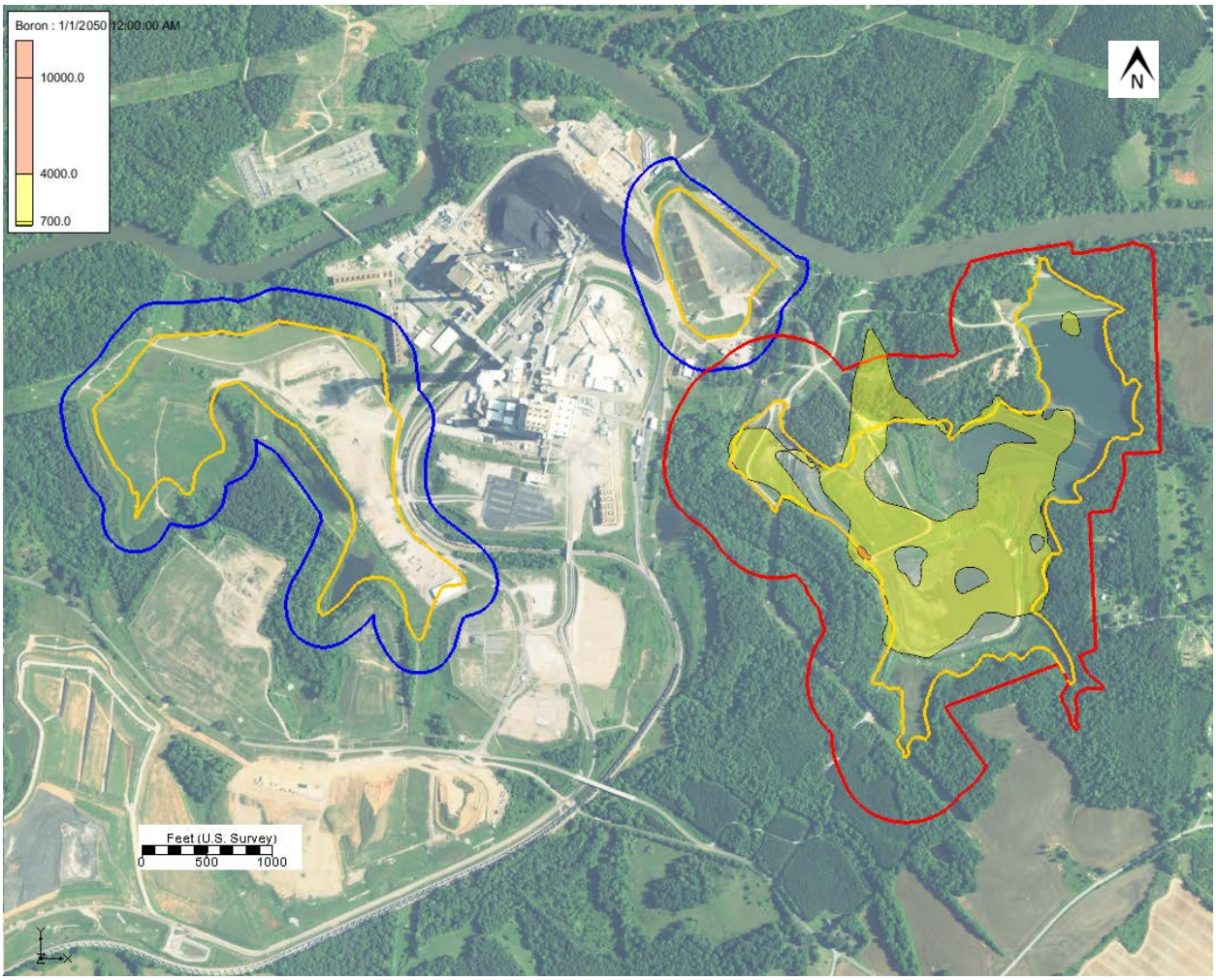

Figure 6-11a. Simulated boron concentrations in the transition zone (layer 15) in 2050 for the final cover scenario. The red outline is the active ash basin potential compliance boundary, the blue outlines are the Former Units 1-4 and the Unit 5 inactive ash basin potential compliance boundaries, and the gold outlines are waste boundaries.

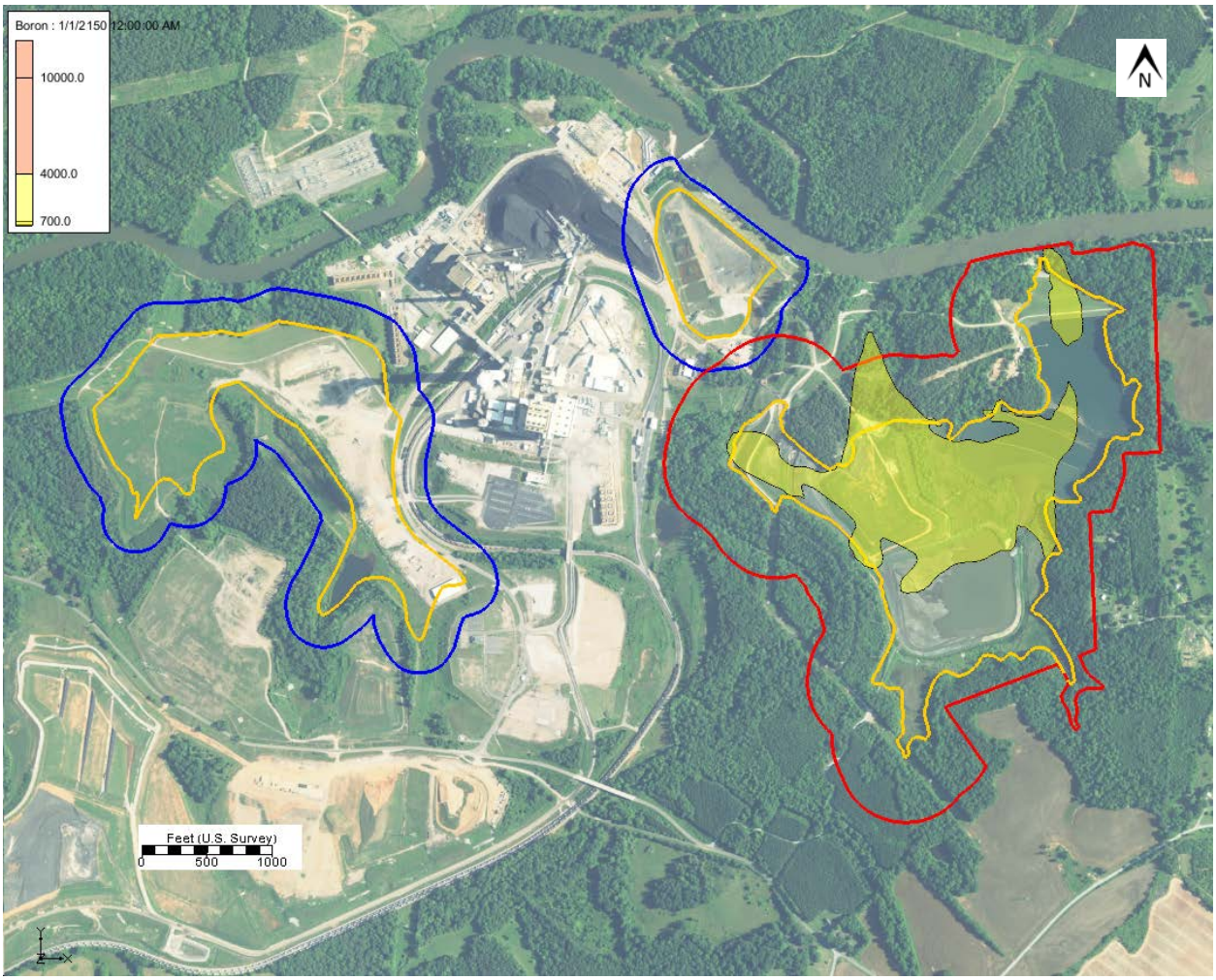

Figure 6-11b. Simulated boron concentrations in the transition zone (layer 15) in 2150 for the final cover scenario. The red outline is the active ash basin potential compliance boundary, the blue outlines are the Former Units 1-4 and the Unit 5 inactive ash basin potential compliance boundaries, and the gold outlines are waste boundaries.

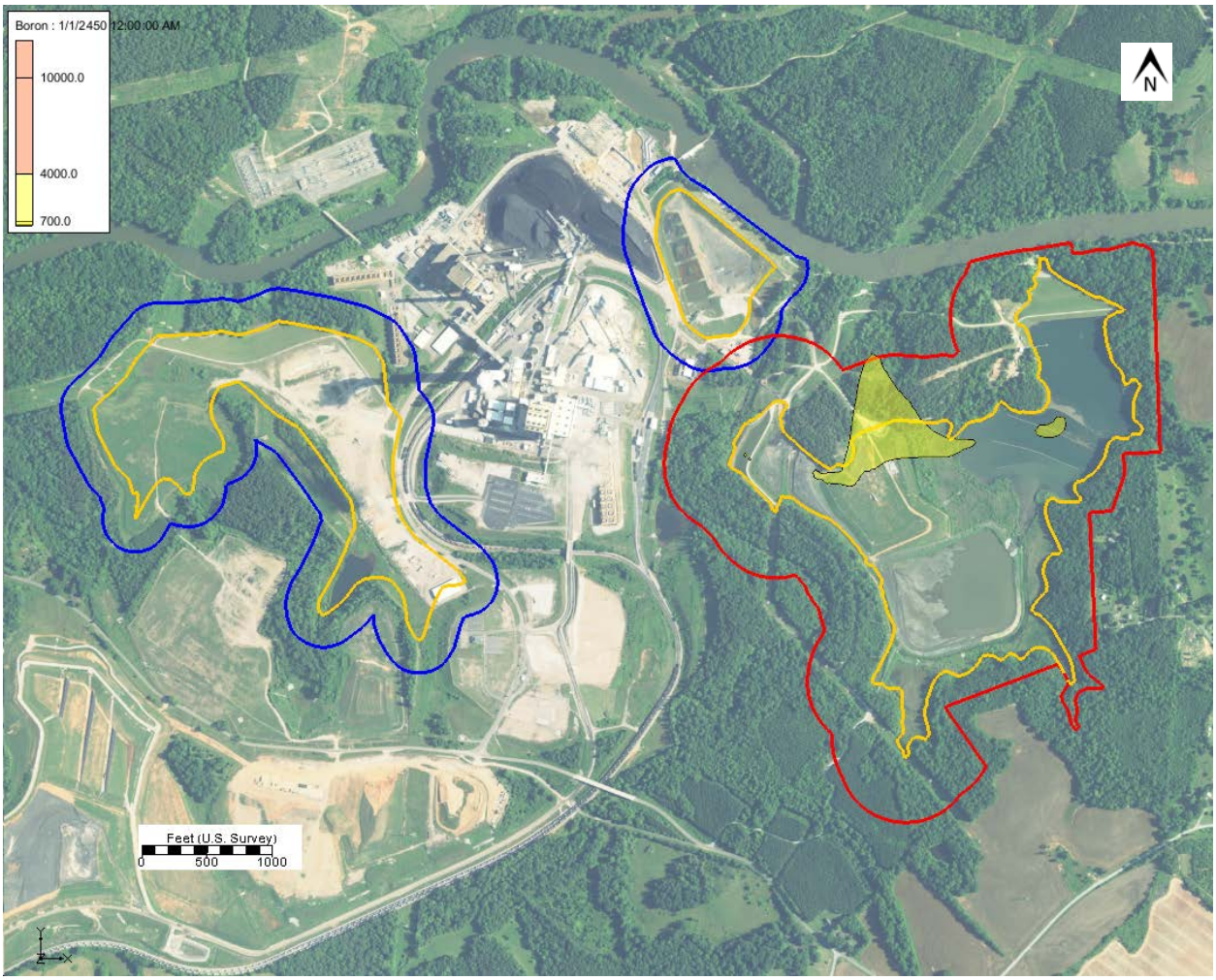

Figure 6-11c. Simulated boron concentrations in the transition zone (layer 15) in 2450 for the final cover scenario. The red outline is the active ash basin potential compliance boundary, the blue outlines are the Former Units 1-4 and the Unit 5 inactive ash basin potential compliance boundaries, and the gold outlines are waste boundaries.

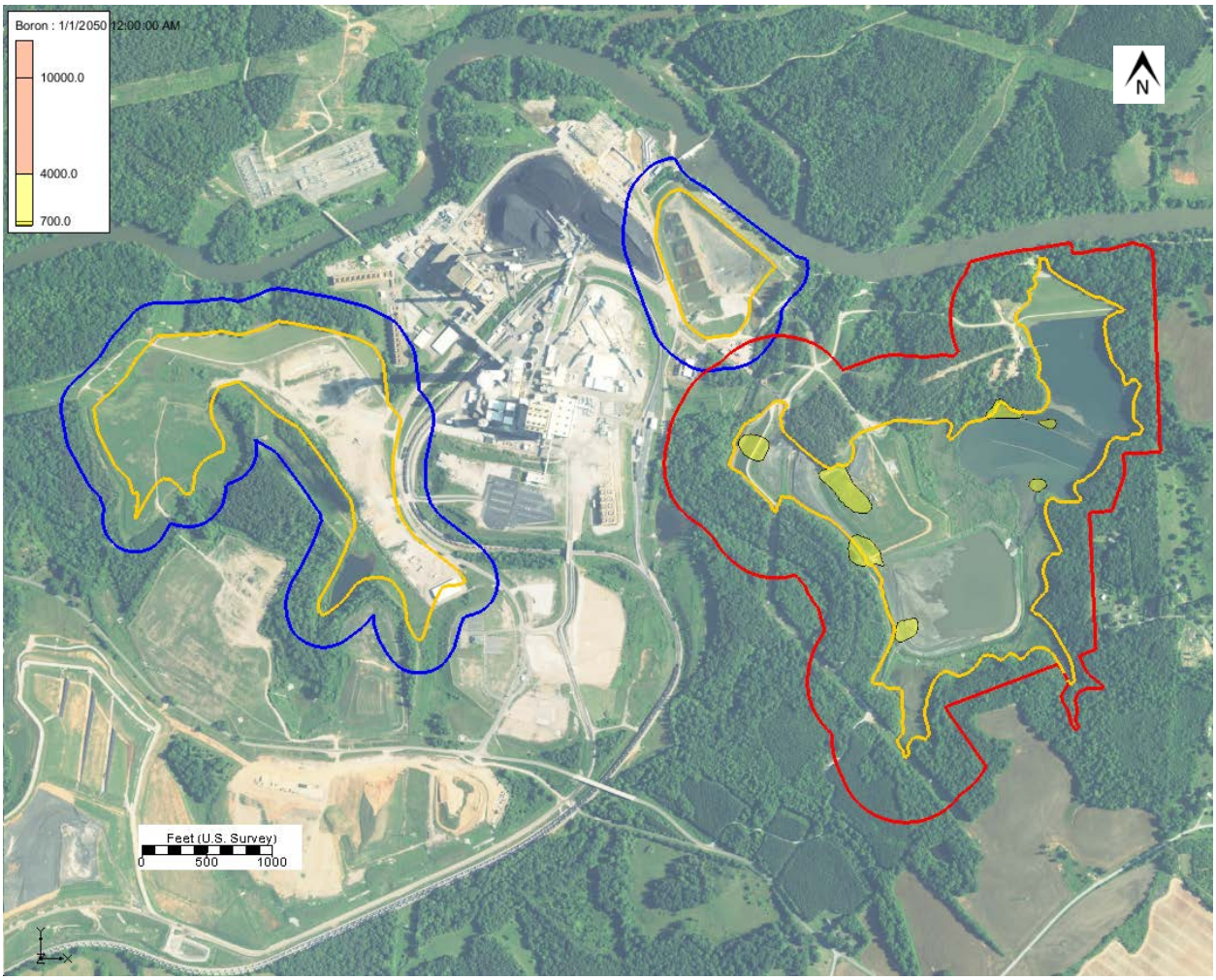

Figure 6-12a. Simulated boron concentrations in the upper bedrock (layer 17) in 2050 for the final cover scenario. The red outline is the active ash basin potential compliance boundary, the blue outlines are the Former Units 1-4 and the Unit 5 inactive ash basin potential compliance boundaries, and the gold outlines are waste boundaries.

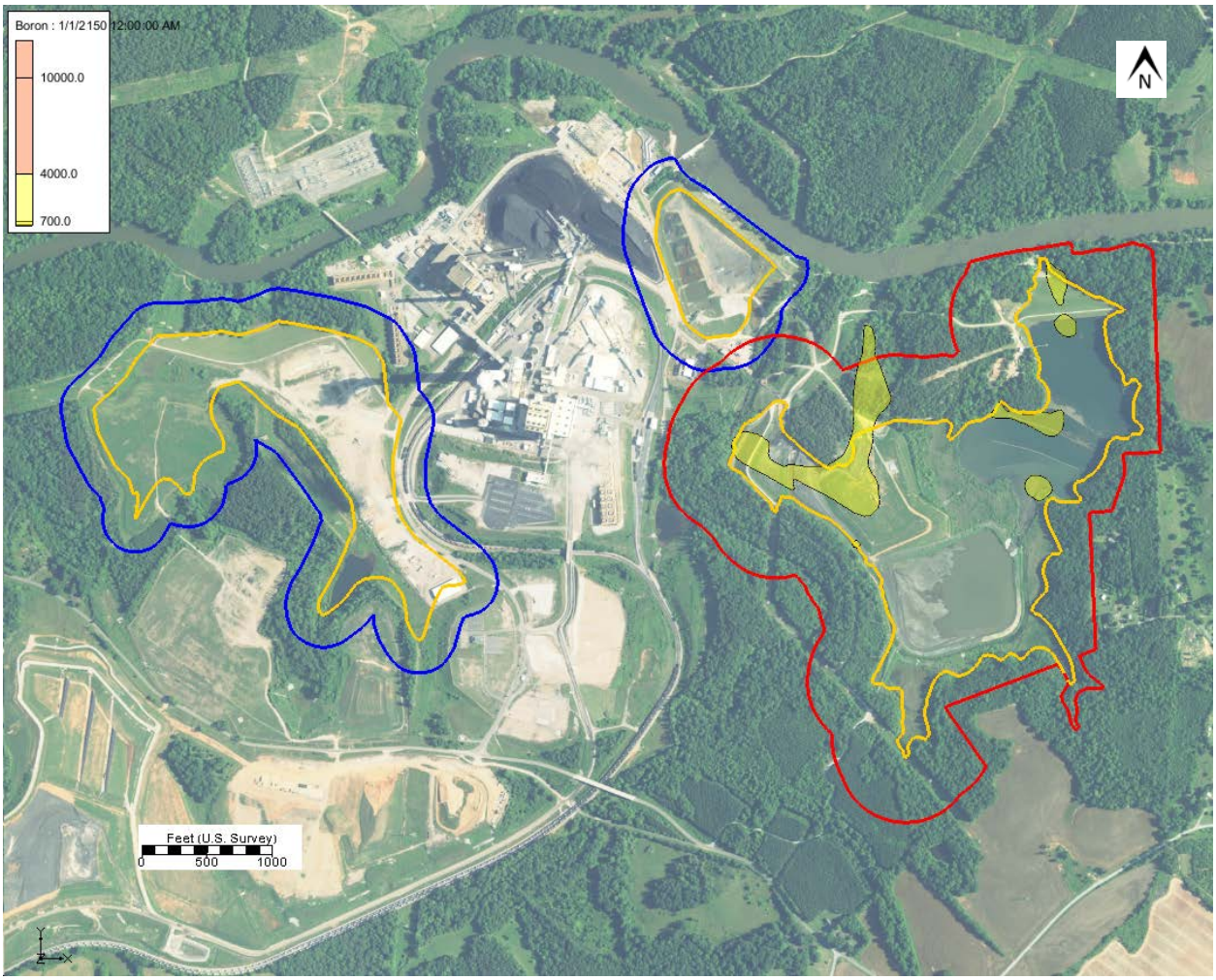

Figure 6-12b. Simulated boron concentrations in the upper bedrock (layer 17) in 2150 for the final cover scenario. The red outline is the active ash basin potential compliance boundary, the blue outlines are the Former Units 1-4 and the Unit 5 inactive ash basin potential compliance boundaries, and the gold outlines are waste boundaries.

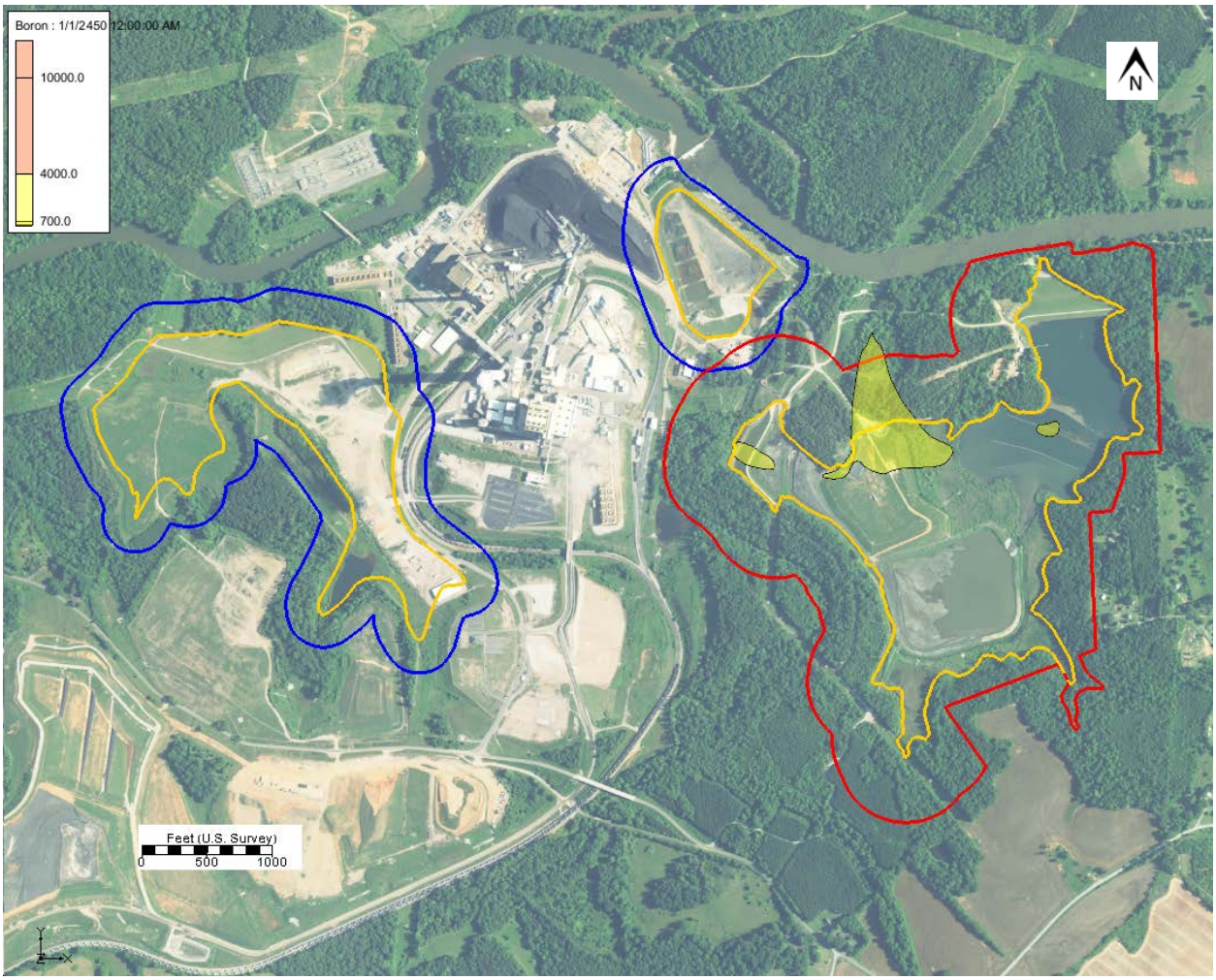

Figure 6-12c. Simulated boron concentrations in the upper bedrock (layer 17) in 2450 for the final cover scenario. The red outline is the active ash basin potential compliance boundary, the blue outlines are the Former Units 1-4 and the Unit 5 inactive ash basin potential compliance boundaries, and the gold outlines are waste boundaries.

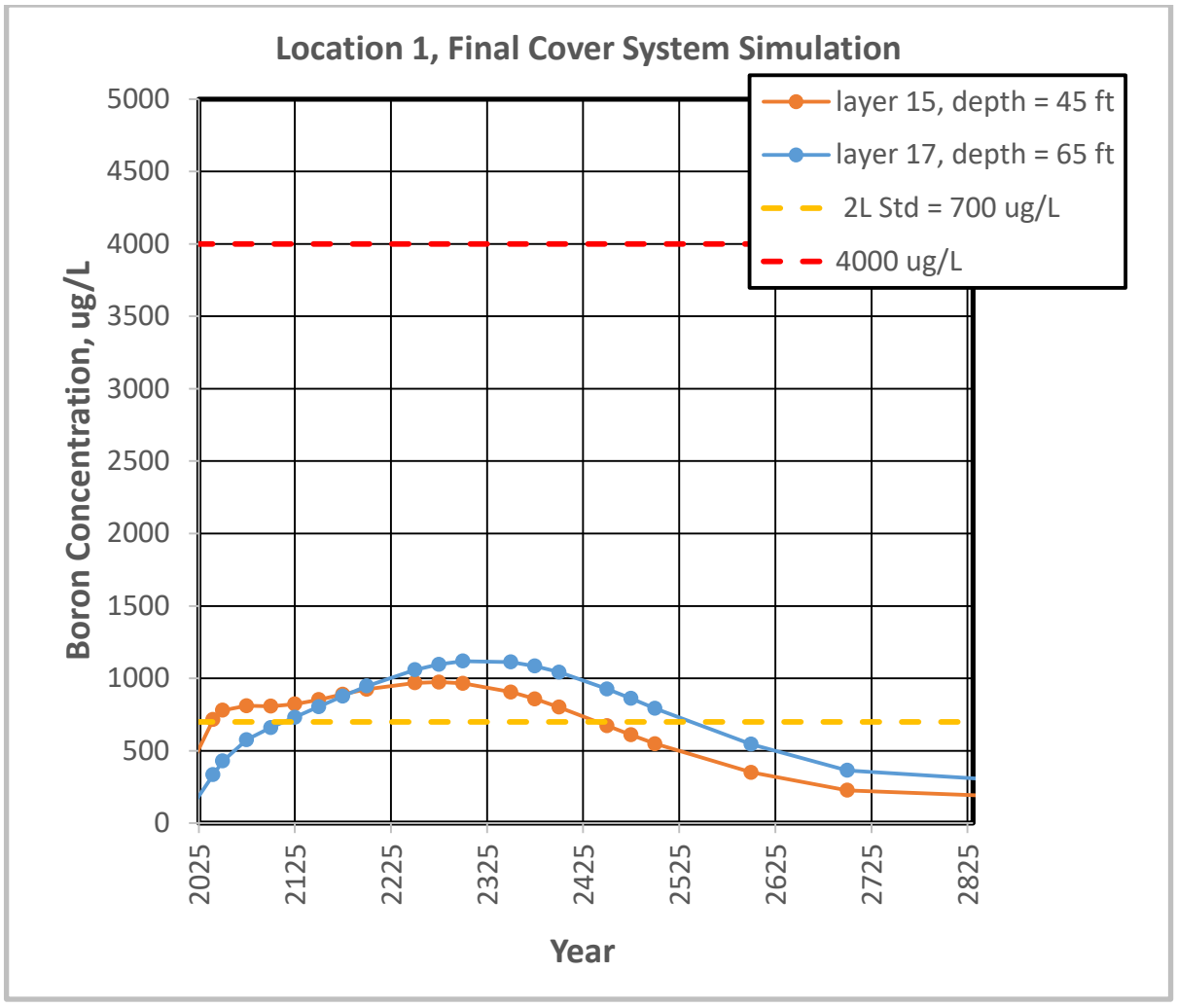

Figure 6-13. Predicted boron concentrations at Point 1 north of the active ash basin for the final cover scenario.

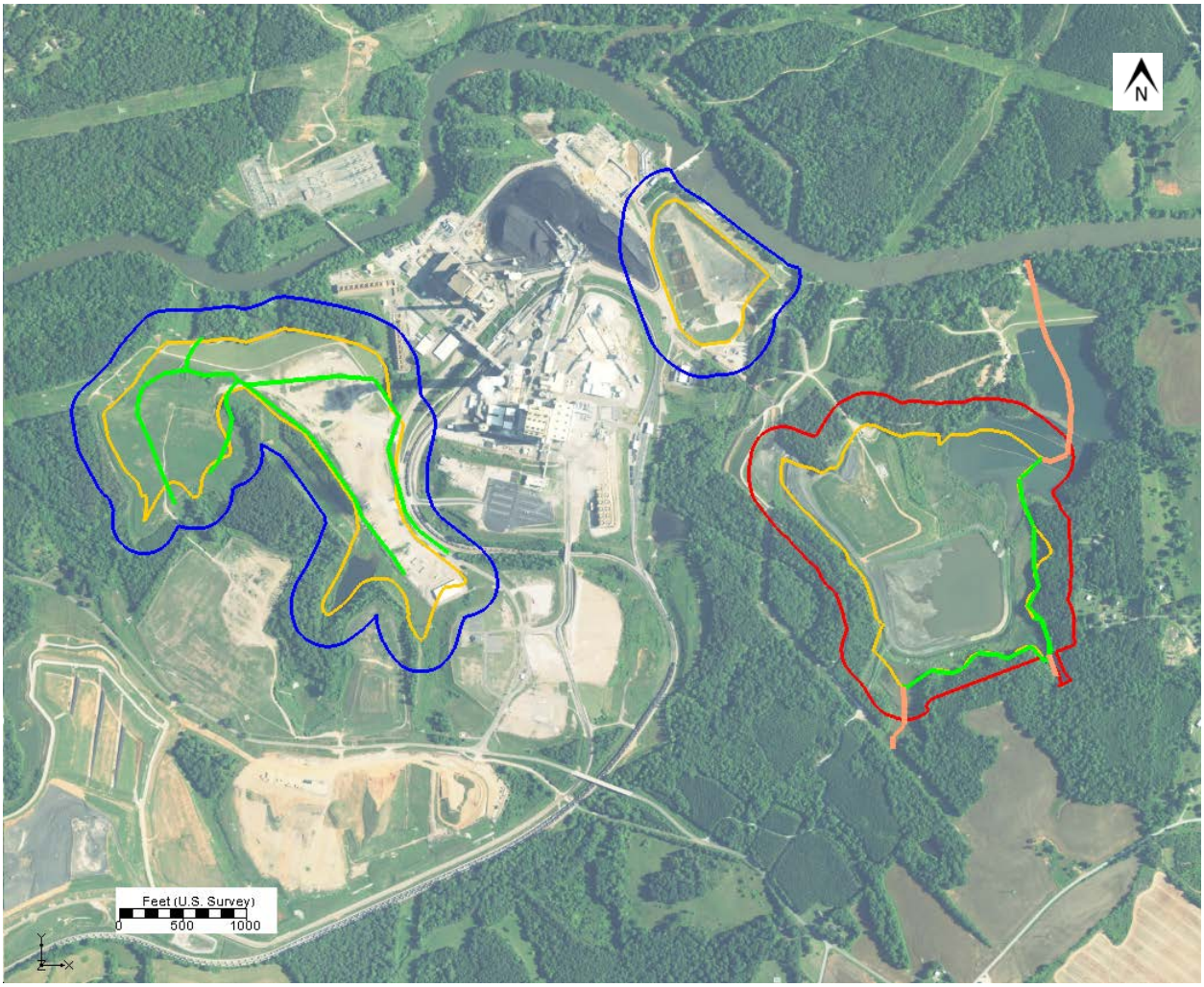

Figure 6-14. Proposed active ash basin drainage system for the hybrid simulations. Proposed active ash basin perimeter drains (green lines) are present five feet along the edge of the cover system. A drain network (orange lines) is used in in the excavated (northern and southern) part of the active ash basin to represent springs and streams that may form. The elevations are set to the top of the saprolite surface, which approximately corresponds to the original ground surface in this part of the basin. Drainage location elevations in Unit 5 inactive ash basin are the same as the final cover scenario and was specified using the draft design from AECOM. The red outline is the active ash basin potential compliance boundary, the blue outlines are the Former Units 1-4 and the Unit 5 inactive ash basin potential compliance boundaries, and the gold outlines are waste boundaries.

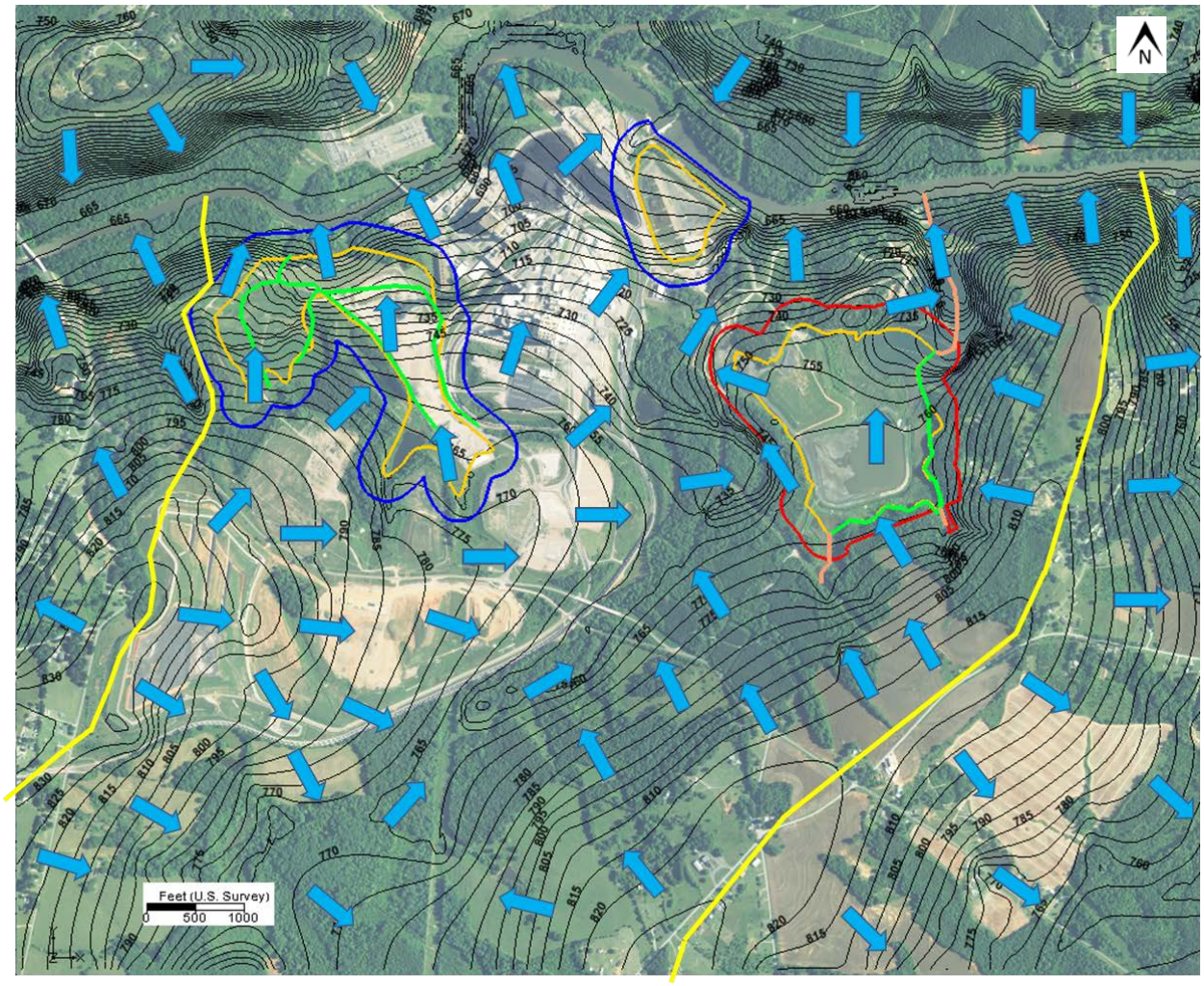

Figure 6-15. Simulated hydraulic heads for the hybrid scenario within the saprolite (layer 9). The red outline is the active ash basin potential compliance boundary, the blue outlines are the Former Units 1-4 and the Unit 5 inactive ash basin potential compliance boundaries, the gold outlines are the waste boundaries, the orange line is a shallow swale, and the green lines are drains. Approximate groundwater divides are yellow lines and approximate flow directions are light blue arrows.

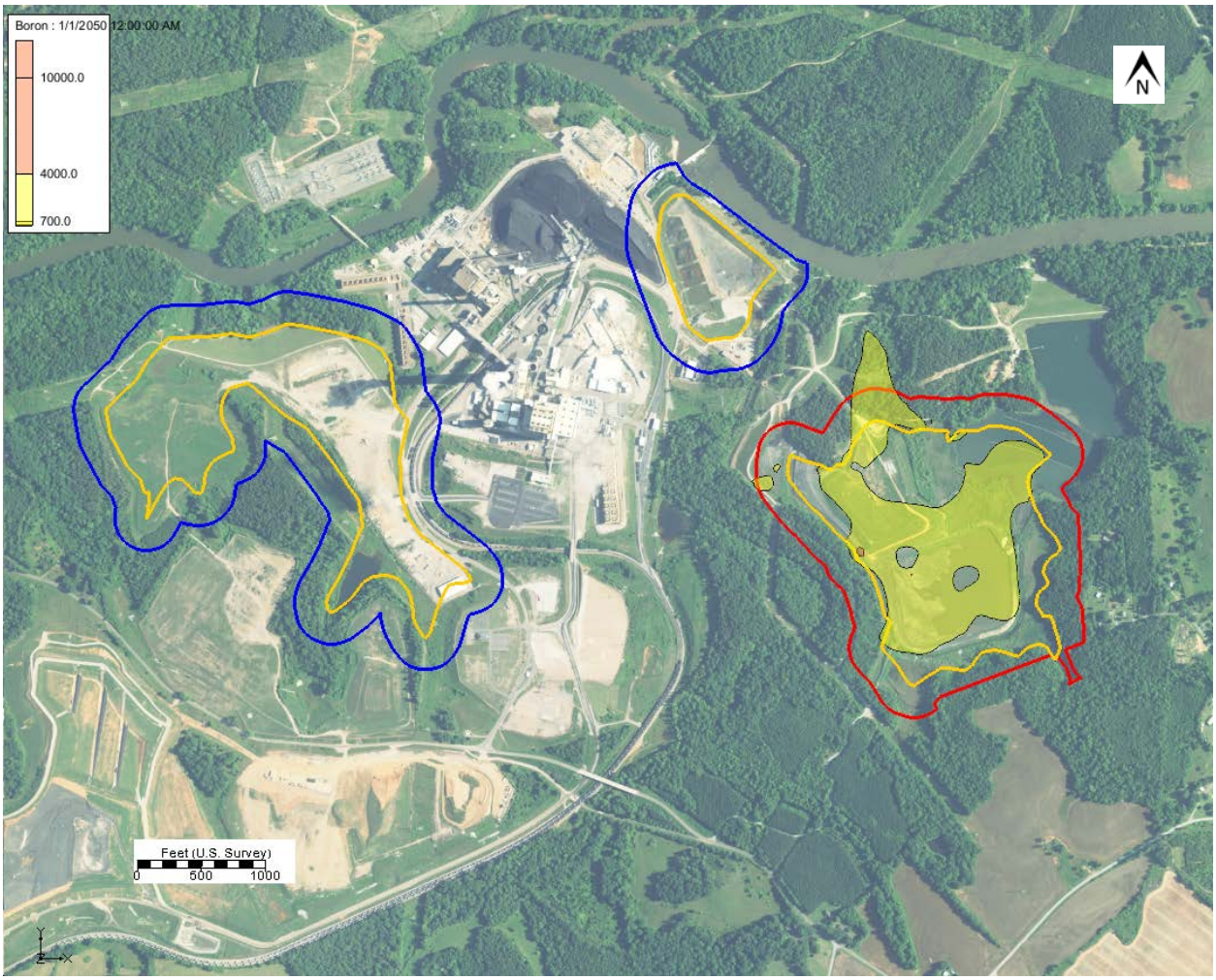

Figure 6-16a. Simulated boron concentrations in the transition zone (layer 15) in 2050 for the hybrid scenario. The red outline is the active ash basin potential compliance boundary, the blue outlines are the Former Units 1-4 and the Unit 5 inactive ash basin potential compliance boundaries, and the gold outlines are waste boundaries.

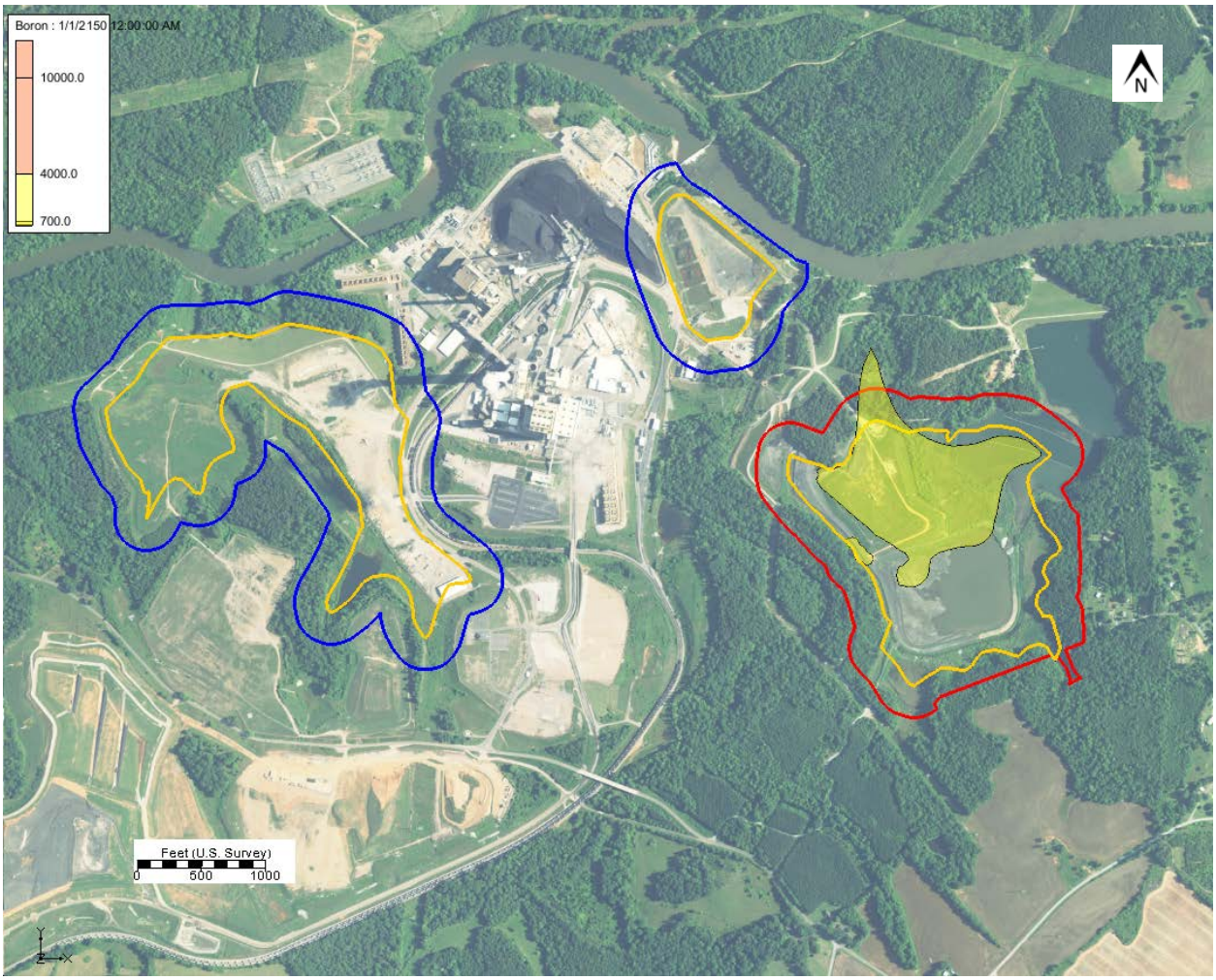

Figure 6-16b. Simulated boron concentrations in the transition zone (layer 15) in 2150 for the hybrid scenario. The red outline is the active ash basin potential compliance boundary, the blue outlines are the Former Units 1-4 and the Unit 5 inactive ash basin potential compliance boundaries, and the gold outlines are waste boundaries.

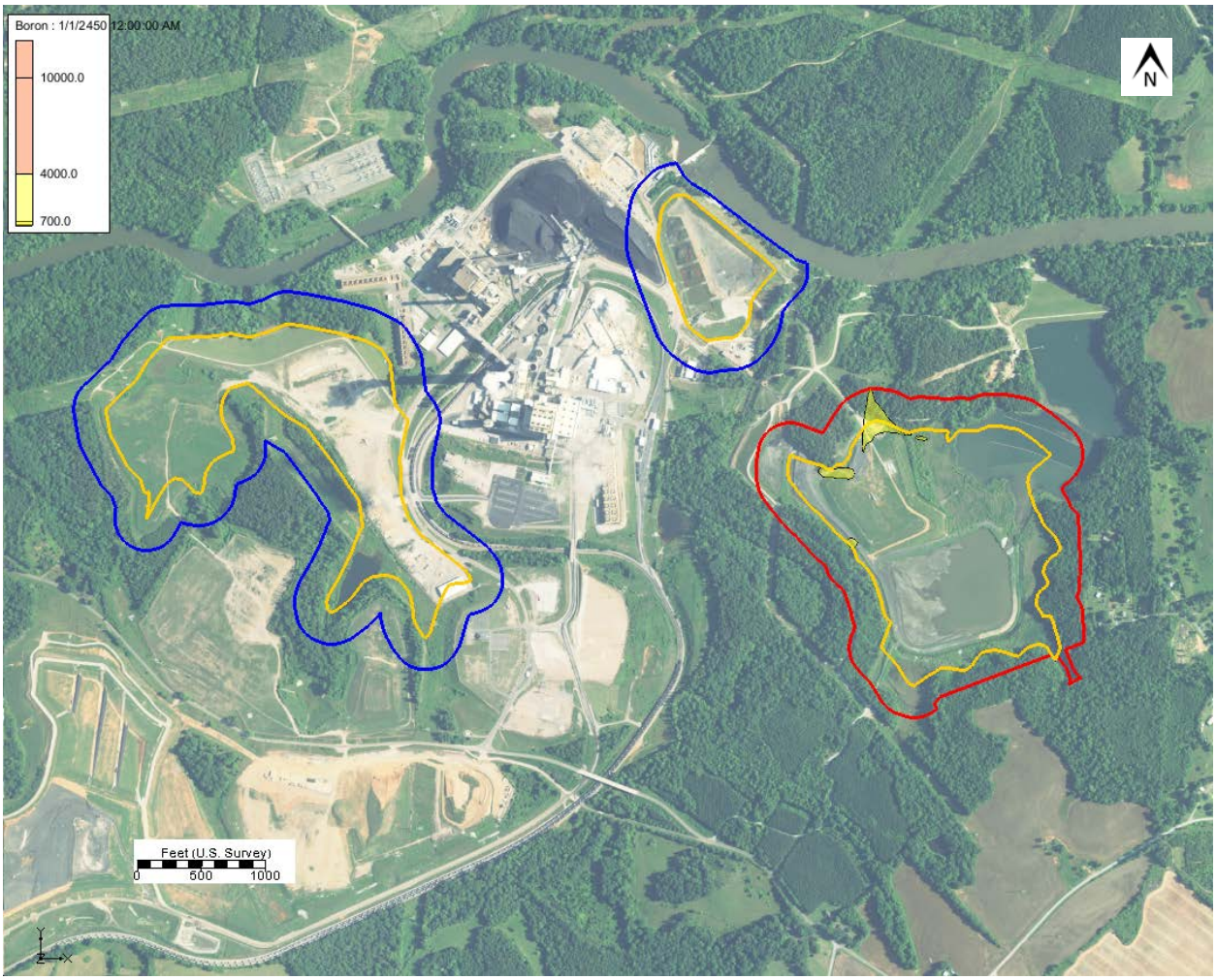

Figure 6-16c. Simulated boron concentrations in the transition zone (layer 15) in 2450 for the hybrid scenario. The red outline is the active ash basin potential compliance boundary, the blue outlines are the Former Units 1-4 and the Unit 5 inactive ash basin potential compliance boundaries, and the gold outlines are waste boundaries.

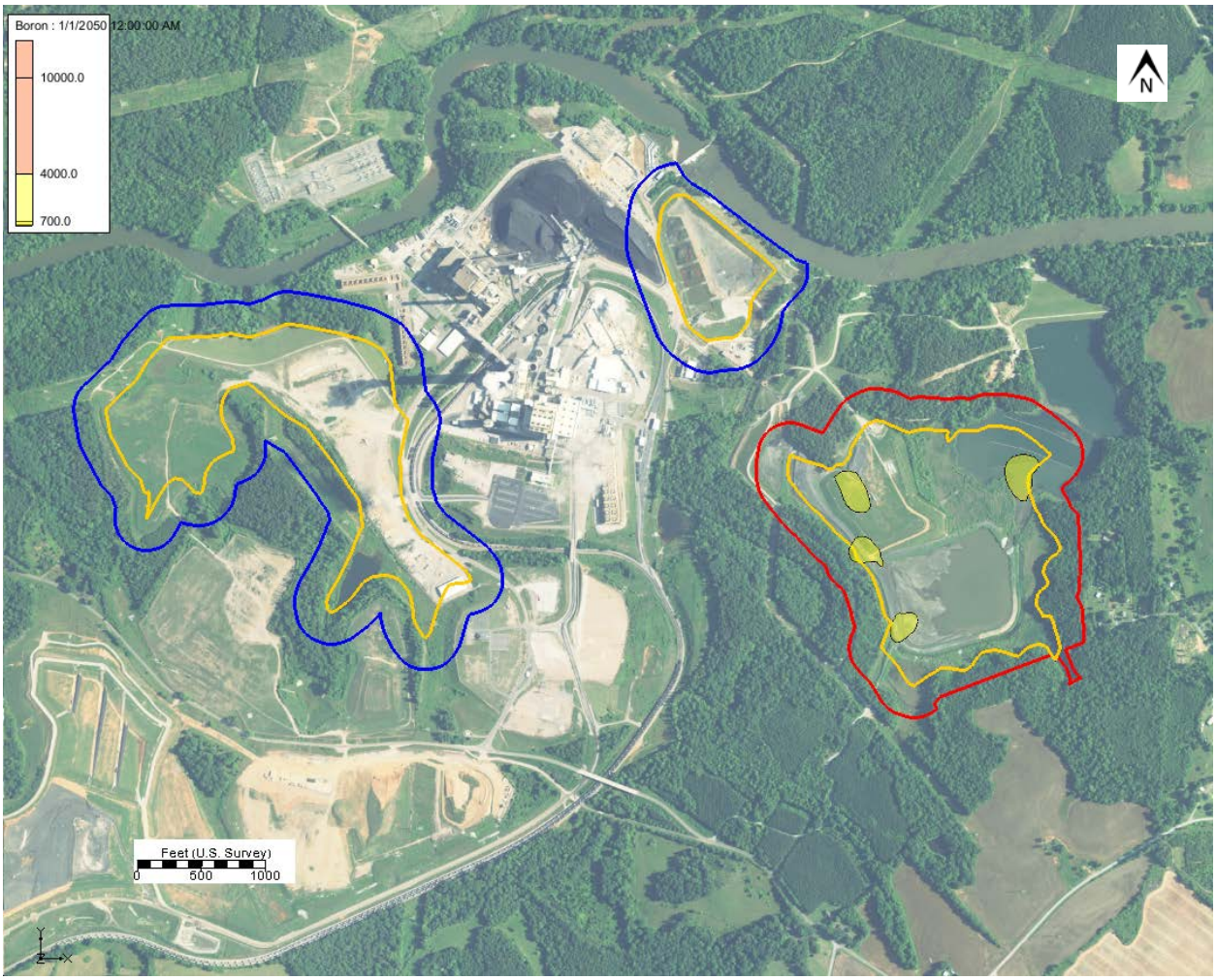

Figure 6-17a. Simulated boron concentrations in the upper bedrock (layer 17) in 2050 for the hybrid scenario. The red outline is the active ash basin potential compliance boundary, the blue outlines are the Former Units 1-4 and the Unit 5 inactive ash basin potential compliance boundaries, and the gold outlines are waste boundaries.

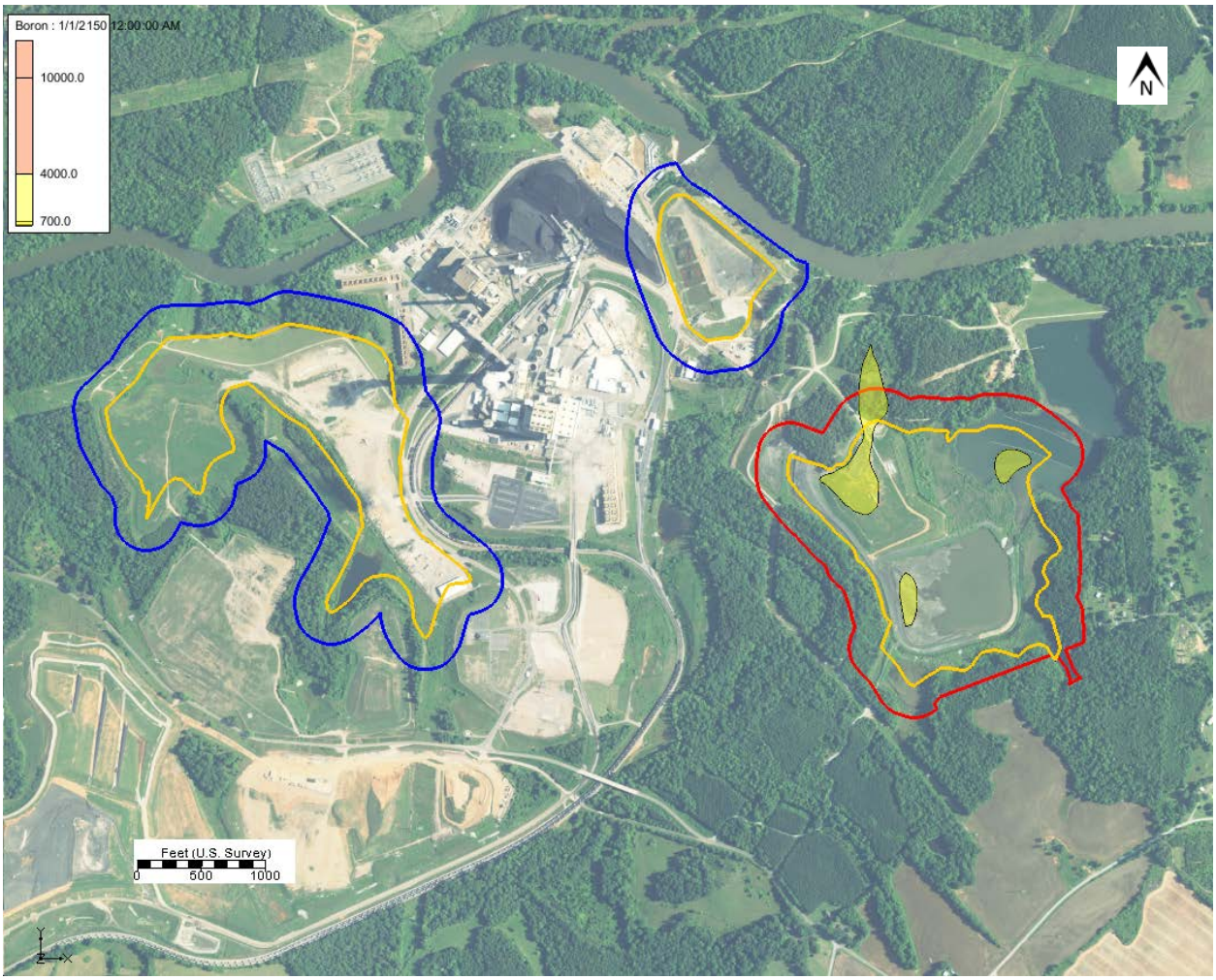

Figure 6-17b. Simulated boron concentrations in the upper bedrock (layer 17) in 2150 for the hybrid scenario. The red outline is the active ash basin potential compliance boundary, the blue outlines are the Former Units 1-4 and the Unit 5 inactive ash basin potential compliance boundaries, and the gold outlines are waste boundaries.

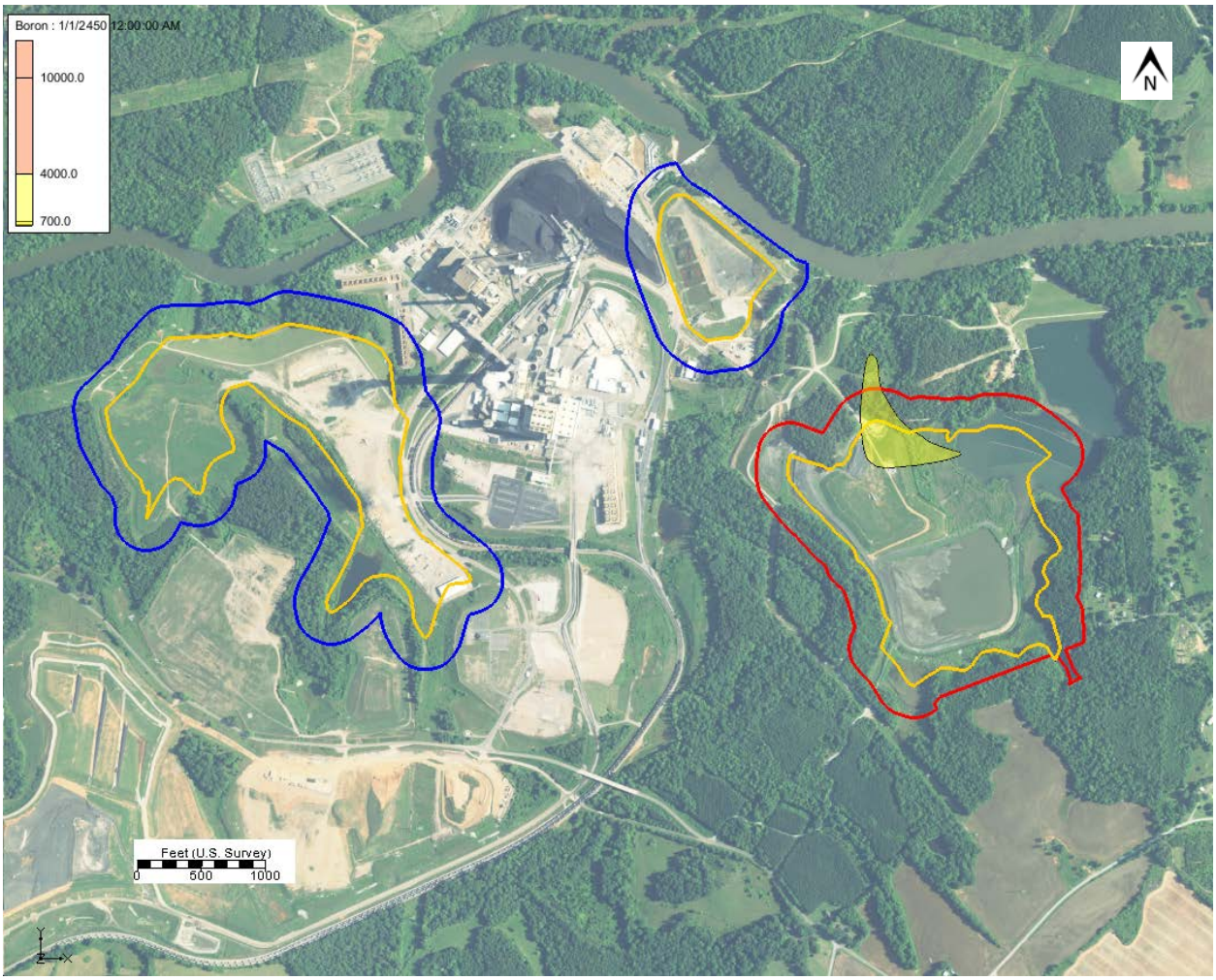

Figure 6-17c. Simulated boron concentrations in the upper bedrock (layer 17) in 2450 for the hybrid scenario. The red outline is the active ash basin potential compliance boundary, the blue outlines are the Former Units 1-4 and the Unit 5 inactive ash basin potential compliance boundaries, and the gold outlines are waste boundaries.

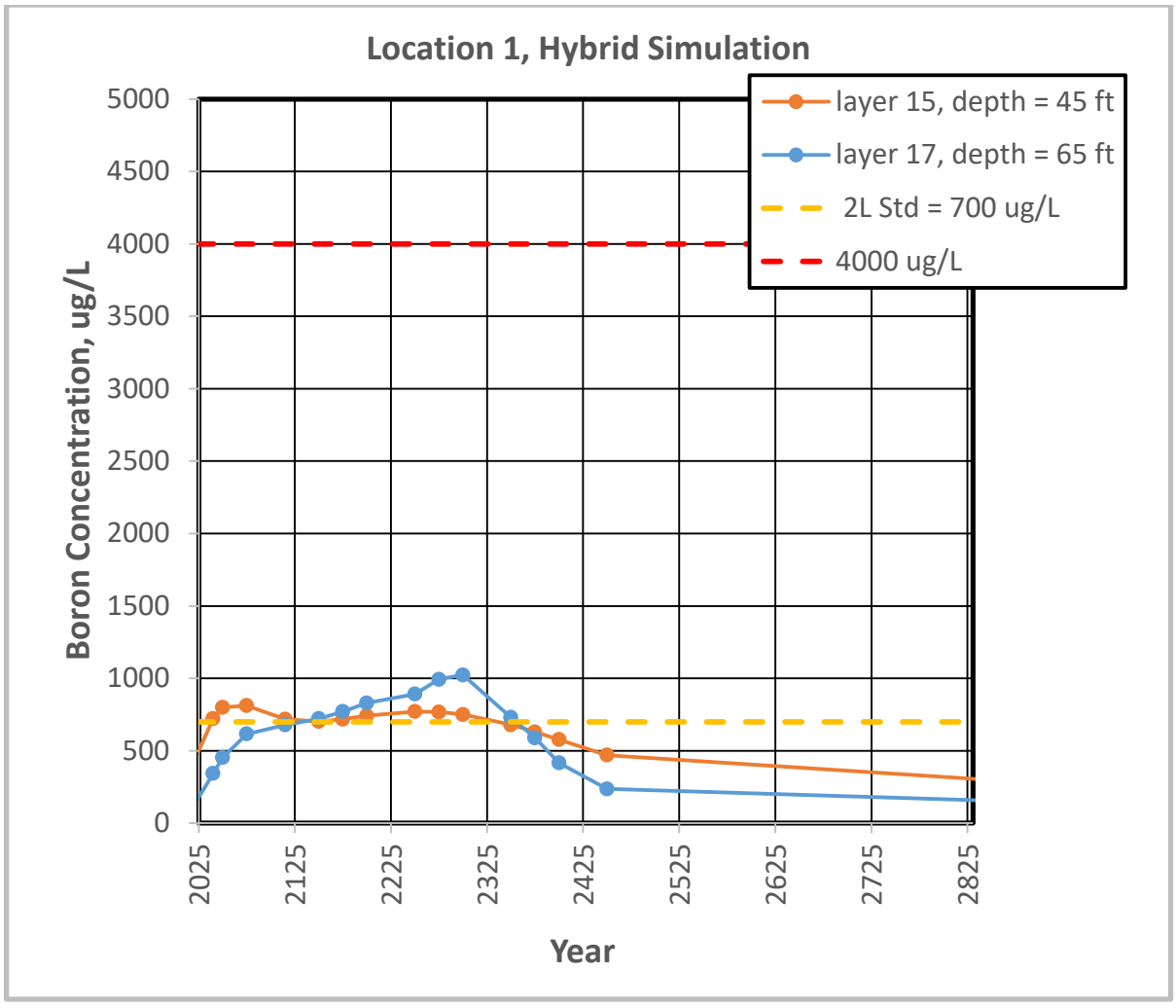

Figure 6-18. Predicted boron concentrations at Point 1 north of the active ash basin for the hybrid scenario.

YEAR	EXCAVATION SIMULATION	FINAL COVER SYSTEM SIMULATION	HYBRID SIMULATION
2050	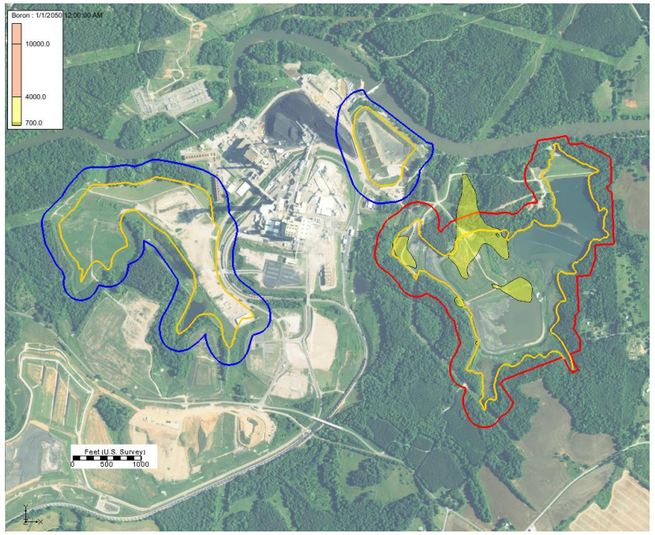	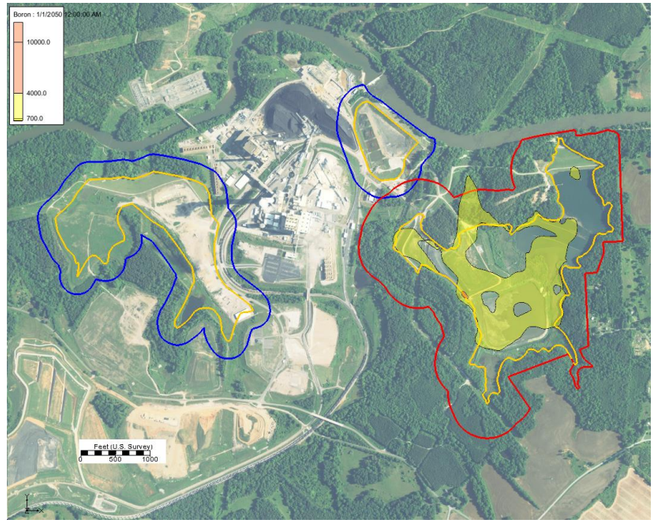	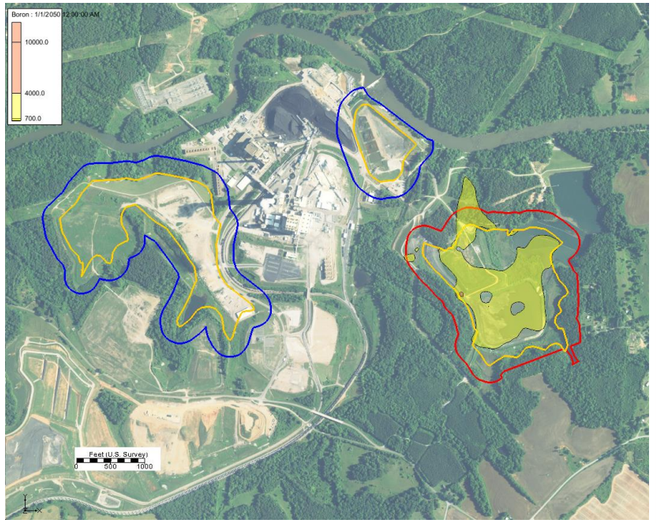
2150	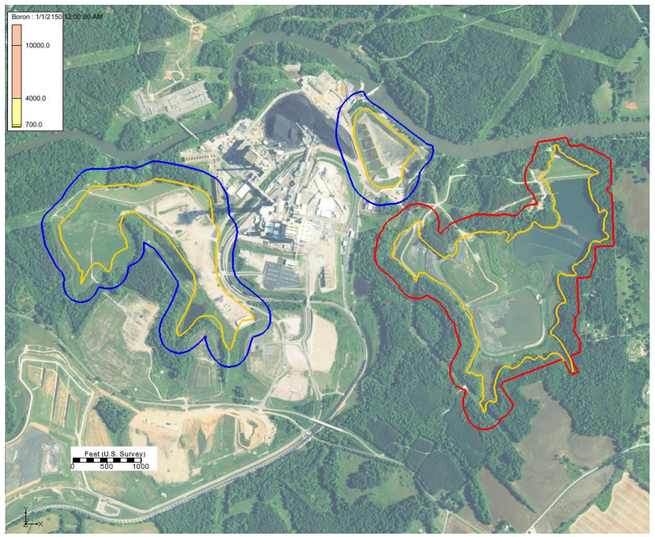	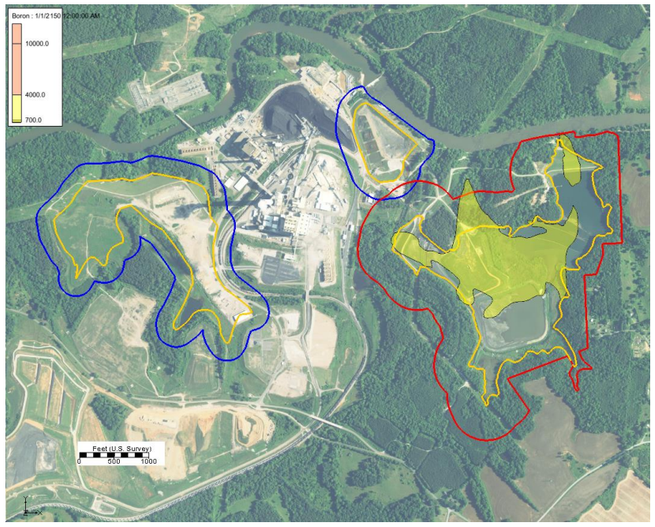	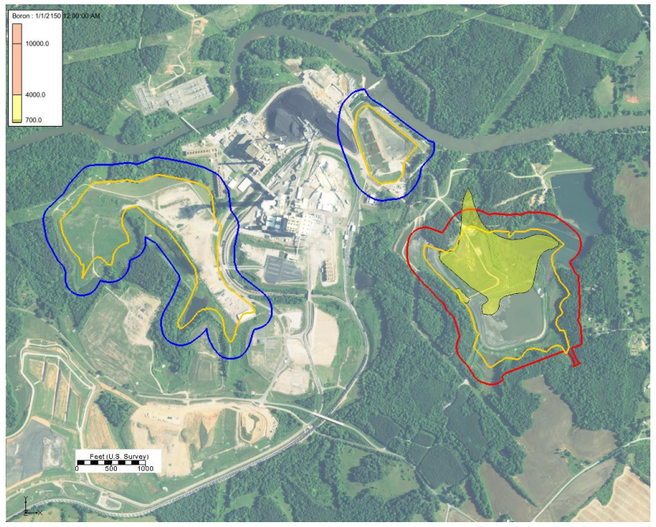

NOTES:
THE START DATES FOR THE THREE MODEL SCENARIOS ARE BASED ON THE COMPLETION DATES FOR THOSE ACTIVITIES. THESE DATES ARE:

- EXCAVATION – YEAR 2027
- FINAL COVER SYSTEM – YEAR 2023
- HYBRID – YEAR 2023

EXISTING COMPLIANCE BOUNDARIES FOR UNIT 5 INACTIVE ASH BASIN AND FORMER UNITS 1-4 ASH BASIN AS DARK BLUE LINES.
CURRENT AND POTENTIAL COMPLIANCE BOUNDARIES FOR ACTIVE ASH BASIN ASSOCIATED WITH BASIN CLOSURE OPTIONS AS RED LINE.
THE WASTE BOUNDARIES ARE SHOWN IN GOLD.

FIGURE 6-19
COMPARISON OF CLOSURE OPTIONS FOR THE TRANSITION FLOW ZONE
MODEL YEARS 2050 AND 2150
CLIFFSIDE STEAM STATION
DUKE ENERGY CAROLINAS, LLC
MOORESBORO, NORTH CAROLINA

P:\Duke Energy Progress.1026\500.Client Attorney Privilege\21.CLIFFSIDE\Abbreviated modeling report\Figures

YEAR	EXCAVATION SIMULATION	FINAL COVER SYSTEM SIMULATION	HYBRID SIMULATION
2250	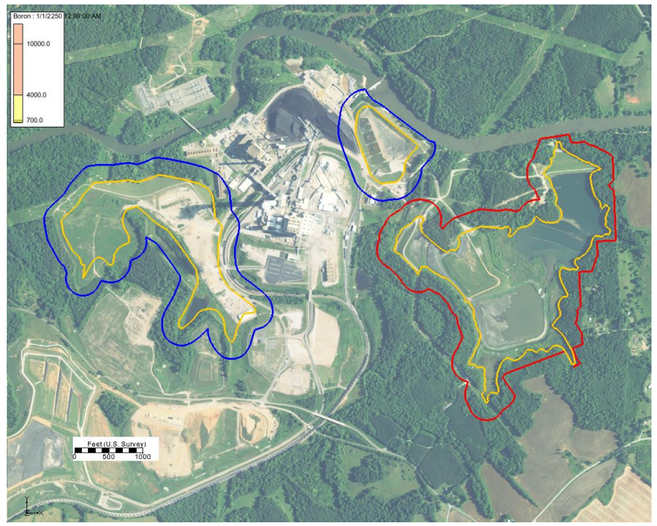	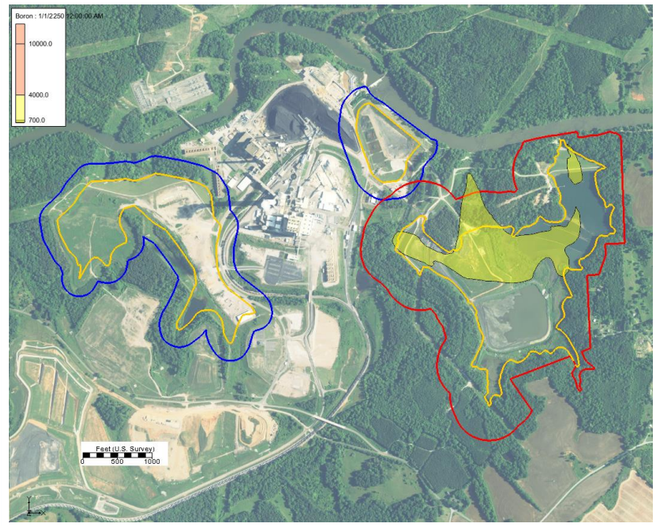	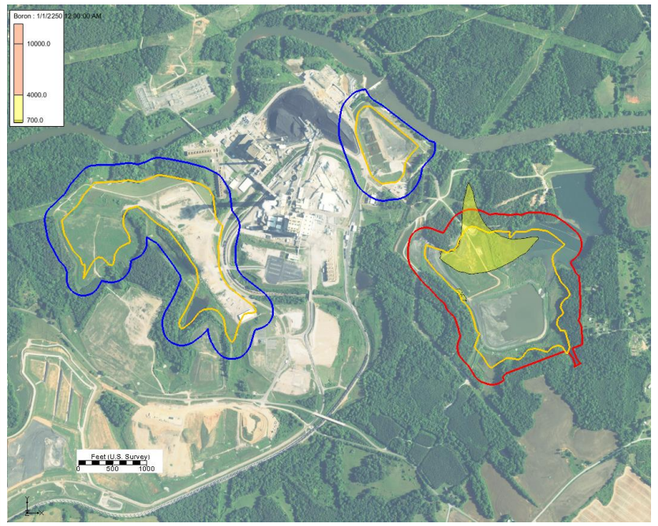
2450	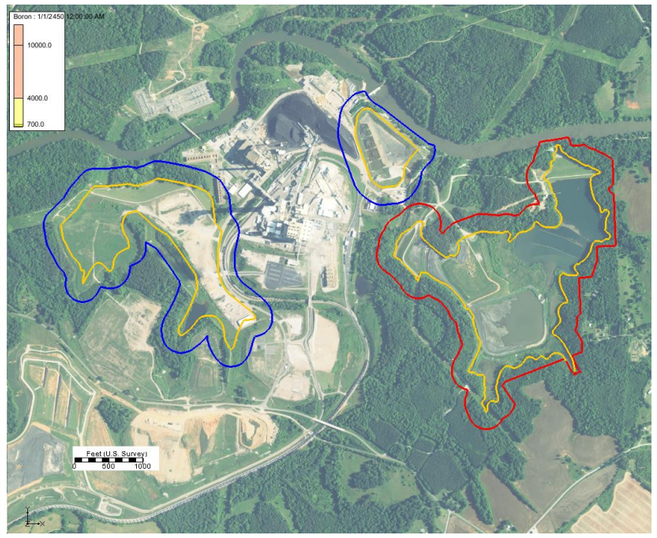	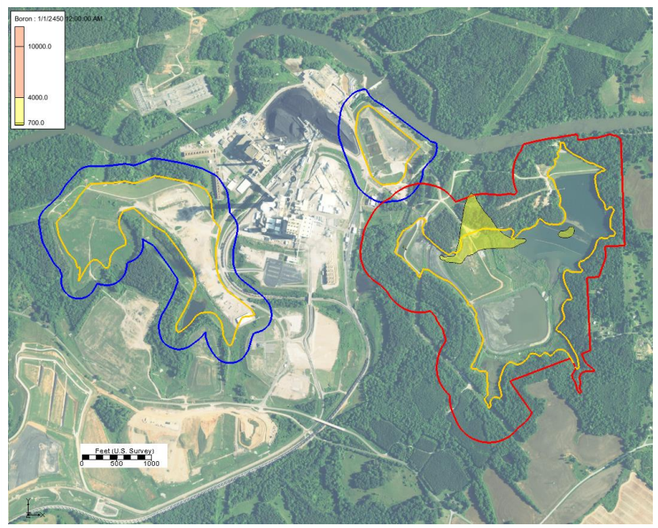	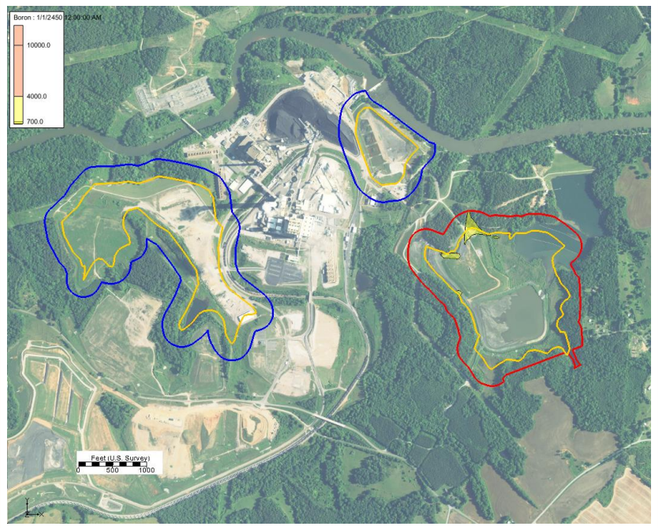

NOTES:
THE START DATES FOR THE THREE MODEL SCENARIOS ARE BASED ON THE COMPLETION DATES FOR THOSE ACTIVITIES. THESE DATES ARE:

- EXCAVATION – YEAR 2027
- FINAL COVER SYSTEM – YEAR 2023
- HYBRID – YEAR 2023

EXISTING COMPLIANCE BOUNDARIES FOR UNIT 5 INACTIVE ASH BASIN AND FORMER UNITS 1-4 ASH BASIN AS DARK BLUE LINES.
CURRENT AND POTENTIAL COMPLIANCE BOUNDARIES FOR ACTIVE ASH BASIN ASSOCIATED WITH BASIN CLOSURE OPTIONS AS RED LINE.
THE WASTE BOUNDARIES ARE SHOWN IN GOLD.

FIGURE 6-20
COMPARISON OF CLOSURE OPTIONS FOR THE TRANSITION FLOW ZONE
MODEL YEARS 2250 AND 2450
CLIFFSIDE STEAM STATION
DUKE ENERGY CAROLINAS, LLC
MOORESBORO, NORTH CAROLINA

P:\Duke Energy Progress.1026\500.Client Attorney Privilege\21.CLIFFSIDE\Abbreviated modeling report\Figures

YEAR	EXCAVATION SIMULATION	FINAL COVER SYSTEM SIMULATION	HYBRID SIMULATION
2050	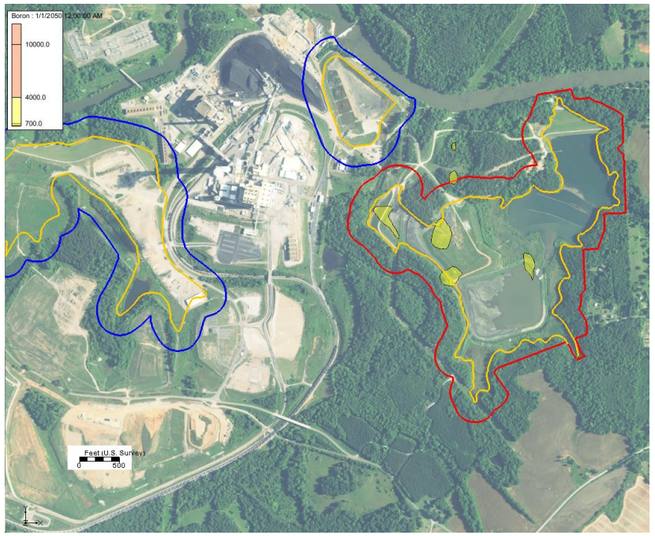	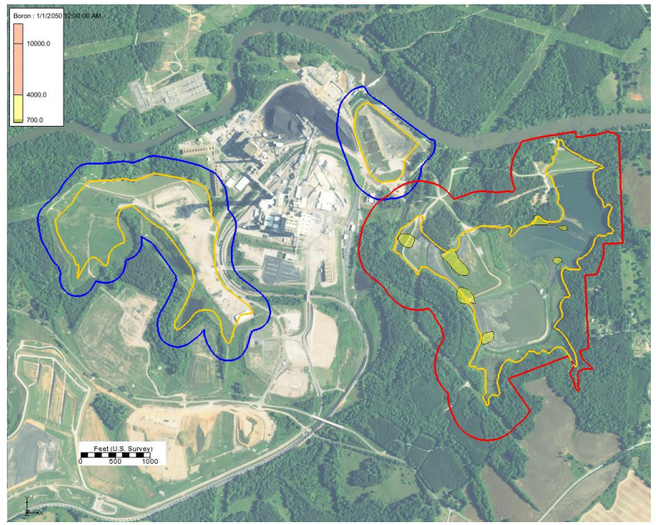	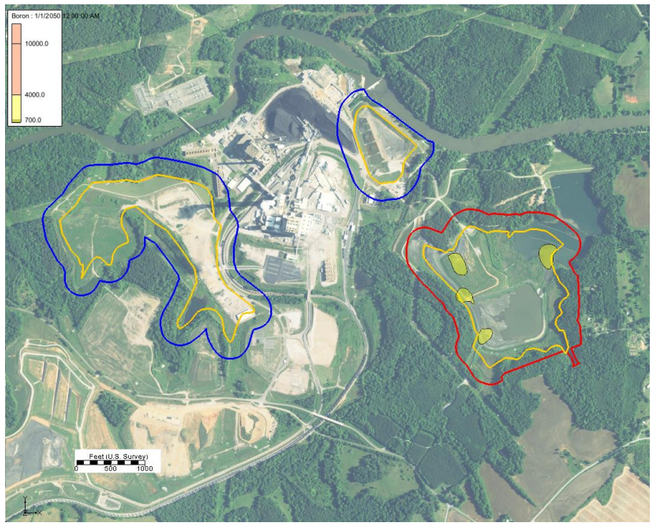
2150	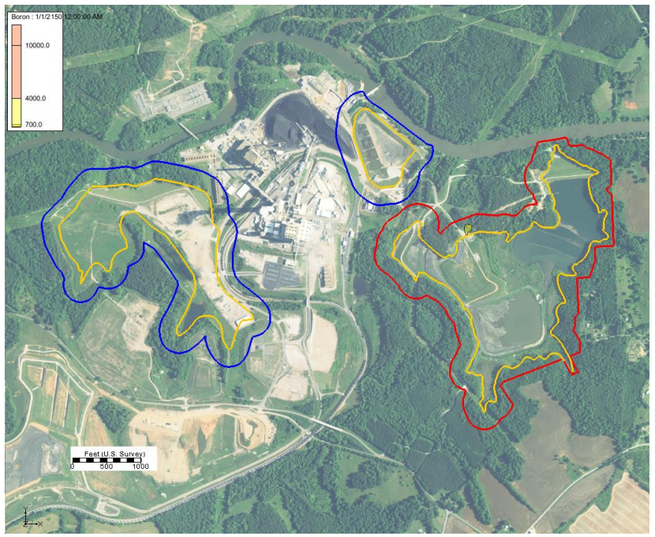	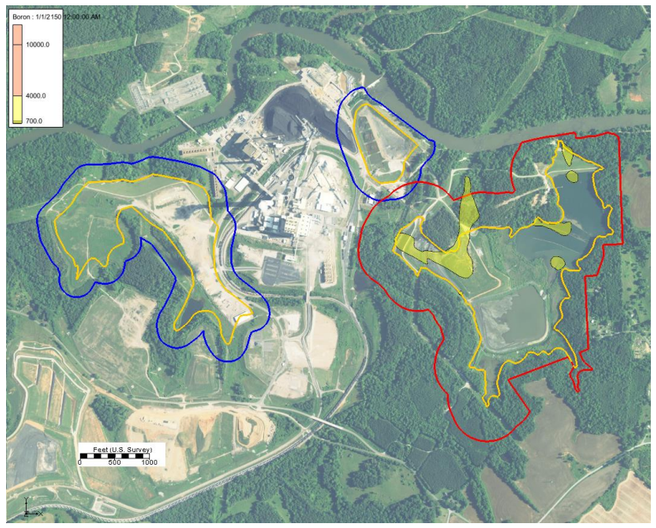	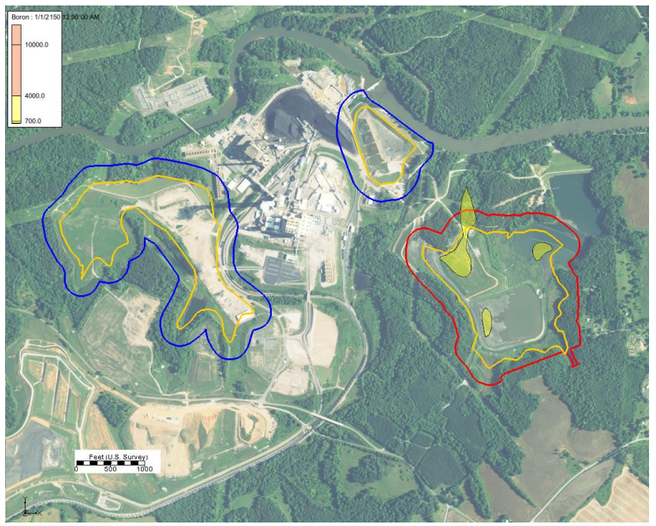

NOTES:
THE START DATES FOR THE THREE MODEL SCENARIOS ARE BASED ON THE COMPLETION DATES FOR THOSE ACTIVITIES. THESE DATES ARE:

- EXCAVATION – YEAR 2027
- FINAL COVER SYSTEM – YEAR 2023
- HYBRID – YEAR 2023

EXISTING COMPLIANCE BOUNDARIES FOR UNIT 5 INACTIVE ASH BASIN AND FORMER UNITS 1-4 ASH BASIN AS DARK BLUE LINES.
CURRENT AND POTENTIAL COMPLIANCE BOUNDARIES FOR ACTIVE ASH BASIN ASSOCIATED WITH BASIN CLOSURE OPTIONS AS RED LINE.
THE WASTE BOUNDARIES ARE SHOWN IN GOLD.

FIGURE 6-21
COMPARISON OF CLOSURE OPTIONS FOR THE UPPER BEDROCK FLOW ZONE MODEL YEARS 2050 AND 2150
CLIFFSIDE STEAM STATION
DUKE ENERGY CAROLINAS, LLC
MOORESBORO, NORTH CAROLINA

P:\Duke Energy Progress.1026\500.Client Attorney Privilege\21.CLIFFSIDE\Abbreviated modeling report\Figures

YEAR	EXCAVATION SIMULATION	FINAL COVER SYSTEM SIMULATION	HYBRID SIMULATION
2250	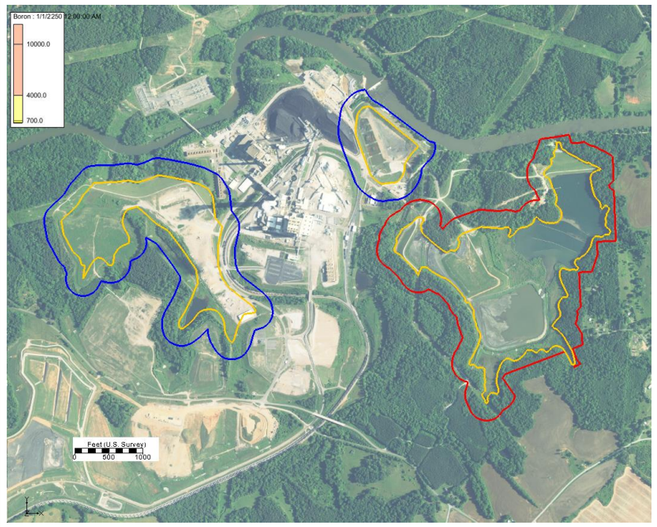	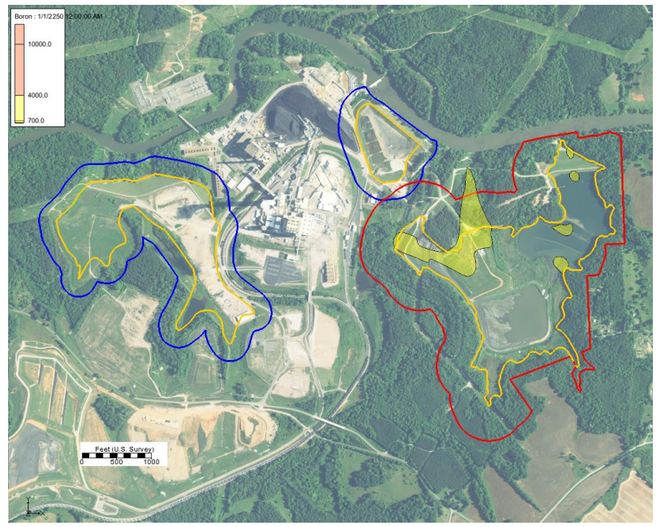	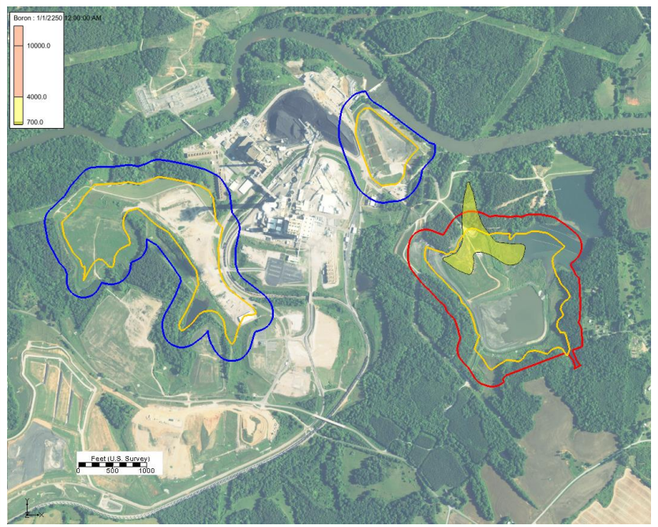
2450	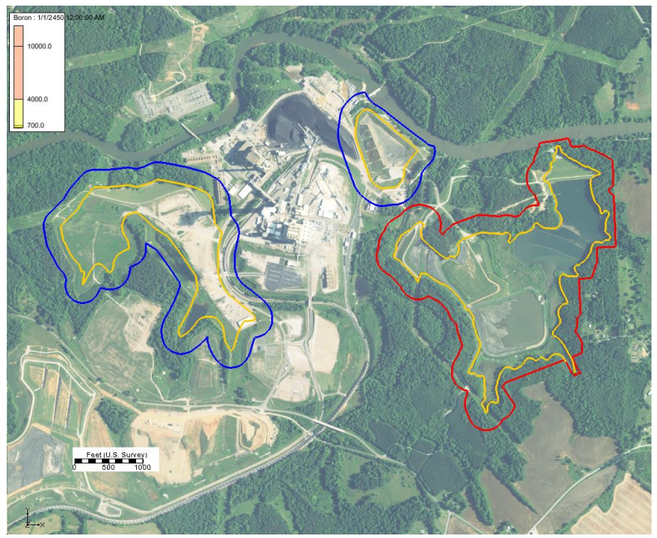	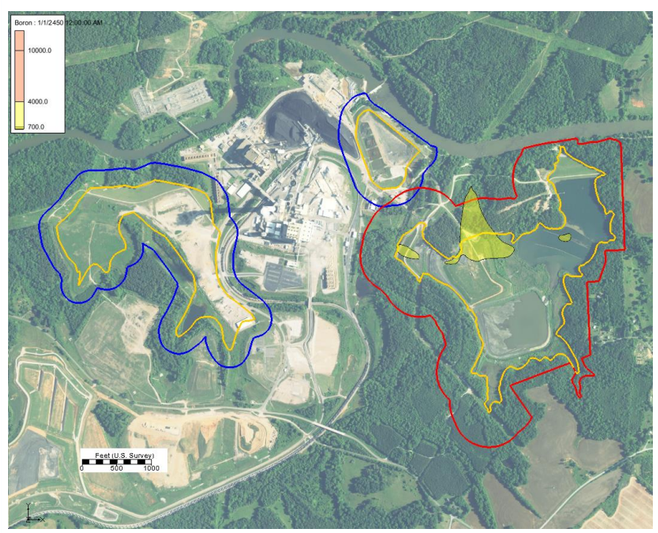	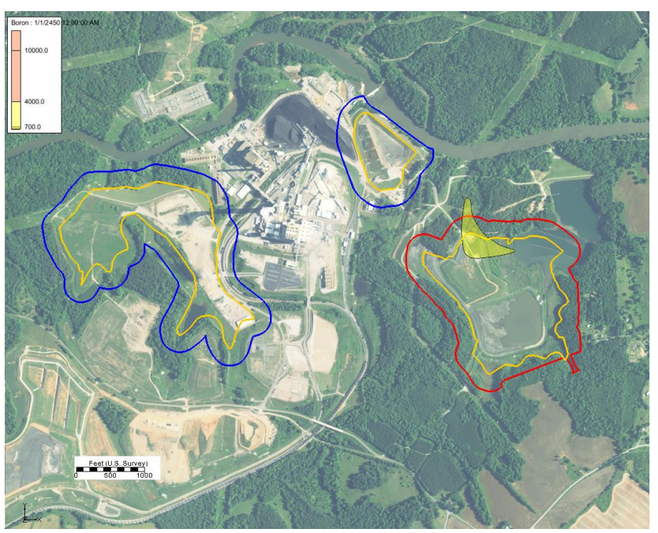

NOTES:
THE START DATES FOR THE THREE MODEL SCENARIOS ARE BASED ON THE COMPLETION DATES FOR THOSE ACTIVITIES. THESE DATES ARE:

- EXCAVATION – YEAR 2027
- FINAL COVER SYSTEM – YEAR 2023
- HYBRID – YEAR 2023

EXISTING COMPLIANCE BOUNDARIES FOR UNIT 5 INACTIVE ASH BASIN AND FORMER UNITS 1-4 ASH BASIN AS DARK BLUE LINES.
CURRENT AND POTENTIAL COMPLIANCE BOUNDARIES FOR ACTIVE ASH BASIN ASSOCIATED WITH BASIN CLOSURE OPTIONS AS RED LINE.
THE WASTE BOUNDARIES ARE SHOWN IN GOLD.

FIGURE 6-22
COMPARISON OF CLOSURE OPTIONS FOR THE UPPER BEDROCK FLOW ZONE
MODEL YEARS 2250 AND 2450
CLIFFSIDE STEAM STATION
DUKE ENERGY CAROLINAS, LLC
MOORESBORO, NORTH CAROLINA

P:\Duke Energy Progress.1026\500.Client Attorney Privilege\21.CLIFFSIDE\Abbreviated modeling report\Figures